Bioactive secondary metabolites from the endophytic microorganisms of the medicinal plant *Bidens pilosa*

Dissertation

zur Erlangung des akademischen Grades doctor rerum naturalium

(Dr. rer. nat.)

vorgelegt dem Rat der Biologisch-Pharmazeutischen Fakultät

der Friedrich-Schiller-Universität Jena

von Apothekerin Randa Abdou

geboren am 21.02.1976 in Kairo, Ägypten

Gutachter:

1. Prof. Dr. Christian Hertweck, Friedrich-Schiller-Universität Jena und Hans-Knöll-Institut (HKI) Jena

2.Prof. Dr. Dirk Hoffmeister, Friedrich-Schiller Universität Jena

3. Prof. Dr. Jörg Durner, Technische Universität München und Helmholtz Zentrum München

Tag der öffentlichen Verteidigung : 14.01.2011

List of contents

List of abbreviations

1D = One Dimensional

2D = Two Dimensional

CC_{50} = Concentration at which 50% cytotoxicity (cell death) is observed

$CDCl_3$ = Deuterated Chloroform

^{13}C NMR = Carbon Nuclear Magnetic Resonance

COSY = Correlated Spectroscopy

DEPT = Distortionless Enhancement by Polarization Transfer

DMSO = Dimethylsulfoxide

D_3OD = Deuterated Methanol

Fig = Figure

GI_{50} = Concentration at which 50% growth inhibition is achieved

HeLa = Human immortal cell line from the cervical cancerous cells of Henrietta Lacks

HMBC = Heteronuclear Multiple-Bond Correlation

HMQC = Heteronuclear Multiple Quantum Coherence

^1H NMR = Proton Nuclear Magnetic Resonance

HPLC = High Performance Liquid Chromatography

HPLC-MS = High Performance Liquid Chromatography Mass Spectrometry (coupling)

HRESIMS = High Resolution Electron Spray Ionization Mass Spectrometry

HSQC = Heteronuclear Single-Quantum Coherence

HUVEC = Human Umbellical Vein Endothelial Cells

K-562 = human immortal erythroleukaemia cells

MeOH = Methanol

MS = Mass Spectrometry

NMR = Nuclear Magnetic Resonance

ppm = Parts Per Million

RP = Reversed Phase

rpm = Rotation Per Minute

TFA = Trifluoroacetic Acid

TLC = Thin Layer Chromatography

UV = Ultraviolet

1. Introduction

1.1. Endophytes

The term endophyte includes all organisms that during a variable period of their life symptomlessly colonise the living internal tissues of their hosts. This definition includes any organisms residing inside a plant host [1]. However the most frequently isolated endophytes are the fungi. Endophytic fungi are found in almost all plants including trees, grasses, algae, mosses and herbaceous plants [1]. Under normal conditions they live within the host plant without causing any symptoms of disease.

Presently no one knows exactly the role of endophytes in nature and their relationship to various host plant species. While some endophytic fungi appear to be ubiquitous (e.g. *Fusarium* spp., *Pestalotiopsis* spp., and *Xylaria* spp.), one cannot state that endophytes are host specific [2]. It is more propable that their associations are developed by chance. Many endophytes of the same species are often isolated from the same plant and only one or a few strains produce a highly biologically active compound in culture. There is a lack of knowledge about what an endophyte produces in culture and what it may produce in symbiosis. The production of certain bioactive compounds by the endophyte in situ may facilitate the domination of its biological niche within the plant or even provide protection to the plant from harmful invading pathogens [2].

Many endophytes are closely related to pathogenic fungi, and are suggested to be derived from them by an extension of latency periods and a reduction of virulence [3]. Moreover endophytic fungi are thought to interact mutualistically with their host plant so that the host plant provides nutrients to the endophyte which in turn produces bioactive substances to enhance the growth and competitiveness of the host in nature [4]. Accordingly endophytes have been identified as a promising source of new pharmacologically active secondary metabolites that might be suitable for medicinal or agrochemical applications.

It is hypothesized that there are no neutral interactions, but that endophyte-host interactions involve a balance of antagonisms. There is always a certain degree of virulence of the fungus causing infection, whereas defense of the plant host limits development of diseases [5].

It has also been estimated that the interaction between fungal endophytes and their host plants is characterized by a finely tuned balance between fungal virulence and plant defense, in which disease symptoms may develop if the association is disturbed by weakened plant defense or increased fungal virulence. There are reports that endophytes become parasites under certain conditions. Thus, host-microbe interactions can range from mutualism through commensalism to parasitism in a continous manner [4]. As disease is the exception in plant microbe interactions, it can be regarded as an unbalanced symbiosis. Commensalism and

mutualism represent the balanced stages of plant microbe interactions. Commensalism provides benefit to the endophyte by enabling an undisturbed existence and nutrient supply without affecting the host. Mutualism, on the contrary is defined as an interaction that is beneficial for both partners. In addition to providing benefits for the endophyte, mutualism often results in stimulated growth of the host. Endophytes can also improve tolerance to abiotic stress [6].

1.2. Plant-endophyte interaction

The interactions between host plants and endophytes are poorly understood. Studies showed that endophytes interact mutualistically when reproducing vertically (systemic) by growing into seeds, and are antagonistic to the host when transmitted horizontally (nonsystemic) via spores [7]. It has been hypothesized that some of these endophytes may have developed genetic systems allowing the transfer of information between themselves and the plant and *vice versa* [8-9]. This would allow rapid dealing with environmental conditions and improve the compatibility with the plant host [9].

One of the estimated mutualistic interactions of endophytes with their host plants is the increase of host resistance to pathogenic microorganisms which is called ‘‘acquired plant defense’’ [10]. It has been reported that grass species infected with systemic endophytes show toxic effects on vertebrate and invertebrate herbivores and pathogens due to the production of several alkaloids by their endophytes [11]. Loline alkaloids, saturated 1-aminopyrrolizidines with an oxygen bridge, were found in endophyte-infected grasses, such as *Festuca* spp. infected with *Neotyphodium* spp. Lolines are potent broad-spectrum insecticides, acting both as metabolic toxins and feeding deterrents depending on the specific insect species. Contrary to ergot and indole diterpene alkaloids, these loline derivatives are less toxic to mammals [12]. Endophytes of woody plants may also provide a protective role for the host plant because they produce several mycotoxins and enzymes that are toxic to certain microbes and invertebrate herbivores [7]. In addition, endophytes may also increase host fitness and competitive abilities. This is achieved by increasing nutrient uptake, germination success, resistance to water stress, resistance to seed predators, tolerance to heavy metals, tolerance to high salinity, and growth rate by acquiring biochemical pathways to produce plant growth hormones. Accordingly, the growth-promoting phytohormone indole-3-acetic acid (IAA) was isolated from cultures of the fungal endophytes *Acremonium coenophialum*, *Aureobasidium pullulans*, *Epicoccum purpurascens* and *Colletotrichum* sp. Together with IAA and indole-3-acetonitrile, cytokinins were produced by an endophytic strain of *Hypoxylon serpens* [13]. In return, plants provide spatial structure,

protection from desiccation and nutrients for the endophyte [7]. It is also possible that the plant may provide the endophyte with compounds essential for the completion of its life cycle or important for its growth or self-defense [14]. Recent studies suggested that plant and endophyte genotypic combinations together with environmental conditions affect the type of interaction between them [10]. It seems that many changing factors in the host such as season, age, environment and location may influence the biology of the endophyte [15]. It had been estimated that about 1.5 million fungal species are present on earth of which only about 7% have been described so far. Almost all vascular plant species examined were found to contain endophytes, which suggests that they are widely spread in the plant kingdom [13]. As many new endophytic species may exist in plants, endophytic microorganisms are considered as important components of microbial biodiversity [16]. Biological diversity is associated with chemical diversity because of the constant chemical changes that exist in ecosystems with hard competitions for survival [15]. Currently, it is hypothesized that ecology has a major impact on the profiles of natural products in filamentous fungi. Climatic factors such as temperature, precipitation, humidity and length of season affect the distribution of fungi. Moreover, several regions such as the tropical forests, the deep sea, sites of extreme temperature, salinity or pH, often provide a source of new microorganisms with the potential for novel secondary metabolites [17]. However, a high fungal diversity is also found in temperate regions, such as those of northern Europe, eastern North America and North Africa [18].

1.3. Biologically active natural products from endophytes

1.3.1. Antimycotic agents from endophytes

Due to the increasing number of AIDS and cancer patients as well as those with organ transplants and autoimmune diseases, the incidence of opportunistic fungal infections has become a life threatening problem [14]. The development of resistance against current medications, the toxic side effects caused by some drugs has created an urgent need for new antifungal agents to overcome these problems. Cryptocandin A is a peptide antimycotic agent effective for the treatment of skin and nail fungal infections [14]. It has been isolated from the endophytic fungus *Cryptosporiopsis quercina* residing in the medicinal plant *Tripterigeum wilfordii* [19]. Other examples include ambuic acid (Fig 1), which has been obtained from *Penicillium microspora* found in several rainforests [20] and the potent antifungal agent jesterone obtained from *Pestalotiopsis jester* [21].

1.3.2. Antibiotic agents from endophytes

The increasing occurrence of multiresistant pathogenic strains has rendered many currently used antimicrobial agents ineffective in treating current infections. Therefore new antibacterial agents are required to overcome this problem. Guanacastepene A (Fig 1) is a diterpenoid produced by an unidentified endophytic fungus from the tree *Daphnopsis Americana* which exhibited potent antibacterial activity against drug resistant strains of *Staphylococcus aureus* and *Enterococcus faecium* [22]. A further example is represented by rhizotonic acid (Fig 1) obtained from an endophyte of *Rhizoctonia* species in *Cynodon dactylon*. These compounds exerted potent antibacterial activity against *Helicobacter pyroli*, which is the causative agent of gastric ulcer [23]. Moreover altersetin (Fig 1) showed significant activity against Gram-positive bacteria and has been produced by endophytic *Alternaria* species [24].

Fig 1. Fungal natural products with antimicrobial activity

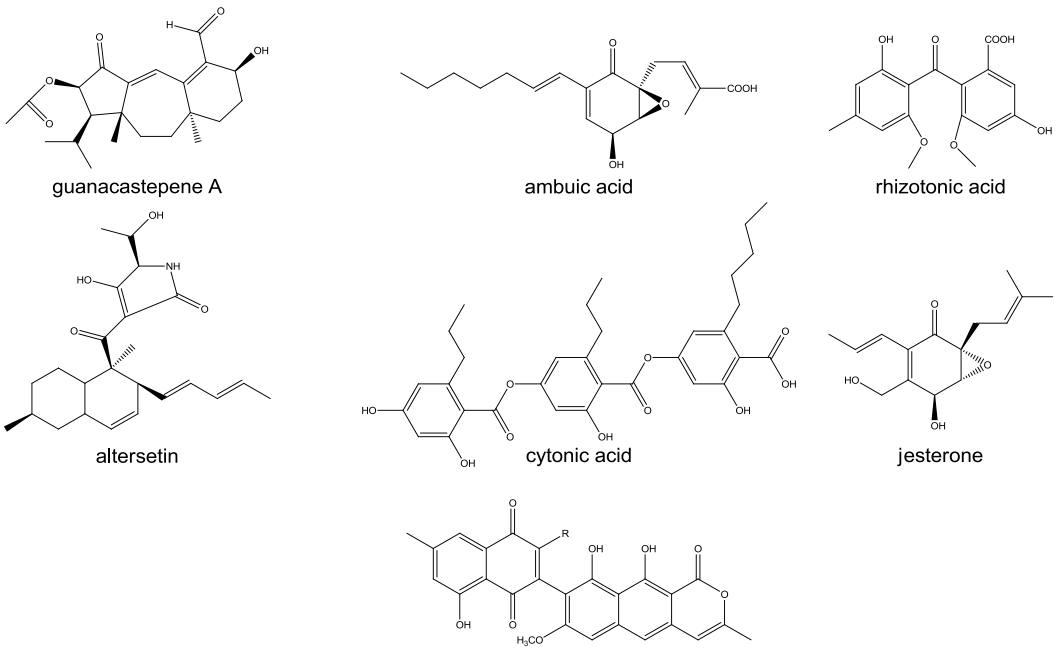

1.3.3. Antiviral agents from endophytes

New antiviral drugs are needed to overcome the increasing development of resistance against current drugs, the side effects and high cost of available therapies as well as the increasing incidence of opportunistic infections in HIV and AIDS patients [15].

Cytonic acids A and B were reported as human cytomegalovirus protease inhibitors from the culture of the endophytic fungus *Cytonaema* sp. isolated from *Quercus* sp. [25]. In addition,

the new quinone-related metabolites, xanthoviridicatins E and F (Fig 1), produced by the endophyte *Penicillium chrysogenum* obtained from an unidentified plant, inhibited the cleavage reaction of HIV-1 integrase [26].

1.3.4. Anticancer agents from endophytes

Taxol is the world`s "first billion dollar" anticancer drug (Fig 2), which has been obtained from the yew tree species, *Taxus* sp. [27]. In 1993 a taxol-producing endophytic fungus *Taxomyces andreanae* from *Taxus brevifolia* was isolated and characterized [8]. A hypothesis of the presence of a genetic recombination of the endophyte with the host during a long evolutionary symbiosis has been proposed to explain the production of taxol by the host plant and its endophyte [28]. Studies on the mechanism of action of paclitaxel revealed that it acts by preventing tubulin molecules from depolymerizing during the process of cell division [29]. Moreover it has been found that taxol acts on tubulin molecules of plant pathogenic fungi in the same way it affects human cancer cells which indicates the protective role taxol provides to the yew tree from which it originates [30].

Another anticancer drug is the indole derivative vincristine (Fig 2) which is used in the treatment of leukemia, lymphoma, breast and lung cancer. This drug was obtained from *Catharanthus roseus* [31]. Recently, a Chinese group reported preliminary evidence that vincristine might be produced by *Fusarium oxysporum* endophytic in the same plant [32] Endophytic fungi were found to produce interesting bioactive metabolites not related to the natural products produced by their host plants like chaetomellic acids A and B (Fig 2), isolated from the culture of the endophyte *Chaetomella acutisea*, were found to be specific inhibitors of farnesyl-protein transferase [33]. Moreover, microcarpalide (Fig 2), a microfilament disrupting agent with weak cytotoxicity to mammalian cells, was characterized from an unidentified endophytic fungus [34].

Another example is the large group of alkaloids known as cytochalasans. Many of these compounds, possessing antitumor and antibiotic activities, were found in endophytic fungi, but unfortunately their cellular toxicity limited their development into pharmaceutical drugs [35]. Chaetoglobosins (Fig 2) are fungal metabolites belonging to the family of cytochalasans. Some chaetoglobosins have been isolated recently from the endophyte *Chaetomium globosum* and were shown to exhibit cytotoxic activities against the human nasopharyngeal epidermoid tumour KB cell line [36].

Fig 2. Fungal natural products with anticancer, immunosuppressive and antioxidant activities

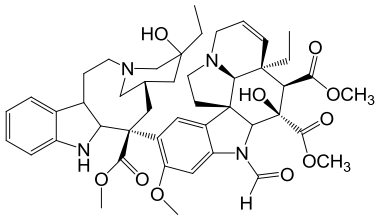

vincristine

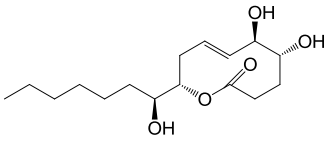

microcarpalide

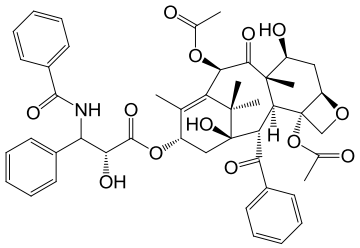

taxol

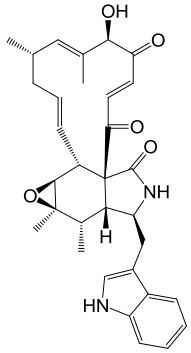

chaetoglobosin A

1.4. Plant selection for isolation of bioactive endophytes

The first step in the search for bioactive endophytes is the choice of a suitable host plant. It is important to understand the methods and rationale used to provide the best opportunities to isolate biologically active endophytic microorganisms as well as ones producing new bioactive compounds. Since the number of plant species in the world is so vast, creative and imaginative strategies must be used to narrow the search for bioactive endophytes [2].

A specific rationale for the collection of each plant for endophyte isolation and natural-product discovery is employed. Several hypotheses determine these plant selection strategies, which have been summed up by Strobel as follows: (i) Plants from unique environments possess new strategies for survival and are interesting to study. (ii) Plants having special uses and biological activities are a promising source for study. In some cases the bioactivity of the plant has nothing to do with its natural products, but originates from its endophyte. (iii) Plants that have an unusual longevity are mostly associated with endophytes with active natural products. (iv) Plants growing in areas of great biodiversity may harbor endophytes with great biodiversity as well [2].

1.5. The plant *Bidens pilosa*

Bidens pilosa is an annual weed distributed widely in the tropical and subtropical regions of the world. It is well-known as hairy beggar ticks or Spanish needles and is reported to be a weed of 31 crops in more than 40 countries [37]. It is a herbaceous plant widely distributed in Africa, America, China, and Japan that is used in traditional medicines for treatment of inflammation and various diseases, including hepatitis and diabetes. The boiling water extract of the aerial parts of *B. pilosa* in Japan has anti-inflammatory and anti-allergic properties [37]. Furthermore, the ethanolic crude extract from the roots of *B. pilosa* contains polyacetylenes and flavonoids that exert in vitro antimalarial activity against *Plasmodium falciparum* [38]. More recently, a study was carried out to examine the possibility of using *B. pilosa* for weed and plant fungus control assuming that the wide distribution of the plant might be due to its antifungal activity against phytopathogens [39]. Phenylpropanoid glucosides, polyacetylenes, a diterpene, flavonoids, and flavone glycosides have been identified from *B. pilosa* [40]. The extracts of *B. pilosa* showed antihyperglycemic, antihypertensive, immunosuppressive and anti-inflammatory, antileukemic, antimalarial, antibacterial, and antimicrobial activities [41]. Concerns regarding this weed have increased since it was noted as an invasive species. With strong invasive strength and effects from climate changes, this noxious weed might be able to extend its dominance to other regions of the world. As a successful strategy against this invasive species has not been achieved yet, research on the utilization of *B. pilosa* for eco-friendly agricultural production is indispensable [39].

All studies performed so far focused on the phenolic constituents of the plant extract, and yet endophytes of *B. pilosa* and their potentially active metabolites have been neglected.

2. Aim of the study

The aim of this study was the investigation of the metabolic profile of the biologically active (antifungal and/or antibacterial as well as cytostatic and/or cytotoxic) endophytic strains of the Egyptian medicinal plant *Bidens pilosa* (*Asteraceae*) to search for new bioactive natural products and find out the role of these metabolites in the interaction with the host plant and the other endophytes. This involved the following steps:

- Isolation of the endophytic microorganisms from the different sterilized plant parts (flower, leaf and stem).
- Screening of all endophytic strains for antimicrobial and cytotoxic activity.
- Screening of all endophytic strains for a stimulant effect on plant immunity using plant cells of *Arabidopsis thaliana*.
- Selection of the strains with antimicrobial activity for cultivation and optimisation of the cultivation conditions (nutrient type, pH, temperature and fermentation duration) of the selected strains followed by their large scale fermentation.
- Isolation and purification of secondary metabolites from the extracts of microbial fermentation using chromatographic methods
- Elucidation of the structures of purified metabolites using spectroscopic techniques
- Evaluation of the identified secondary metabolites for their antifungal, antibacterial, cytostatic and cytotoxic activities.
- Testing the effect of the antifungal endophytic strain extracts on the growth of the other endophytes in agar diffusion assays.
- Investigation of the metabolic profile and antifungal activity of cocultures formed of endophytic strains exerting antifungal activities in their pure cultures.

3. Results and discussion

3.1. Isolation of endophytes and cultivation

Samples of *B. pilosa* were collected near Cairo, Egypt. After surface sterilization of the fresh, healthy, aerial plant parts 11 endophytic fungal strains were isolated. To monitor the production of secondary metabolites of the isolates each strain was cultivated in four different culture media, a malt extract (M4), a caseine–flesh peptone (M5), a cornsteep (M25) and a dextrose–yeast (M26) medium, both as shaken and as stationary culture. Screening assays for antimicrobial activity were performed. Results of these screening assays showed that altogether 6 out of the 11 isolated strains showed antimicrobial activities. The strain that exerted the highest antimicrobial effects was strain number 20076003 which was later on identified as *Botryosphaeria rhodina* on the basis of ITS sequence.

3.2. Chromatographic fractionation of the extract of strain 1 (*Botryosphaeria rhodina*):

The extraction of the strain was carried out by mixing culture filtrate and mycelium together and then extracting with ethylacetate. When the ethylacetate extract obtained was tested for antimicrobial activity significant antibacterial and antifungal activities were observed for the strain in all culture media and especially for the stationary culture in medium M25 (Table 1). High antifungal activity against various test strains (*Sporobolomyces salmonicolor, Saccharomyces cerevisiae, Candida albicans, Penicillium notatum, Penicillium avellanea, and Aspergillus terreus*) was detected in agar diffusion assays. In addition a cytotoxic assay was performed on this extract against HeLa, HUVEC and K-562 cancer cell lines. Results revealed potent cytostatic activity against HUVEC and K-562 cell lines as well as strong cytotoxicity against HeLa cell lines (Table 2). Accordingly large scale reproduction of the strain (40 L) in medium M25 under the optimized culture conditions was carried out. The crude extract obtained (18 g) was liberated from lipophilic components (4.5 g) by extracting with hexane and was subjected to flash chromatographic separation on silica gel (using hexane: ethyl acetate/ 9:1), followed by open column chromatography with Sephadex LH-20 (eluted with MeOH). Activity-guided fractionation was performed by testing the resulting fractions against *Aspergillus terreus*, which proved to be the most sensitive test strain towards the crude extract (Table 1). The active fractions were subjected to further purification on open column chromatography and repeated preparative RP-HPLC using an acetonitrile/ water gradient. Active fractions contained botryorhodine A (**1**) and B (**2**) (Fig. 5), which are chemically related as based on retention time and UV spectra, and seemed to belong to a complex of four aromatic metabolites (compounds **1–4**).

Table 1: Antimicrobial activity[a] of the extract of *Botryosphaeria rhodina*

B. rhodina				
Microorganism	in M4	in M5	in M25	in M26
Sporobolomyces salmonicolor	29	23	32	23
Saccharomyces cerevisae	15	-	22	16
Candida albicans	16	13	24	17
Penicillium notatum	19	15	35	22
Penicillium avellanea	20	15	37	22
Aspergillus terreus	25	18	44	30
Bacillus subtilis	31	20	39	26
Escherichia coli	35	28	42	34
Staphylococcus aureus	32	24	39	29
Mycobacterium vaccae	37	22	50	41

a = measured in terms of the diameter of the inhibition zone in millimeters

Table 2. Antiproliferative (GI_{50}) and cytotoxic (CC_{50}) activities of the extract of *Botryosphaeria rhodina* in medium M25

Strain	Antiproliferation		Cytotoxicity
	Huvec (GI_{50} in µg mL^{-1})	K-562 (GI_{50} in µg mL^{-1})	HeLa (CC_{50} in µg mL^{-1})
B. rhodina	4.3	4.5	3.7

3.2.1. Structure elucidation of compounds 1-4 (botryorhodines A-D):

Compound **1** has a molecular formula of $C_{16}H_{12}O_6$ as indicated by HRESIMS and ^{13}C NMR data (Table 3). The ^{1}H NMR spectrum exhibited signals corresponding to two aromatic methyl groups (δ 2.26; 2.41 ppm), three aromatic protons (δ 6.47; 6.54; 6.59 ppm), one hydroxyl proton (δ 9.79 ppm) and one aldehyde proton (δ 10.57 ppm). The ^{13}C NMR spectrum revealed the presence of 16 carbons of which two were methyl groups (δ16.7; 21.4 ppm), one aldehyde carbonyl (δ 191.9 ppm) and one ester carbonyl group (δ 164.5 ppm). From HSQC and HMBC data (Fig 4) the presence of two aromatic phenyl groups was concluded. HMBC data indicated that the first ring contained a methyl group (δ 2.41 ppm), which was correlated with a methine carbon at δ 116.9 ppm (C-5) and an ester carbonyl carbon (C-7) at δ 164.5 ppm. Furthermore, the aldehyde moiety was correlated to the same carbon C-5 and to an OH-bonded carbon (C-4, δ 163.8 ppm). The second phenyl

group is substituted with two *meta* coupled protons at δ 6.54 ppm (H-3) and δ 6.47 ppm (H-10) as well as a methyl group at δ 16.7 ppm which was correlated with a methine carbon (C-10) at δ 114.2 ppm and two quaternary carbons (C-6) at δ 131.2 ppm and (C-5) at δ 141.2 ppm on the basis of HMBC correlations (Fig 4). The presence of another oxygen-bound carbon was deduced from the correlations observed for the proton at δ 6.54 ppm (H-3') with two quaternary carbons, C-5' at δ 141.2 ppm and C-4' at δ 144.0 ppm. This correlation together with a strong HMBC correlation between H-1' and C-5' and a COSY correlation between
H-1' and the methyl protons H-7' led to the complete deduction of the substitution pattern of ring b. This was furthermore supported by comparisons with previously reported NMR data [42-44]. Contrary to the downfield shift observed for the oxygen bonded carbons C-2, C-5' and C-4' an upfield shift was observed for C-1 (δ 111.5 ppm), thus suggesting its connection to a carbonyl carbon. Consequently, both phenyl groups are connected by a seven-membered ring containing an ether linkage and an ester bridge, revealing compound **1** (Fig 3) to be a new depsidone, for which the name botryorhodine A was proposed [45].

Compound **2** (Fig 3) was obtained as a second product with significant antifungal activity. From HRESIMS and ^{13}C NMR data (Table 3) the molecular formula $C_{17}H_{14}O_6$ was deduced, thus suggesting that **2** is a homologue of **1** with an additional methyl group. The ^{13}C NMR signal at δ 194.6 ppm and the ^{1}H NMR signal at δ 10.71 ppm attached to it on the basis of HSQC correlations confirmed the presence of the aldehyde function. Its proton was correlated with an OH-bearing quaternary carbon at δ 165.4 ppm and a methine carbon (C-5, δ 118.1 ppm) on the basis of HMBC correlations (Fig 4). This proton (H-5) is in turn correlated with its neighboring methyl carbon at δ 22.3 ppm, as well as a quaternary carbon connected to the ester carbonyl group (C-1) at δ 114.0 ppm on the basis of HMBC (Fig 4). The second aromatic ring bears two methyl groups, a hydroxyl group and a single proton, as deduced from the ^{13}C NMR, HSQC and HMBC correlations. One of the methyl groups (C-8') is correlated with the OH-bearing carbon (C-2', δ 155.0 ppm) and the quaternary carbon bound to an oxygen atom (C-4', δ 145.3 ppm). The protons of the second methyl group on the other hand are correlated with the methine aromatic carbon (C-1', δ 114.3 ppm), the quaternary carbon bound to the same methyl group (C-6', δ 128.3 ppm) and a carbon bound to an oxygen atom (C-5', δ 144.0 ppm). This information fully established the substitution pattern of **2** (Fig 3). By comparison of the deduced structure with literature data it was found that **2** is identical with a compound produced at first in the context of the total synthesis of the depsidone dechloropannarin, a lichen (*Psoroma sp*.) metabolite [46]. The structure of **2** was also proposed for a minor product in an extract of *Erioderma chilense* solely on the basis of

its chromatographic properties [47]. This is the first report of the isolation and spectral assignment (Table 3, 4) as well as antifungal (Table 5) and cytostatic activities (Table 6, Fig 5) of nordechloropannarin (botryorhodine B) [45].

Compound **3** (botryorhodine C, Fig 3) appeared also as a major metabolite of the extract. It showed no antifungal activity but exhibited antibacterial activity against *Bacillus subtilis* in agar diffusion assays (MIC = 1265.80 µM). Its molecular formula was determined as $C_{17}H_{16}O_6$ on the basis of HRESIMS and ^{13}C NMR data (Table 3). The spectral data of compound **3** (Table 3, 4) are similar to those of **1** indicating that both might have the same basic skeleton. However, the ^{13}C NMR spectrum lacks an aldehyde signal, but shows a methylene signal (δ 54.8 ppm, DEPT). The chemical shift suggested that this methylene is located in the periphery of a phenyl and is connected to a hydroxyl group. This was further supported by the HMBC correlations (Fig 4) between the methylenic protons and the carbons C-2 (δ 162.5 ppm), C-4 bearing an OH group at δ 163.0 ppm and the quaternary carbon (C-3) at δ 117.0 ppm. Compound **3** also differs from **1** in the additional methyl group at C-3', which is also present in **2** (Fig 3). The compound was found to be a new depsidone for which the name botryorhodine C was given [45].

Compound **4** (botryorhodine D**,** Fig 3), a minor product from the fraction of compound **3**, has a molecular formula of $C_{16}H_{14}O_6$ as indicated by HRESIMS and ^{13}C NMR. The ^{1}H NMR and ^{13}C NMR spectral data (Tables 3, 4) showed close similarity to those of compound **3** suggesting that both compounds have the same basic framework. In contrast to compound **3** the ^{1}H NMR (Table 4) shows only two methyl proton signals (δ 2.37, 2.43 ppm) but three aromatic proton signals of which one appeared at δ 6.60 ppm and two at δ 6.44 ppm. On the basis of HMBC correlations (Fig 3) it was confirmed that the C-8 methyl group of **3** is lacking as in the b-ring of **1**. These spectral data identified **4** as a new depsidone for which the name botryorhodine D was suggested (Fig 3) [45].

Fig 3. Chemical structures of botryorhodines A-D

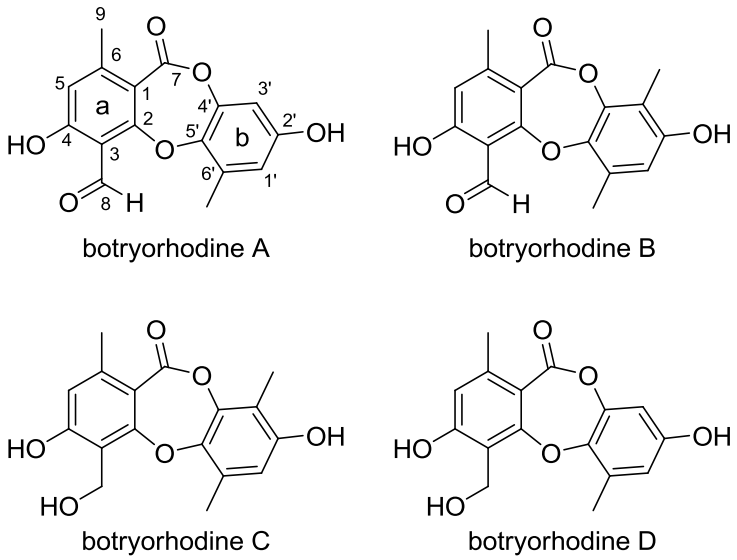

Fig 4. HMBC correlations of botryorhodines A-D

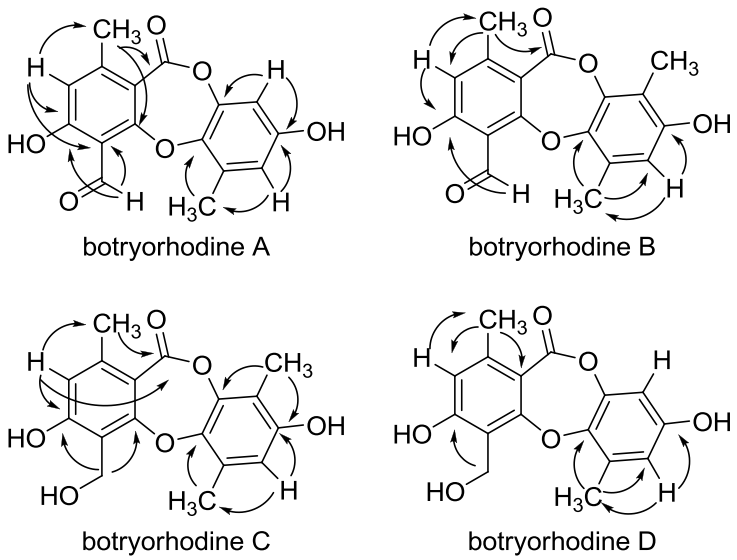

Table 3. ^{13}C NMR data for botryorhodines A-D

Position	δ ^{13}C			
	botryorhodine A	botryorhodine B	botryorhodine C	botryorhodine D
1	111.5, qC	114.0, qC	113.6, qC	113.7, qC
2	161.8, qC	163.4, qC	162.5, qC	162.5, qC
3	112.3, qC	112.1, qC	117.0, qC	117.0, qC
4	163.8, qC	165.4, qC	163.0, qC	162.8, qC
5	116.9, CH	118.1, CH	116.2, CH	116.2, CH
6	152.0, qC	155.6, qC	145.9, qC	146.1, qC
7	164.5, qC	166.4, qC	166.0, qC	165.7, qC
8	191.9, CH	194.6, CH	54.8, CH_2	54.7, CH_2
9	21.4, CH_3	22.3, CH_3	21.4, CH_3	21.4, CH_3
1′	114.2, CH	114.3, CH	114.1, CH	115.2, CH
2′	155.1, qC	155.0, qC	153.9, qC	155.9, qC
3′	105.3, CH	116.1, qC	115.3, qC	105.9, CH
4′	144.0, qC	145.3, qC	144.7, qC	145.8, qC
5′	141.2, qC	144.0, qC	144.1, qC	143.7, qC
6′	131.2, qC	128.3, qC	128.6, qC	132.8, qC
7′	16.7, CH_3	17.1, CH_3	16.9, CH_3	17.2, CH_3
8′		9.2, CH_3	9.2, CH_3	

3.2.1.1. Bioactivity of botryorhodines A-D

One may speculate on the role of these compounds in the microbial interaction. Depsidones have been reported to act as photoprotectors limiting the deleterious effects of UV through their antioxidant activity [48-49]. Furthermore, they may modulate microbial populations living within or attacking the plant. Thus the antimicrobial efficacy of compounds **1–4** against test strains *A. terreus* and *B. subtilis* were performed using nystatin as a positive control for the antifungal activity, ciprofloxacin for the antibacterial activity and methanol as a negative control. Compounds **1** and **2** are active against both microorganisms while **3** and **4** do not have antifungal activity (Table 5) but show weak antibacterial activity (MIC 400 µg mL^{-1} for **3** and 475 µg mL^{-1} for **4**). The minimum inhibitory concentration of compound **1** against *A. terreus* was found to be 7.81 µg mL^{-1}, while the reference nystatin has a MIC-value of 15.63 µg mL^{-1}. Compound **2** also showed antifungal activity against *A. terreus* (MIC 49.70 µM).

Table 4. ^{1}H NMR data of botryorhodines A-D

Position	δ ^{1}H (*J* in Hz)			
	botryorhodine A	botryorhodine B	botryorhodine C	botryorhodine D
1				
2				
3				
4				
5	6.59, *s*	6.73, *s*	6.59, *s*	6.60, *s*
6				
7				
8	10.57, *s*	10.71, *s*	4.95, *s*	4.94, *s*
9	2.41, *s*	2.48, *s*	2.38, *s*	2.37, *s*
1′	6.47, *d* (3.0)	6.46, *s*	6.43, *s*	6.44, *s*
2′				
3′	6.54, *d* (3.0)			6.44, *s*
4′				
5′				
6′				
7′	2.26, *s*	2.30, *s*	2.39, *s*	2.43, *s*
8′		2.19, *s*	2.12, *s*	
OH	9.79, *s*			

The finding that **3** and **4,** both lacking the aldehyde group of **1** and **2**, showed no antifungal activity suggests the possible importance of this functional group for antifungal activity. To evaluate the cytotoxicity and antiproliferative effects of **1** and **2** they were subjected to cytotoxicity assays against HeLa, K-562 and HUVEC cell lines (Table 6, Fig 8). Compounds **1** and **2** exhibited potent antiproliferative activity against K-562 and HUVEC (Table 6). In both assays, the two compounds showed significant antiproliferative activity over a wide concentration range with **2** covering the wider range. As for the cytotoxic assay against HeLa cancer cell line CC_{50} values of 29.09 μg mL^{-1} and 11.43 μg mL^{-1} were obtained for compounds **1** and **2**, respectively. Compounds **3** and **4** on the contrary did not show any antiproliferative activity. The observed antifungal activity of botryorhodine A (**1**) and B (**2**) is intriguing as endophytes may be producing bioactive substances that may be involved in a

host–endophyte relationship and can have the capacity to control plant pathogens [39]. To test whether the endophyte metabolites have the potential to protect the host plant from fungal infections, they were also tested against the phytopathogen *Fusarium oxysporum*. Indeed, **1** and **2** were active with a MIC of 57.50 µg mL^{-1} and 75.00 µg mL^{-1} observed for **1** and **2** respectively. Compounds **3** and **4** on the contrary were inactive (Table 5).

Table 5. Antifungal activities of botryorhodines A-D

Compound	botryorhodine A	botryorhodine B	botryorhodine C	botryorhodine D
MIC (µg mL^{-1}) against *A. terreus*	7.81	15.63	0	0
MIC (µg mL^{-1}) against *F. oxysporum*	57.50	75.00	0	0

Table 6: Antiproliferative (GI_{50}) and cytotoxic (CC_{50}) activities of botryorhodines A and B

Antiproliferative activity			Cytotoxicity
Compound	GI_{50} (HUVEC)	GI_{50} (K-562)	CC_{50} (HeLa)
botryorhodine A	0.50 µg mL^{-1}	0.25 µg mL^{-1}	29.09 µg mL^{-1}
botryorhidine B	0.02 µg mL^{-1}	0.001 µg mL^{-1}	11.43 µg mL^{-1}

Fig 5. Antiproliferative and cytotoxic activities of botryorhodines A and B against HUVEC, K-562 and HeLa cancer cell lines

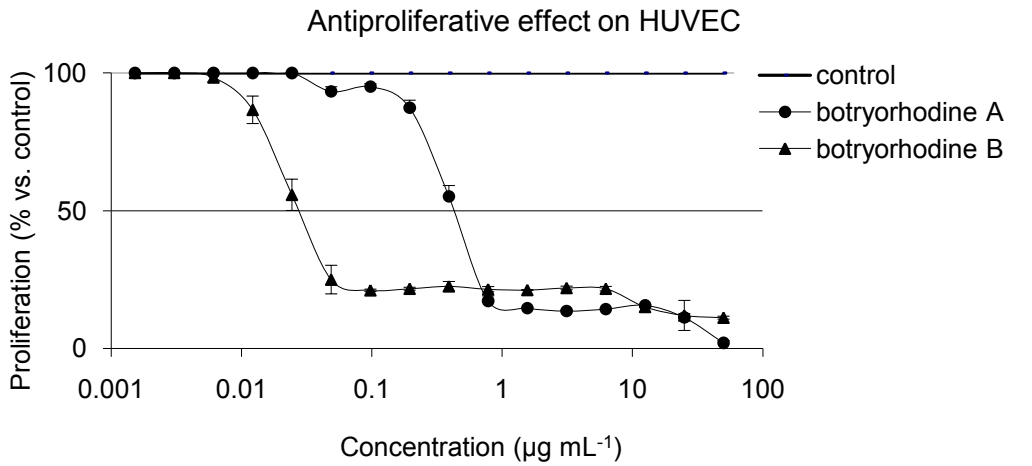

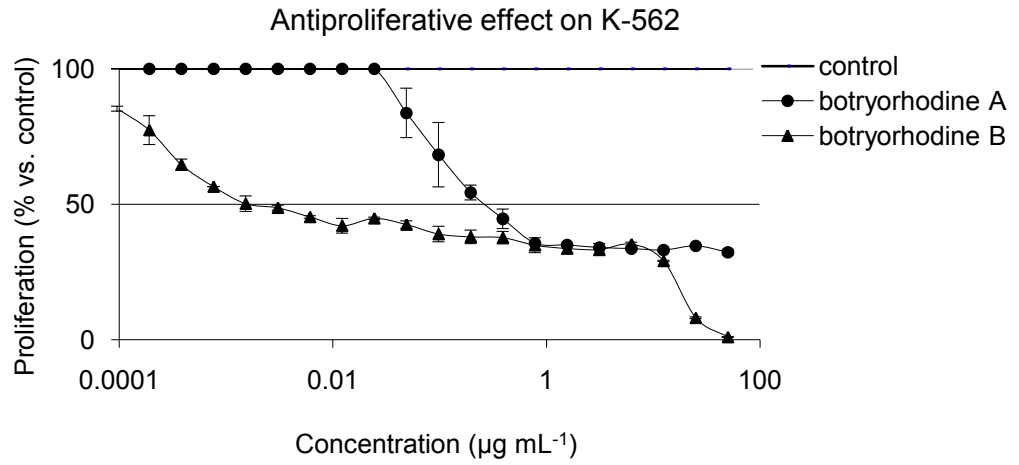

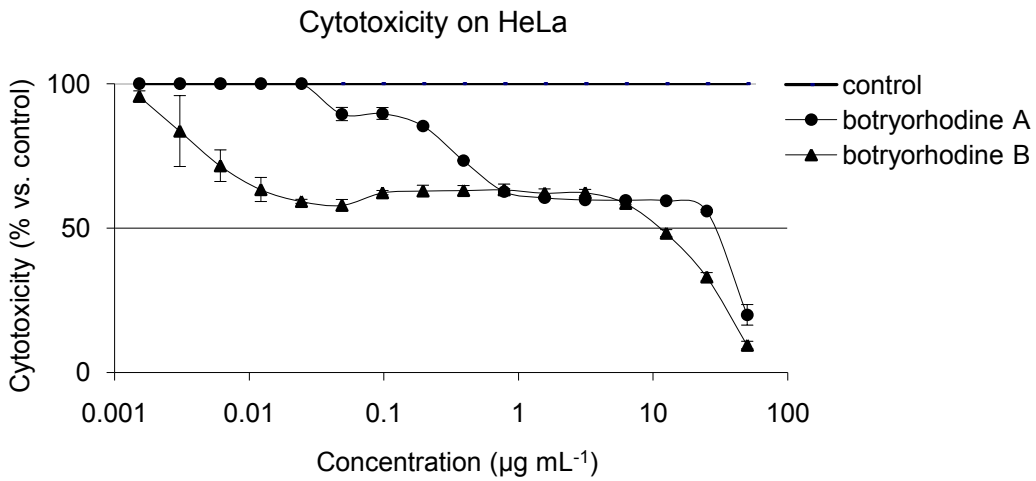

3.2.2. Structure elucidation of compound 5 (botryorhodine E):

The compound was isolated from the fraction containing the two antifungal compounds botryorhodines A (**1**) and B (**2**). The HRESI-MS exhibited a strong peak at *m/z* 275.1050 $[M+H]^+$ (calcd 275.1054) indicating a molecular formula of $C_{14}H_{14}O_5$ for the compound. The ^{1}H-NMR spectrum of the compound showed two proton singlets each representing a methyl group at δ 2.2 and 1.8 ppm, three proton signals for three hydroxyl groups and one aldehyde proton signal at δ 10.4 ppm. Furthermore four aromatic proton signals were observed with two *meta* coupled doublets at δ 6.14 and 6.25 ppm. The number of carbons suggested by the HRESIMS was confirmed by the ^{13}C-NMR spectrum which also revealed the presence of two methyl groups and one aldehydic functional group represented by a carbon signal at δ 193.6 ppm. From the COSY and HMBC correlations it was concluded that the compound consisted of two aromatic rings. The first ring is a tetrasubstituted aromatic ring while the second ring is a trisubstituted one. The substitution pattern of the first ring was deduced from the HMBC correlations (Fig 7, Table 7) observed between the aldehydic proton and the adjacent hydroxylated quaternary carbon appearing at δ 162.4 ppm (C-2'). The aromatic proton at δ 6.37 ppm (H-5') is in turn correlated with the second aromatic primary carbon of this ring, an adjacent methyl carbon C-7' (δ 22.3 ppm) and the quaternary carbons C-1' and C-2'. As for the second ring correlations were observed between the aromatic proton at δ 6.14 ppm (H-6) and the quaternary carbon at δ 155.1 ppm (C-5) bearing a hydroxyl group, the methyl carbon C-7 (δ 15.9 ppm) and the aromatic primary carbon at δ 101.8 ppm (C-4) whose proton is *meta* coupled with this proton (*J*= 2.5 *Hz*). The methyl protons on the other hand showed HMBC correlations (Fig 7) with both aromatic primary carbons of this ring as well as with the quaternary carbon at δ 150.0 ppm (C-2). Since an oxygen atom was still missing according to the suggested molecular formula and the chemical shifts of the quaternary carbons C-6' and C-2 were δ 150.3 and 150.0 ppm respectively, both rings were connected with each other via an ether bond. Thus the compound appeared to be a new diphenylether (Fig 6) for which the name botryorhodine E has been suggested.

To evaluate the antimicrobial activity of the compound it was tested against the fungus *Penicillium notatum* and the bacterium *Bacillus subtilis*, where it showed weak antifungal and weak antibacterial activities. It was also tested for cytotoxicity where it exerted antiproliferative effects against HUVEC cell line with a GI_{50} value of 17 µg mL^{-1} and K-562 cell line with a GI_{50} value of 11 µg mL^{-1} as well as cytotoxicity against Hela cancer cell line with a CC_{50} value of 12 µg mL^{-1} (Fig 8).

Previously, diphenyl ether derivatives have been reported as secondary metabolites of fungi belonging to the genera *Pestalotiopsis* [50], *Xylaria* [51], *Phoma* and *Oospora* [52].

Some diphenyl ether analogues were reported to inhibit farnesyl-protein transferase [52], endothelin binding [53], and vascular endothelial growth factor (VEGF)-induced tube formation of human umbilical vein endothelial cells (HUVECs) [54]. Diphenyl ethers (DPEs) are also an important class of herbicides that strongly inhibit the protoporphyrinogen oxidase enzyme which is a key enzyme in the chlorophyll/heme biosynthetic pathway. This enzyme catalyzes the oxidation of protoporphyrinogen IX to protoporphyrin IX (PPIX) [1]. Herbicides are the most widely used class of pesticides, accounting for more than 60% of all pesticides applied in agriculture [2]. Recently a new member of bioactive diphenyl ethers, neoplaether (Fig 6) has been isolated from the culture of *Neoplaconema napellum* IFB-E016, an endophytic fungus residing in the leaves of *Hopea hainanensis*. It has been reported to exert cytotoxic activity against the human nasopharyngeal epidermoid tumor KB cell line, with an IC_{50} value (13.0 mg mL^{-1}) comparable to that of 5-fluorouracil (2.5 mg mL^{-1}) co-assayed as a reference material. Furthermore, in vitro antifungal activity was examined, using *A. niger, C. albicans* and *T. rubrum* as test organisms, and neoplaether showed obvious activity against *C. albicans* with its MIC value of 6.2 mg mL^{-1} (that of amphotericin co-assayed as positive control against *C. albicans* was 1.5 mg mL^{-1}), whereas no growth inhibition to *A. niger* and *T. rubrum* could be detected when it was tested at 100 mg mL^{-1}.

Fig 6.Chemical structure of botryorhodine E and neoplaether

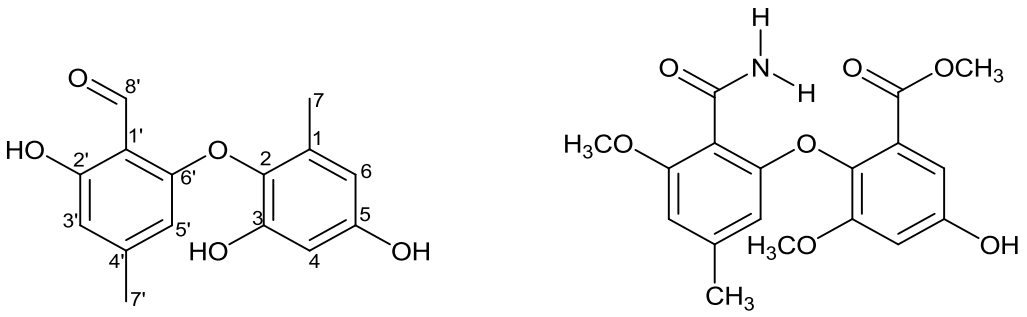

Fig 7. Key HMBC correlations of botryorhodine E

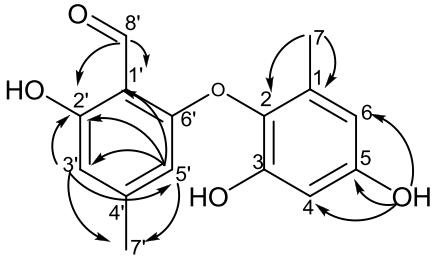

Table 7. NMR spectroscopic data (150MHz, DMSO-d_6) of botryorhodine E

Position	δ ^{13}C	δ ^{1}H (*J* in *Hz*)	HMBC
1	131.7, qC		
2	150.0, qC		
3	161.2, qC		
4	101.8, CH	6.25, *d* (2,7)	1, 2, 5, 6
5	155.1, qC		
6	107.8, CH	6.14, *d* (2.7)	1, 4, 5, 7
7	15.9, CH3	1.82, *s*	1, 2, 4, 6
1′	108.5, qC		
2′	162.4, qC		
3′	104.2, CH	5.84, *s*	1’, 2’, 5’, 7’, 8’
4′	131.8, qC		
5′	110.0, CH	6.37, *s*	1’, 2’, 3’, 7’
6′	150.3, qC		
7′	22.3, CH3	2.22, *s*	3’, 5’, 6’
8′	193.6, CHO	10.40, *s*	1’, 2’, 5’
3-OH		9.37, *s*	1, 2, 4
5-OH		9.24, *s*	4, 5, 6
2′-OH		11.75, *s*	1’, 2’, 5’, 6’

Fig 8. Antiproliferative and cytotoxic activity of botryorhodine E against HUVEC, K-562 and HeLa cell lines

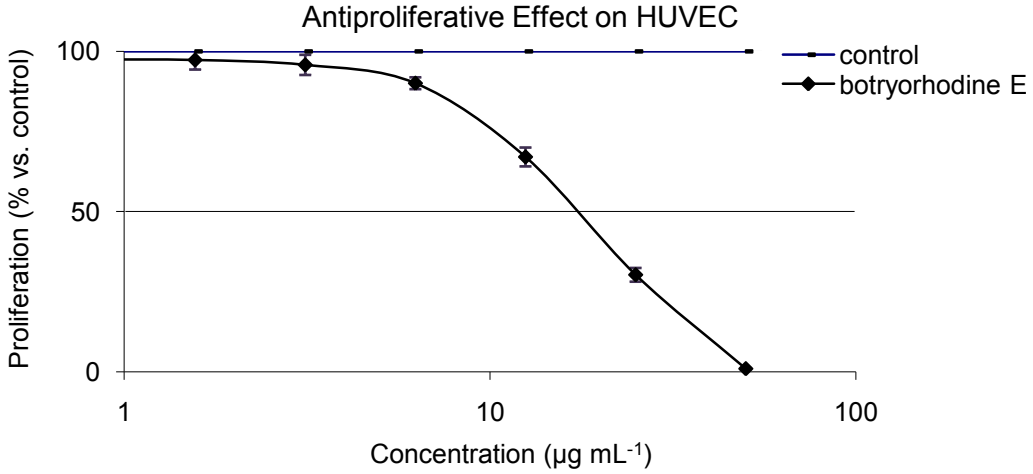

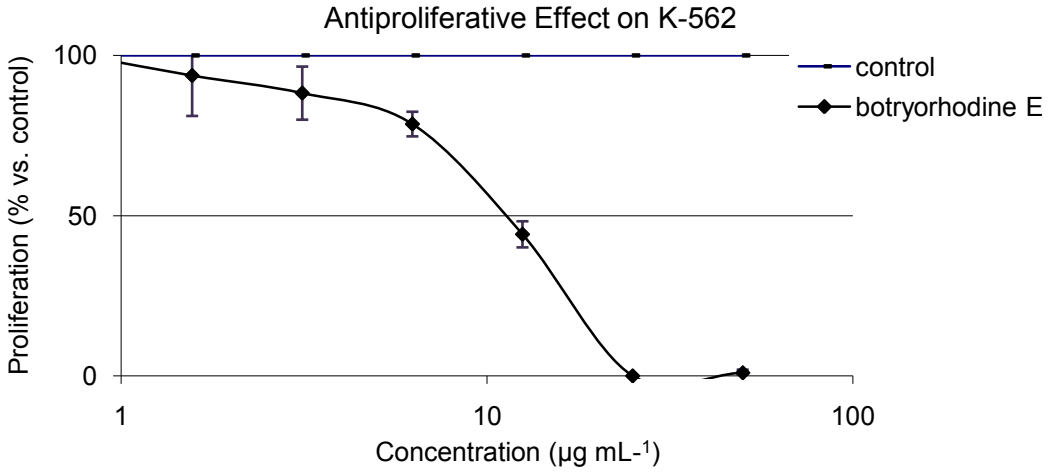

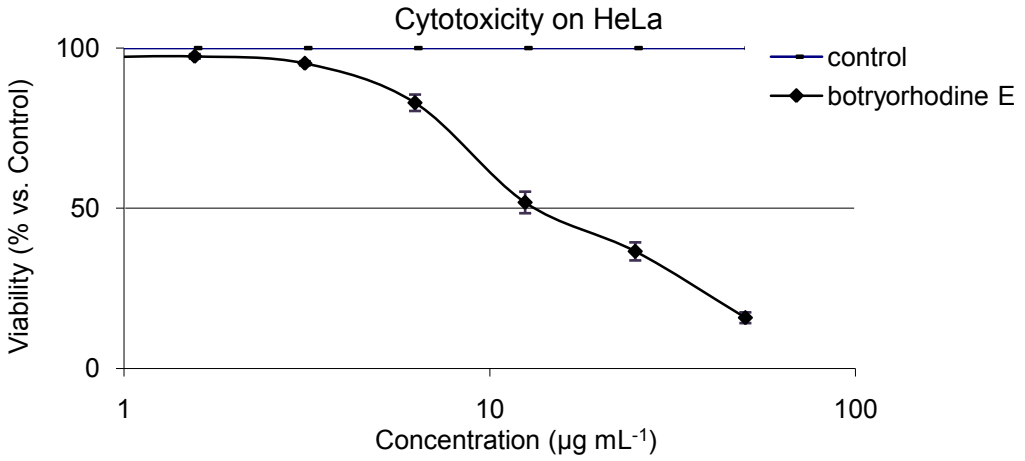

3.2.3. Structure elucidation of compound 6 (preussomerin C):

A strong peak at m/z 395.0850 $[M-H]^-$ for $C_{21}H_{17}O_8$ was suggested for the compound by HRESIMS analysis indicating 13 degrees of unsaturation. The compound showed characteristic bis-spirobisnaphthalene NMR signals due to the presence of an oxygenated tetrasubstituted aromatic ring, one oxygenated trisubstituted aromatic ring, a phenolic hydroxyl group and two spiroketal quaternary carbons. In addition the ^{1}H and ^{13}C NMR data (Table 8) showed signals for two epoxides bearing methines (H-2 and H-3), one oxygenated methane and one methylene. The ^{1}H-^{1}H COSY spectrum in acetone-d6 showed correlations of H-1 with H-2; H-2 with H-1 and H-3 as well as H-2' with H-3' which indicated the presence of two isolated proton spin systems corresponding to C1-C3 and C1'-C3' subunits of the compound. In the HMBC spectrum correlations were observed between H-1 and C-6, C-9, C-3, C-5 as well as between H-2 and C-10, C-9, C-3, C-4 which confirmed that the C1-C3

subunit is attached to C-10 and C-4. On the other hand correlations were observed between H-2' and C-1', C-10', C-3' and C-4' as well as H-3' and C-1', C-5', C-10' and C-4' which confirmed the attachment of the C1'-C3 'subunit to C5'-C10'.

This spectral data led to the deduction of the structure of this compound which was proven to be preussomerin C (Fig 9) by comparison with literature data. The absolute configurations at C-1, C-2, C-3, C-1' and C-3' were presumed to be the same as for the known compound on the basis of identical NMR data of the corresponding structural parts [55].

The general characteristics of this class of compounds include two unsaturated decalin units connected via 3 oxygen bridges through two spiroketal carbons located in each of the upper and lower decaline units. The stereochemistry was previously determined on the basis of crystallography and chemical degradation experiments performed on preussomerin A (Fig 9). It has been found that the bis-spirobisnaphthalene unit is essential for the high activity because all tested bis-spirobisnaphthalene metabolites were reported to be of more potent nematicidal activity than naphthalenone metabolites [56].

Preussomerin C has been reported previously to possess antibacterial, antifungal, antiplasmoidal as well as weak nematicidal activity against a plant parasitic and fungal feeding nematode that causes profound destruction of pine forests especially in Asian countries. Furthermore it has been found to possess ras farnesyl protein transferase inhibitory activities [56]. In another study other naphthoquinone spiroketals have been isolated from an endophytic fungus *Edenia gomezpompae* isolated from the leaves of *Callicarpa acuminata (Verbenaceae)* in Mexico [57]. These compounds exerted allelochemical activity by showing antifungal activity against several phytopathogens as well as growth inhibitory activity against other endophytic fungi isolated from the same plant [57].

Fig 9. Chemical structures of preussomerins C and A

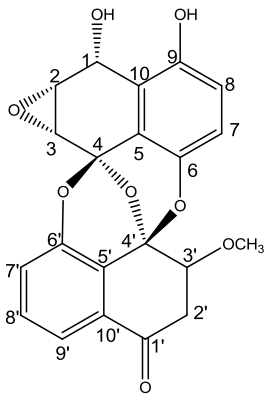

preussomerin C

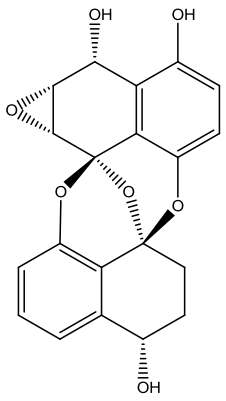

preussomerin A

Table 8. NMR data (150MHz, acetone-d_6) of preussomerin C

Position	δ ^{13}C	δ ^{1}H (*J* in *Hz*)	HMBC
1	69.3, CH	5.63, *s*	3, 4, 6, 7, 9
2	53.2, CH	3.91, *dd* (4.2; 0.5)	1, 3, 4, 9, 10
3	53.0, CH	4.03, *d* (4.2)	1, 2, 4, 5, 6
4	96.3, qC		
5	114.3, qC		
6	143.4, qC		
7	117.4, CH	6.75, *d* (9.0)	1, 4, 5, 6, 9, 10
8	120.7, CH	6.75, *d* (9.2)	1, 4, 5, 6, 9, 10
9	152.3, qC		
10	117.3, qC		
1’	193.8, qC		
2’a	41.5, CH_2	2.98, *dd* (18.1; 2.7)	1’, 3’, 4’, 10’
2’b		3.35, *dd* (18.1; 3.2)	1’, 3’, 4’, 10’
3’	80.3, CH_2	4.32, *dd* (2.9; 2.9)	1’, 2’, 3’-OMe, 4’, 5’, 6’, 10’
4’	94.9, CH		
5’	121.6, qC		
6’	151.8, qC		
7’	122.0, qC	7.12, *dd* (8.1; 1.0)	4’, 6’, 9’, 10’
8’	131.6, CH	7.43, *dd* (7.8; 7.8)	1’, 5’, 6’, 7’, 10’
9’	120.3, CH	7.53, *dd* (7.6; 1.0)	1’, 4’, 5’, 6’, 7’, 8’
10’	132.0, CH		
3’-OMe	59.5, OCH_3	3.91, s	

A cytotoxic assay was conducted on preussomerin C to test its antiproliferative effect on HUVEC and K-562 and its cytotoxicity on HeLa cancer cell lines. Results showed moderate cytostatic activity against HUVEC and K-562 cell lines with GI_{50} values of 9.0 and 12.4 µg mL^{-1} respectively as well as moderate cytotoxicity against HeLa cell line with a CC_{50} value of 18.7 µg mL^{-1} (Fig 10).

Fig 10. Antiproliferative and cytotoxic activity activity of preussomerin C against HUVEC, K-562 and HeLa cancer cell lines

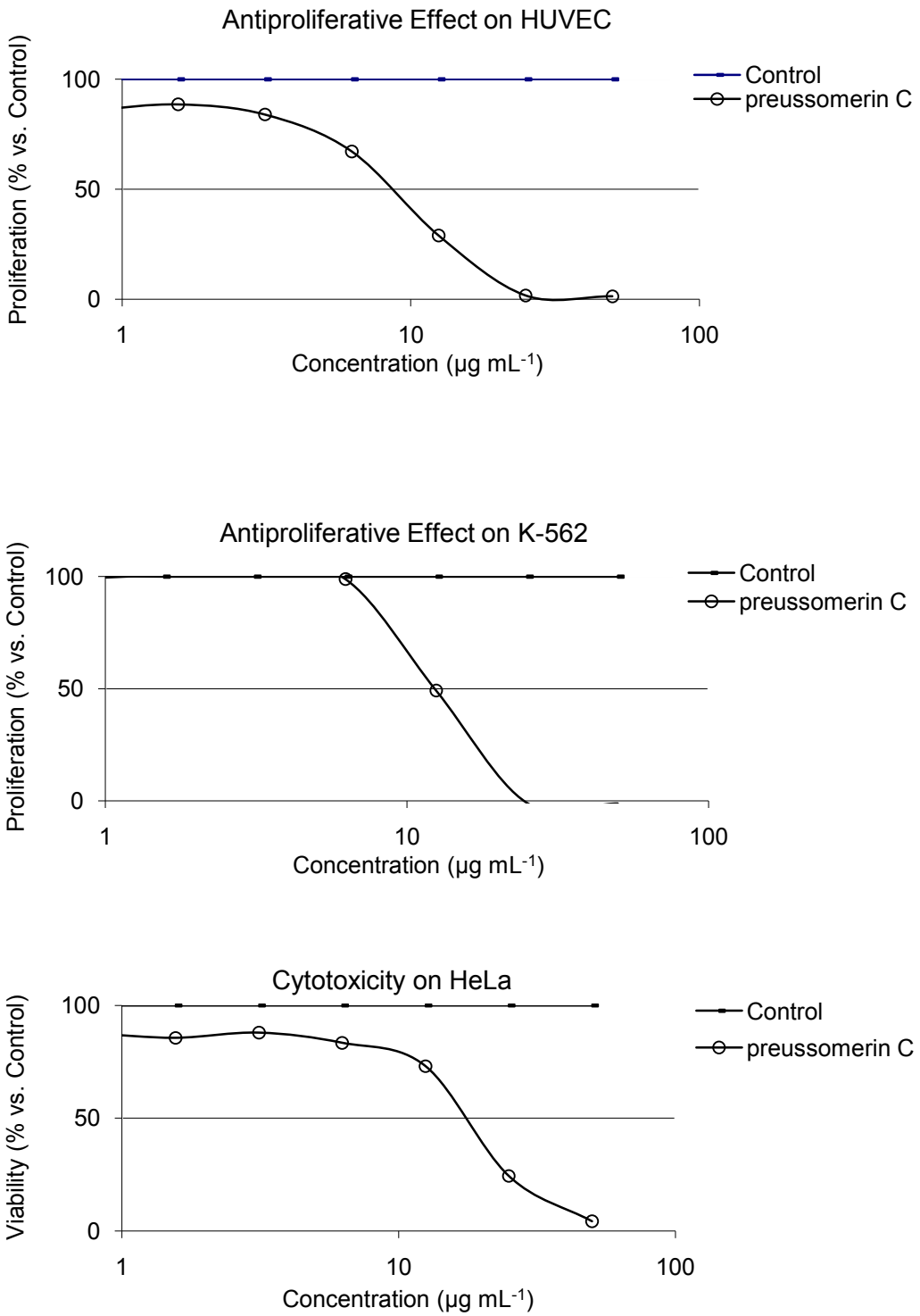

3.2.4. Identification of compound 7 (4-hydroxy mellein):

Furthermore hydroxymellein (Fig 11) was identified as a secondary metabolite of this endophytic fungal strain by dereplication with a database and comparison with an authentic sample. A molecular formula of $C_{10}H_{10}O_4$ (m/z 195.1549 $[M+H]^+$) was determined for the compound by HRESI-MS. Measurement of the optical activity and comparison with literature data identified the isolated isomer as 3*R*, 4*R*-(-)-4-hydroxymellein. Hydroxymellein is a 3, 4 dihydroisocoumarin belonging to the family of pentaketides as well as related compounds with different substitution patterns on the phenyl moiety [58]. Because of its relationship with the ochratoxins, a group of potent mycotoxins reported for the first time from *Aspergillus ochraceus* but also produced by other genera including *Penicillium,* it is also named ochracin [59]. Hydroxymellein was previously isolated from many fungal species. The detection of hydroxymellein is not surprising since it has been reported to be a phytotoxic compound previously isolated from another *Botryosphaeria* strain called *Botryosphaeria obtuse* [60] as well as from the fungus *Sphaeropsis sapinea* which is pathogenic to the plant *Pinus radiata* [61] and also from *B. rhodina* before [62].

A moderate antifungal activity in agar diffusion assays against *Ustilago violacea* was reported [63]. The reported isolation of mellein and 4-hydroxymellein from unhealthy samples of the upper part of declining pine (*Pinus radiata*) plants, with observed symptoms of foliage chlorosis, drying of needles and cankers on branches gives an indication on the phytotoxic effect of these metabolites on the plant. The detection of 4-hydroxymellein is quite interesting as it indicates the possible pathogenic effect *B. rhodina* might exert on its host plant. It is assumable that the endophyte *B. rhodina* which is known of being a phytopathogen in many plants [64] was a latent pathogen at the time it was isolated from its healthy host plant *B. pilosa.*

Fig 11. Chemical structure of 4-hydroxymellein

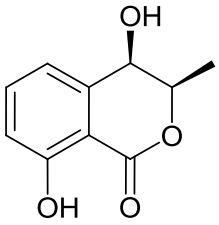

3*R*, 4*R*-(-)-4-hydroxymellein

3.2.5. Identification of compound 8 (indole-β-carboxylic acid):

Indole-β-carboxylic acid was identified as an endophyte metabolite in the extract of its pure culture (by comparison with an authentic sample). Like the phytohormone indole acetic acid compound **5** (Fig 12) belongs to the plant auxins, which are responsible for growth stimulation and elongation of plants. It has been previously reported that endophyte-infected plants often grow faster than non-infected ones [65-66]. This effect is either due to the endophytes production of phytohormones such as indole-3-acetic acid, cytokines and other plant growth promoting substances and/or owing to the fact that endophytes could have enhanced the host's uptake of nutritional elements such as nitrogen and phosphorus [13]. Thus, the one meter height often observed for *B. pilosa* [67] could be referred at least partly to the production of indole-β-carboxylic acid by its endophyte.

Fig 12. Chemical structure of indole-β-carboxylic acid

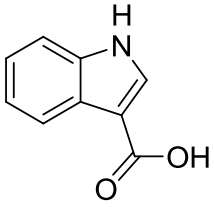

3.2.6. Discussing the investigated metabolic profile of *B. rhodina*:

Botryosphaeria rhodina (also known as *Lasiodiplodia theobromae*) is a multiinfectious microorganism that causes considerable crop damage, particularly to tropical fruits. It spoils many farm products in tropical regions and is one of the main pathogens responsible for the decay of fruits [64]. Therefore, the search for the toxins involved in this decay has been the focus of various studies and resulted in the identification of the toxin (3*S*, 4*R*)-3-carboxy-2-methyleneheptan-4-olide as well as decumbic acid from the culture filtrate of *L. theobromae* isolated from rotted mango branches in Miyako islands, Okinawa, Japan [64]. In addition, the macrophorins E, F and G were isolated from *B. berengeriana* and showed potent antifungal and antibacterial activity against phytopathogenic fungi as well as cytotoxic effects [68].

Botryorhodines A-D (**1–4**) belong to the group of depsidones, which are typically found in lichens [69-72]. Only a few depsidones have been isolated from non-lichen sources, such as auranticins A and B from the mangrove fungal isolate *Preussia aurantiaca* [73], emeguisins (Fig 13) from the ascomycete *Emericella unguis* [44] and the depsidones garcinisidone B–F (Fig 13) from two species of *Garcinia* plants, *Garcinia neglecta* and *Garcinia puat* [74-75]. Only recently, depsidones from endophytic fungi have been reported: excelsione (Fig 13)

from an endophytic fungus from the New Zealand endemic tree *Knightia excelsa* [76] and the depsidones from the endophytic fungus BCC 8616 isolated from a leaf of the Hala-Bala evergreen forest in Thailand [44]. It was previously reported that lichen metabolites exert a variety of biological actions including antibiotic, antimycobacterial, antiviral, anti-inflammatory, and analgesic, antipyretic, antiproliferative and cytotoxic effects [77]. Although various pharmacologically relevant activities of lichen metabolites have been recognized, their therapeutic potential has not yet been fully explored. An improved access to depsidones may aid in identifying new leads with therapeutic potential [77].

By producing three antifungal and three antibacterial compounds this endophytic fungus thus provides broad spectrum antimicrobial activity to protect itself from competing invaders and/or the plant from phytopathogens. This is in agreement with previous reports of suppressed pathogenic attack, removed contaminants and promoted plant growth and yield by endophytic fungi [78]. The identification of the auxin indole carboxylic acid as a major metabolite of the strain supports these suggestions since it is most propably involved in stimulated growth of the host plant whose height can reach a length of one meter [67]. Moreover, the detection of the phytotoxin 4-hydroxymellein together with the pathogenic effect previously reported for *B. rhodina* [79] suggest that this endophyte might be a latent pathogen since no symptoms of diseases were observed on the plant at the time of collection.

Fig 13. Chemical structures of depsidones from non-lichen sources

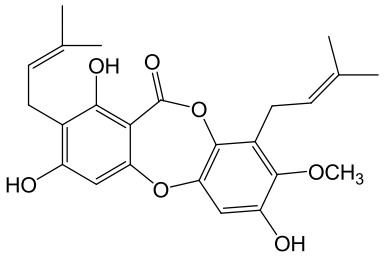

garcinisidone A

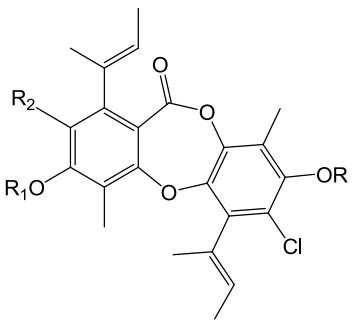

emeguisin A: R= H; R_1= H; R_2= H
emeguisin B: R= H; R_1= CH_3; R_2= H
emeguisin C: R= CH_3; R_1= H; R_2= Cl

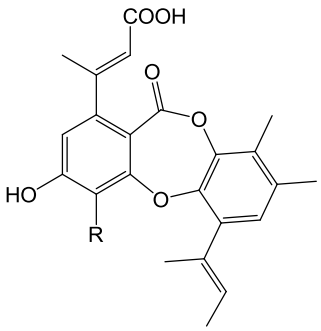

auranticin A: R= CH_2OH
auranticin B: R= COH

3.3. Strain 2: *Aspergillus neoniger*

The second strain selected for investigation of its metabolic content was strain 20076001 which was identified as a new *Aspergillus neoniger* strain by ITS sequence comparison. A cytotoxic assay was performed on the crude extract and revealed potent cytotoxicity (Table 9) for the strain against HeLa cell lines (CC_{50} value of 2.7 µg mL^{-1}) as well as cytostatic activity against HUVEC and K-562 cell lines (GI_{50} values of 3.5 and 3.2 µg mL^{-1} respectively). Thus the strain was selected for large scale fermentation (40 L) under the optimized growth conditions (stationary culture in medium M5) and afterwards it was extracted with ethyl acetate and yielded an extract with a dry weight of 13 g which was defatted with n-hexane to give a final extract of 9 g. This methanolic extract was exposed to column chromatographic fractionation using hexane: ethyl acetate (9:1) and then polarity was gradually increased till 100 % ethyl acetate. The obtained fractions were spotted and visualized using thin layer chromatography and the fractions exhibiting similar chromatographic behavior were combined to give a total number of 14 main fractions. These were subjected to antimicrobial activity tests in agar diffusion assays and the results obtained showed antimicrobial activity for fractions F2, F3, F5 and F15 and only partial activity for F9. Therefore further purification was carried out on fractions F2, F3, F5 and F15 on Sephadex LH-20 followed by preparative column chromatography using reversed phase silica and a solvent mixture of acetonitrile and water. These purifications resulted in the isolation of six pure compounds as well as the phytohormone indole carboxylic acid.

Table 9. Antiproliferative and cytotoxic activities of the extract of *Aspergillus neoniger* in medium M5

	Antiproliferative Effect		Cytotoxicity
Strain	HUVEC GI_{50} [µg mL^{-1}]	K-562 GI_{50} [µg mL^{-1}]	HeLa CC_{50} [µg mL^{-1}]
A. neoniger	3.5	3.2	2.7

3.3.1. Structure elucidation of compounds 9-12:

A strong peak at *m/z* 557.1545 $[M+H]^+$ for a molecular formula of $C_{31}H_{24}O_{10}$ was deduced from HRESIMS for compound **9**. The ^{1}H-NMR spectrum showed signals for six aromatic protons, two methyls and three methoxy protons. In addition two hydroxyl proton signals were represented by signals at δ 14.9 and 15.1 ppm. Their downfield shift suggests their chelation with neighbouring carbonyl functional groups. These two carbonyl functions were represented by a carbon signal at δ 183.9 ppm (C-4) in the ^{13}C-NMR spectrum. The ^{13}C-NMR spectrum showed 31 carbon signals and together with the DEPT spectrum the presence of

six primary carbons, two methyl groups and three methoxy groups was confirmed. The NMR spectra and the UV spectrum indicated that this compound was a naphthopyrone dimer. In the first subunit of the structure correlations were observed between the two *meta* coupled protons at δ 6.1 ppm (H-9') and 6.6 ppm (H-7') as well as between each of them and the quaternary carbon at δ 106.6 ppm (C-10') positioned at the junction of the two phenyl rings of the naphthyl moiety. The only proton of the pyrone ring appearing at δ 6.21 ppm (H-3') was correlated with the neighbouring methylenic carbon (δ 20.1 ppm) and its adjacent quaternary carbon at δ 168.4 ppm (C-2').

As for the second part of the structure HMBC correlations were observed between the hydroxyl proton at δ 14.9 ppm and C-9', C-8' and C-5'a. In addition correlations were also found between the second hydroxyl proton at δ 15.1 ppm and C-5', C-5'a and C-4'a. The only proton (H-3) of the pyrone ring was like in the first subunit correlated with the neighbouring methyl carbon at δ 20.2 ppm and C-2'.

Furthermore the aromatic proton at δ 7.1 ppm (H-9') was correlated with C-7', C-5'a, C-6' and C-9'. The second aromatic proton (H-10') of this naphthyl ring moiety was in turn correlated with C-4'a, C-4', C-10'a and C-5'a. From the chemical shifts and HMBC correlations (Table 10, 11) observed for this compound it was concluded that it was composed of two linear naphthopyrone moieties connected with each other (Fig 14). By comparison of the obtained structure and NMR data with literature it was found to be dianhydroaurasperone C which has been previously isolated from *Aspergillus tubingensis* isolated from the rhizosphere of the Sonoran desert plant *Fallugia paradoxa* [80].

Compound **10** has the same mass and molecular formula of compound **1** as determined by the HRESIMS. The UV absorption spectrum in methanol and the NMR data (Table 10, 11) were very similar to those of compound **1** suggesting the presence of a naphthopyrone. The ^{1}H NMR spectrum showed two methyl proton signals at δ 2.1 and 2.4 ppm as well as three singlets for three methoxy proton signals at δ 3.6, 3.9 and 3.3 ppm. Furthermore six aromatic proton signals were observed at δ 6.15, 6.18, 6.2, 6.5, 7.1 and 7.2 ppm. These observations were furthermore supported by the DEPT spectrum which confirmed the presence of five tertiary carbons at δ 55.0, 56.1, 61.4, 20.1, 20.2 ppm and six primary carbons at δ 96.7, 106.6, 106.5, 96.4, 105.2 and 100.3 ppm.

In addition the presence of two due to chelation downfield shifted hydroxyl protons was indicated by the appearance of two singlet proton signals at δ 14.9 and 15.1 ppm. HMBC correlations were observed between (H-7) at δ 6.5 ppm and C-5a as well as between (H-9) at δ 7.1 ppm and C-5a, C-10 and C-6. The naphthalene moiety was furthermore confirmed by

HMBC correlations between the hydroxyl group at δ 15.1 ppm and C-4a, C-5 and C-5a. In the pyrone ring HMBC correlations were observed between the methyl protons at δ 2.4 ppm (CH_3-2) and C-2, C-3. The dimeric nature of the compound was concluded from the appearance of HMBC correlations and ^{13}C-NMR signals revealing the presence of a second naphthopyrone moiety. By comparing the concluded chemical structure with literature data, it was shown to be the structure of aurasperone D (Fig 14), a toxic naphthopyrone dimer previously isolated from *A. niger* isolated from mango fruits infected with the fungal strain [81].

Compound **11** has a molecular formula of $C_{32}H_{26}O_{10}$ as was suggested for it by HRESIMS. The ^{1}H NMR spectrum revealed the presence of two methyl proton signals at δ 2.1 and 2.4 ppm as well as four methoxy proton signals at δ 3.3, 3.6, 3.8 and 3.9 ppm. In addition six aromatic proton signals and two chelating hydroxyl proton signals at δ 14.9 and 15.1 ppm were observed. The UV, ^{1}H-and ^{13}C-NMR spectra showed close similarity to aurasperone D. The only difference was the appearance of an additional methoxy group in this compound represented by a carbon signal at δ 54.9 ppm in the ^{13}C-NMR spectrum. These data suggested the structure presented in Fig 14 for the compound, which was found to be aurasperone A after comparison with literature data [80-81].

Compound **12** was determined to have the molecular formula $C_{31}H_{24}O_{10}$ by HRESIMS and ^{13}C-NMR spectroscopy, which indicated 20 degrees of unsaturation. The presence of hydroxyl groups and conjugated carbonyl functionalities was deduced from the downfield shift of the corresponding hydroxyl proton signals at δ 14.9 and 15.1 ppm in the ^{1}H-NMR spectrum. The UV spectrum of the compound showed strong absorption bands at 384, 281, 248 and 225 nm and was very similar to that of aurasperone A and D as well as its ^{1}H and ^{13}C NMR spectra which suggested a dimeric naphthoypyrone for the compound. The ^{13}C NMR spectrum displayed 31 signals which consisted of two methyls, three methoxy groups, six methine and 20 quaternary carbons. The ^{1}H-NMR spectrum also showed two methyl singlets (δ 2.40 and 2.55 ppm), three methoxy singlets (δ 3.42, 4.07, 3.57 ppm), six aromatic protons (two *meta*-coupled doublets at δ 6.15 and 6.62 ppm, four signals at δ 6.50, 6.20, 7.10 and 7.25 ppm) as well as two phenolic hydroxyls (δ 14.8; 15.1 ppm). The HMBC spectrum showed correlations for the first naphthoypyrone moiety of the compound identical to those of aurasperone A [78-79]. HMBC correlations were observed for the proton at δ 7.25 ppm (H-10') with the carbon signals at δ 152.3, 103.4, 109.8 and 184.1 ppm corresponding to C-10'a, C-4a, C-5a and C-4; thus confirming the linear arrangement of this naphthopyrone moiety.

In the second part of the compound HMBC correlations were observed between the proton signal at δ 6.50 ppm (H-3') and the carbon signals at δ 107.7 ppm (C-4'a) as well as between the hydroxyl proton at δ 13.2 ppm and the carbon signals at δ 109.9 ppm (C-3'), 107.7 ppm (C-4'a) and the quaternary carbon at δ 155.6 ppm (C-5'). These correlations suggested the angular arrangement of this naphthopyrone moiety and confirmed this compound of being the naphthopyrone dimer asperpyrone D (Fig 14) [82].

Fig 14. Chemical structures of compounds **9-12**

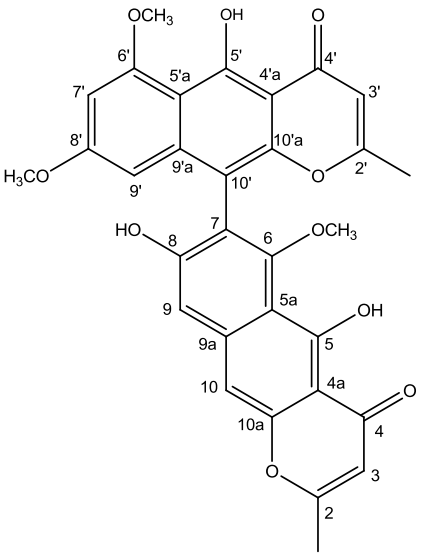

dianhydroaurasperone C (**9**)

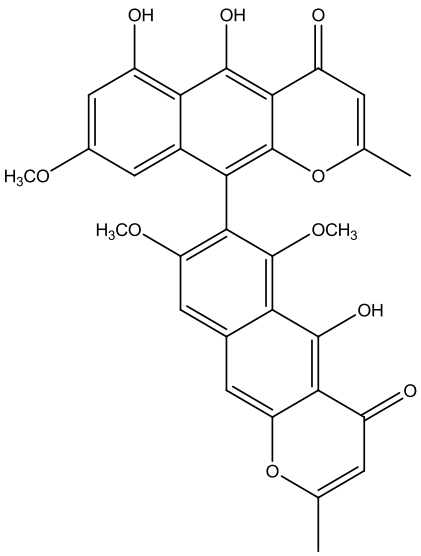

aurasperone D (**10**)

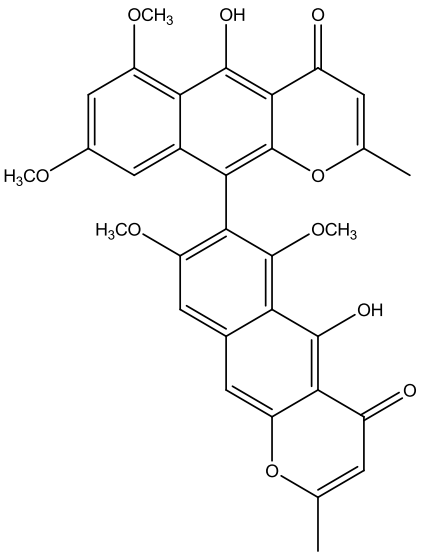

aurasperone A (**11**)

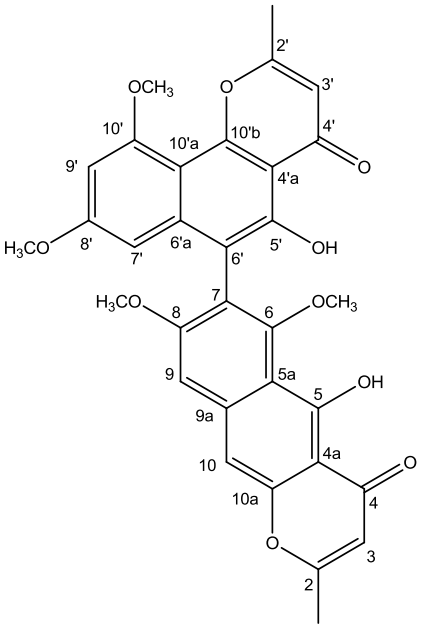

asperpyrone D (**12**)

Table 10. ^{13}C NMR data of compounds **9-12**

Position	δ ^{13}C (**1**)	δc (**2**)	δc (**3**)	δc (**4**)
2	168.8, qC	168.5, qC	168.8, qC	168.0, qC
3	104.8, CH	105.6, CH	105.8, CH	105.7, CH
4	184.0, qC	183.5, qC	183.9, qC	184.1, qC
4a	103.3, qC	103.2, qC	103.9, qC	103.4, qC
5	160.5, qC	161.2, qC	160.9, qC	161.2, qC
5a	108.7, qC	107.6, qC	108.2, qC	109.8, qC
6	158.4, qC	158.5, qC	159.9, qC	157.1, qC
7	116.7, qC	96.4, CH	117.2, qC	116.8, qC
8	160.5, qC	157.8, qC	159.8, qC	152.7, qC
9	103.4, qC	104.9, CH	103.1, CH	105.2, CH
9a	140.0, qC	139.9, qC	139.9, qC	140.0 qC
10	100.3, qC	115.7, qC	101.4, CH	100.4, CH
10a	151.6, qC	151.4, qC	150.1, qC	152.3, qC
CH_3-2	20.2, CH_3	20.2, CH_3	20.1, CH_3	20.1, CH_3
OCH_3-6	61.4, OCH_3		61.2, OCH_3	61.2, OCH_3
OCH_3-8		61.4, OCH_3	61.3, OCH_3	
2’	167.4, qC	168.8, qC	167.9, qC	168.0, qC
3’	105.3, CH	106.7, CH	105.7, CH	109.7, CH
4’	183.9, qC	183.9, qC	184.0, qC	182.4, qC
4’a	106.5, qC	103.3, qC	103.2, qC	106.7, qC
5’	159.5, qC	160.4, qC	161.2, qC	154.6, qC
5’a	107.5, qC	108.5, qC	104.9, qC	105.6, qC
6’	160.4, qC	160.6, qC	158.6, qC	139.9, qC
7’	96.4, CH	96.7, CH	96.5, CH	95.8, CH
8’	159.2, qC	159.5, qC	159.5, qC	152.8, qC
9’	96.7, CH	100.4, CH	96.6, qC	96.9, CH
9’a	140.1, qC	139.4, qC	139.5, qC	158.9, qC
10’	106.6, qC	105.4, qC	110.4, qC	103.8, qC
10’a	149.5, qC	150.2, qC	151.6, qC	154.9, qC
CH_3-2’	20.1, CH_3	20.1, CH_3	20.2, CH_3	20.2, CH_3
OCH_3-6‘	55.2, OCH_3	55.0, OCH_3	55.1, OCH_3	
OCH_3-8‘	56.1, OCH_3	56.1, OCH_3	56.3, OCH_3	56.2, OCH_3
OCH_3-10‘				56.4, OCH_3

Table 11. ^{1}H NMR data of compounds **9-12**

Position	δ ^{1}H (*J* in *Hz*) (**1**)	δ ^{1}H (*J* in *Hz*) (**2**)	δ ^{1}H (*J* in *Hz*) (**3**)	δ ^{1}H (*J* in *Hz*) (**4**)
2				
3	6.22, *s*	6.21, *s*	6.31, *s*	6.20, *m*
4				
4a				
5				
5a				
6				
7		6.52, *s*		
8				
9		7.12, *s*	7.39, *s*	7.10, *d* (9.6)
9a				
10			7.40, *s*	7.25, *d* (8.1)
10a				
CH3-2		2.40, *s*	2.13, *s*	2.40, *s*
OH-5	15.11, *s*	15.12, *s*		14.80, *s*
OCH3-6	3.40, *s*		3.64, *s*	3.57, *d* (5.2)
OCH3-8		3.55, *s*		
OH-8	14.90, *s*			15.10, *s*
2’				
3’	6.21, *s*	6.20, *s*	6.21, *s*	6.50, *d* (2.3)
4’				
5’				
5’a				
6’				
7’	6.64, *d (*2.4)	6.25, *d* (2.1)	6.15, *d* (2.2)	6.62, *d* (2.22)
8’				
9’	6.15, *d* (2.3)	7.37, *d* (2.1)	6.58, *d* (2.1)	6.15, *dd* (2.13; 2.23)
9’a				
10’				
10’a				
CH3-2’	2.13, *s*	2.15, *s*	2.18, *s*	2.55, *s*
OH-5’		14.90, *s*	14.92, *s*	13.29, *s*
OCH3-6’	3.65, *s*	3.63, *s*	3.84, *s*	
OCH3-8’	3.94, *s*	3.97, *s*	3.95, *s*	3.42, *d* (5.24)
OCH3-10’				4.07, *d* (5.26)

3.3.2. Structure elucidation of compounds 13 and 14:

Compound **13** has a molecular formula of $C_{40}H_{35}N_6O_4$ as was determined by HRESIMS which was also confirmed by the NMR data. A monosubstituted aromatic ring was represented by the appearance of five aromatic proton signals (H-19 – H-23) and five corresponding aromatic methine carbon signals (C-19 – C-23). This aromatic ring is obviously connected to a methylene group at δ 36.66 ppm through a HMBC correlation between the proton at δ 7.05 ppm and the carbon signal at δ 36.66 ppm as well as a correlation between the proton signal at δ 7.1 ppm and the same carbon signal at δ 36.7 ppm. These correlations clearly revealed the first subunit of this compound as being a phenyl alanyl group. A disubstituted aromatic ring is represented by the appearance of four aromatic proton signals (H-5 – H-8) and four corresponding aromatic methine carbons (C-5 – C-8).

From the HMBC correlations it became clear that the quaternary carbons at δ 148.6 ppm (C-9) and 134.2 ppm (C-4) are the substituted carbons of this aromatic ring which are connected to an olefinic quaternary carbon represented by a carbon signal at δ 59.3 ppm (C-3) through HMBC correlation with the proton appearing at δ 6.66 ppm (H-6).

The high chemical shift of the quaternary carbon of this aromatic ring δ 148.6 ppm (C-9) suggests its connection to a heteroatom. These NMR data were characteristic for a tryptophan subunit of the structure. This characteristic olefinic quaternary carbon at δ 59.3 ppm (C-3) was correlated with the methylenic protons at C-12 (δ 3.25 & 2.40 ppm). Furthermore this methylenic group was connected to an aromatic ring through HMBC correlations with an aromatic quaternary carbon at δ 126.3 ppm (C-24).

By analyzing the correlations of this aromatic ring it was observed that it belongs to a second tryptophan unit of the structure. This was furthermore supported by the HMBC correlations of the proton at δ 7.51 ppm (H-27) with the quaternary carbon at δ 108.9 ppm (C-32), the high chemical shift observed for C-29 (δ 135.5 ppm) suggesting its connection to an imine group and the correlation of the methylenic protons H-33 at δ 3.05 and 3.09 ppm with C-29 (δ 135.5 ppm). The remaining second phenyl alanyl group was concluded from HMBC correlations observed between the protons at H-33 (δ 3.05 and 3.09 ppm) with two carbonyl functional groups at δ 169.6 ppm (C-36) and 168.8 ppm (C-39) and two alpha methine protons at δ 3.51 ppm (H-34) and 4.12 ppm (H-37).

The comparison of the obtained structural suggestion (Fig 15) and NMR data (Table 12) with literature indicated that this compound is the unusual unsymmetrical diketopiperazine dimer asperazine, which has been reported previously as a secondary metabolite of a marine derived fungus *Aspergillus niger* derived from a Caribbean Hyrtios sponge [83]. The linkage

of the two subunits through the aryl ring of tryptophan in this compound contrasts to the situation in other diketopiperazine dimers. A similar example is the terrestrial fungal metabolite chaetocin, which is a diketopiperazine dimer through the tryptophan units [84]. The other closest analogues are the plant secondary metabolites hodgkinsine and psychotridine [85].

The ^{1}H and ^{13}C NMR data of compound **14** (asperazine A) revealed, that this compound was a homologue of asperazine (**13**) with the same molecular weight and molecular formula. The major differences between both compounds were the higher chemical shift of C-3 (δ 72.7 ppm) which suggested its attachment to a nitrogen atom and the lower chemical shift of C-24 (δ 111.4 ppm). In addition C-24 in this compound appears in the DEPT spectrum as a primary carbon while it was a quaternary one (δ 126.3 ppm) in asperazine. Thus a connection of the two subunits of this dimer through a C-N bond from C-3 to the inolic nitrogen was very probable. This was furthermore supported by HMBC correlations (Fig 16) from the methylenic protons (H-12) to C-11, C-13, C-28 and C-29 as well as from H-31 to C-3, C-28 and C-29. These spectral data confirmed the suggested connection of the two subunits of the compound through a C-N bond and led to the deduction of the structure presented in figure 15 for this compound. By comparing this deduced structure with literature data it was found that it has never been published before.

Fig 15. Chemical structures of compounds **13** and **14**

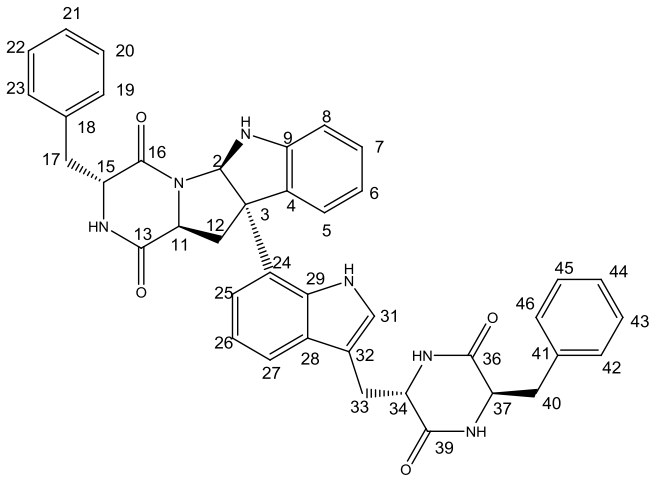

asperazine (**13**)

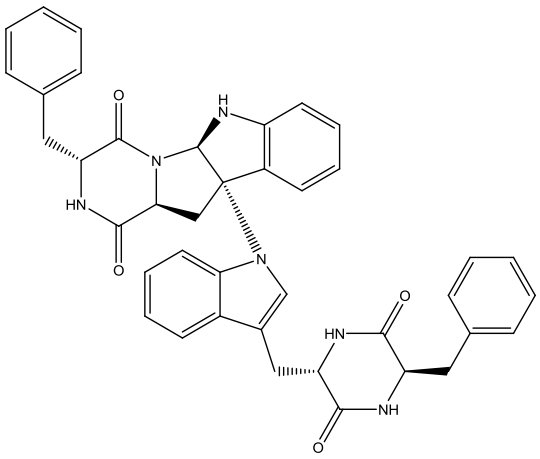

asperazine A (**14**)

Fig 16. Key HMBC correlations of asperazine and asperazine A (**13**, **14**)

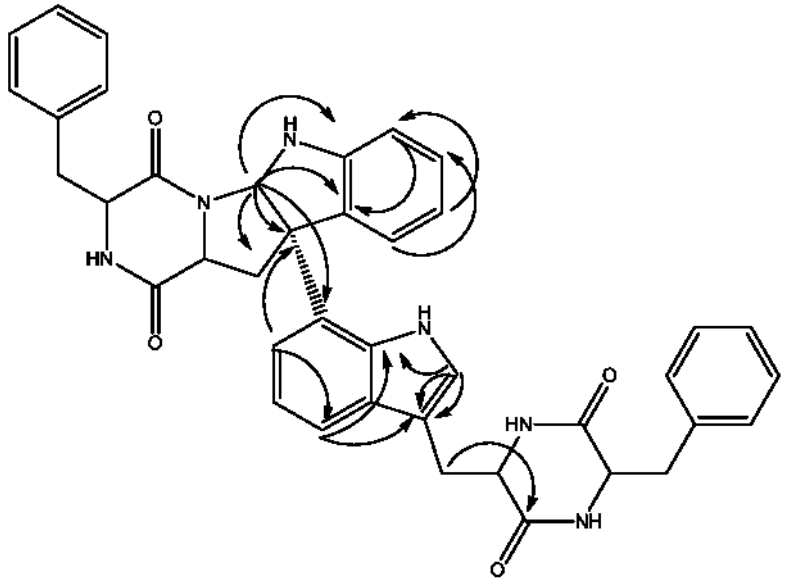

asperazine (**13**)

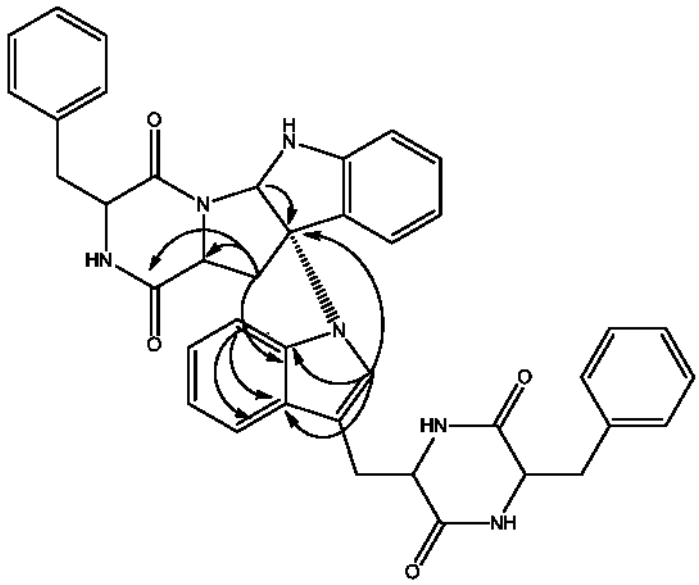

asperazine A (**14**)

Table 12. NMR data (125 MHz, DMSO-d_6) of compounds **13** & **14**

Position	δ ^{13}C (**13**)	δ ^{13}C (**14**)	δ ^{1}H (*J* in *Hz*) (**13**)	δ ^{1}H (*J* in *Hz*) (**14**)
1	NH	NH	6.14, *br s*	6.14, *br s*
2	84.2, CH	81.8, CH	5.71, *d* (1)	5.71, *d* (1)
3	59.3, qC	72.7, qC		
4	134.2, qC	128.4, qC		
5	123.2, CH	122.2, CH	6.74, *dd* (7.0; 1.1)	6.70, *dd* (7.0; 1.2)
6	118.3, CH	118.3, CH	6.51, *dd* (7.1; 1.2)	6.57, *dd* (7.3; 1.1)
7	128.4, CH	128.2, CH	7.02, *m*	7.07, *m*
8	110.2, CH	110.1, CH	6.69, *d* (7.5)	6.72, *d* (7.5)
9	148.6, qC	147.9, qC		
11	57.8, CH	58.1, CH	3.32, *dd* (7.5; 9.5)	4.10, *dd* (7.5; 9.5)
12	39.6, CH_2	39.0, CH_2	3.25, *dd* (14.1; 7.5); 2.40, *dd* (14; 9.5)	3.09, *dd* (14.1; 7.5); 2.90, *dd* (14.1; 9.5)
13	170.0, qC	166.8, qC		
14	NH	NH	6.18, *br s*	6.18, *br s*
15	57.1, CH	55.4, CH	3.59, *ddd* (4.5; 5; 5.5)	3.40, *ddd* (4.5; 5.0; 5.5)
16	168.9, qC	167.6, qC		
17	36.7, CH_2	37.1, CH_2	2.95, *dd* (13.5; 5.5); 2.70, *dd* (13.5; 5.3)	3.02, *dd* (13.5; 5.5); 2.71, *dd* (13.5; 5.0)
18	137.7, qC	136.0, qC		
19	130.1, CH	129.7, CH	7.12, *m*	7.10, *m*
20	126.6, CH	126.5, CH	7.20, *m*	7.12, *m*
21	128.0, CH	127.9, CH	7.05, *m*	7.21, *m*
22	126.9, CH	126.8, CH	7.22, *m*	7.19, *m*
23	129.5, CH	129.7, CH	7.10, *m*	7.10, *m*
24	126.3, qC	111.4, CH		
25	120.2, CH	119.4, CH	7.12, *m*	7.12, *m*
26	120.6, CH	121.3, CH	7.12, *m*	6.91, *m*
27	119.0, CH	119.3, CH	7.51, *dd* (7.0; 1.1)	6.93, *dd* (7.0; 1.1)
28	130.5, qC	129.5, qC		
29	135.5, qC	134.7, qC		
30	NH	NH	8.41, *br s*	8.41, *br s*
31	125.2, CH	125.5, CH	6.918, *d* (2.5)	7.16, *d* (2.5)
32	108.9, qC	108.3, qC		
33	30.2, CH_2	29.0, CH_2	3.05, *dd* (3.5; 14.5); 3.09, *dd* (5.5; 14.5)	3.22, *dd* (3.5; 14.5); 3.01, *dd* (5.5, 14.5)
34	56.4, CH	54.4, CH	3.51, *ddd* (3.5; 5.5; 6.1)	3.62, *ddd* (3.5; 5.5; 6.0)
35	NH		6.16, *br s*	
36	169.6, qC	167.7, qC		
37	60.5, CH	54.4, CH	4.12, *dd* (5.6; 4.5)	3.63, *ddd* (5; 6; 4.5)
38	NH	NH	6.49, *d* (4.5)	6.49, *d* (4.5)
39	168.8, qC	167.8, qC		
40	40.7, CH_2	40.0, CH2	3.06, *dd* (14.3; 6.2); 2.93, *dd* (14.2; 5.2)	3.31, *dd* (14.2; 6.0); 2.05, *dd* (14.2; 5.0)
41	137.7, qC	136.0, qC		
42	131.6, CH	130.1, CH	7.12, *m*	7.11, *m*
43	130.2, CH	129.6, CH	7.12, *m*	7.08, *m*
44	128.7, CH	127.9, CH	7.27, *m*	7.22, *m*
45	130.2, CH	129.6, CH	7.12, *m*	7.08, *m*
46	131.6, CH	130.1, CH	7.12, *m*	7.11, *m*

3.3.3. Bioactivity of compounds 9-14

The isolated compounds of strain 2 were subjected to antimicrobial activity tests against *Bacillus subtilis* and *Penicillium avellaneum* and cytotoxic assays against HeLa, HUVEC and K-562 cell lines. Dianhydroaurasperone C (**1**) was inactive in the agar diffusion assays performed on the chosen microbial test strains. In the cytotoxic assay it showed weak cytotoxicity by exhibiting GI_{50} and CC_{50} values higher than 50 µg mL^{-1}. These results are matching with literature data stating the absence of cytotoxic activity for dianhydroaurasperone C against other cancer cell lines (NCI-H460, human non-small cell lung cancer, MIA Pa Ca-2, human pancreatic cancer, MCF-7, human breast cancer, SF-268, human CNS cancer, WI-38, normal human primary fibroblast cells) [86].

Aurasperone D (**2**) was reported to produce marked central nervous system depressant effects in albino mice and rats leading to death by respiratory failure in a dose of 50 mg/kg after intraperitoneal injection [81]. This information represents a serious threat for the public health since prolonged ingestion of infected mango preparations may cause mental deficiencies [81]. The cytotoxic assay of the compound revealed potent cytotoxicity against HeLa cell lines with a CC_{50} value of 2.4 µg mL^{-1} as well as strong cytostatic activity against HUVEC and K-562 cell lines with GI_{50} values of 4.3 and 4.7 µg mL^{-1} respectively (Table 13).

The cytotoxic assay performed on aurasperone A (**3**) demonstrated rather weak cytotoxic activity against HeLa cell line as well as weak cytostatic activities against HUVEC and K-562 cell lines (CC_{50} and GI_{50} values higher than 50 µg mL^{-1}) (Table 13).

In a study performed on asperpyrone D (**4**) it was reported to have no cytotoxic and no antimicrobial activity [82]. This was confirmed by the negative results of the antibacterial and antifungal activity tests performed against *B. subtilis* and *P. avellaneum*. However, the compound exhibited highly potent cytotoxic activity against HeLa cell lines (CC_{50} = 2.7µg mL^{-1}) and also significant cytostatic activities against HUVEC and K-562 cancer lines with GI_{50} values of 4.3 and 2.7 µg mL^{-1}, respectively (Table 13).

Asperazine (**5**) was reported to be of specific cytotoxic activity against leukemia cell lines while it showed no antibacterial or antifungal effects. It was first isolated from a marine derived *A. tubingensis* (reported as *A. niger*) by Varuglu et al. An analogue was later described by Ovenden et al., also from an *A. tubingensis* strain [87]. Even though asperazine was previously found to be cytotoxic against leukemia, another study reported it to be noncytotoxic [87]. Our assay for cytotoxicity revealed moderate cytotoxicity against HeLa cell lines and also moderate cytostatic activity against HUVEC and K-562 cell lines for asperazine, by exhibiting a CC_{50} value of 19.2 µg mL^{-1} and GI_{50} values of 31.4 and 24.6 µg mL^{-1}, respectively (Table 13). A study previously conducted on extracts from 140 *A. niger*,

177 *A. tubingensis*, one *A. vadensis* and 47 *Aspergillus acidus* strains for the production of asperazine showed that none of the *A. niger* strains produced asperazine, whereas a consistent production was observed in *A. acidus* and *A. tubingensis* [88]. Owing to this limited distribution within the group, asperazine seems to be a chemical marker that can be used to differentiate less toxic species such as *A. acidus* and *A. tubingensis* from similar but more toxic species such as *A. niger* [88]. Here the production of asperazine by the new strain, *A. neoniger* is reported for the first time.

For compound (**6**) on the contrary no activity has been previously reported. The cytotoxic assay perfomed in our lab revealed it of being of rather weak cytotoxic activity against HeLa cell lines as well as weak cytostatic activity against HUVEC and K-562 cell lines (Table 13). No antimicrobial activity was detected for the compound. This is the first report of the spectral assignments and cytotoxic activity of this asperazine analogue.

Table 13. Antiproliferative and cytotoxic activities of compounds **9-14**

	Antiproliferative Effect		Cytotoxicity
Compound	HUVEC GI_{50} [µg mL^{-1}]	K-562 GI_{50} [µg mL^{-1}]	HeLa CC_{50} [µg mL^{-1}]
Dianhydroaurasperone C (**9**)	>50	>50	>50
Aurasperone D (**10**)	4,3	4,7	2,4
Aurasperone A (**11**)	>50	>50	>50
Asperpyrone D (**12**)	4,3	2,7	2,7
Asperazine (**13**)	31.4	24.6	19.2
Asperazine A (**14**)	40.5	>50	34.4

The detection of these cytotoxic metabolites in an *A. neoniger* strain is not surprising as its closest analogue, *A. niger* is involved in a number of reports on toxicity of food or feed contaminated with molds [89]. Black mold is a storage disease caused by *A. niger* on both colored and white cultivars of onions (*Allium cepa*). Although signs of the pathogen are most obvious on the outer scales, the disease is not limited to the exterior portion of the bulb [89]. Malformins were also detected in the extract of black molded onions produced by *A. niger* and several other members of the *A. niger* group of *Aspergillaceae*. Malformins are cyclic pentapeptides which were given this name because they caused malformation in plants. They were also found to be toxic to a variety of bacteria and to prevent IL-1 induced procoagulant changes in human endothelial cells [89] **.** Among the toxic metabolites isolated from *Aspergillus* species are the aspergillomarasmines which were isolated from *A. oryzae* as phytotoxins [90]. Furthermore they were shown to have inhibitory effects on angiotensin-converting enzymes [91]. Another example is cyclopiazonic acid (Fig 17), which is an indole-

tetramic acid and a natural food/feed contaminant [92]. Mycotoxicoses caused by this compound have been observed in several animals. Cyclopiazonic acid is also related to debilitating illnesses in cattle and man in India [93]. Ochratoxin A (Fig 17), a nephrotoxic and carcinogenic compound, is considered the most toxic among the ochratoxins. The toxin is receiving attention because it is a common food contaminant. Ochratoxins are derived primarily from *A. ochraceus and Penicillium verrucosum* but ochratoxin A was first reported from an *A. niger* species [94].

Fig 17. Chemical structures of toxic metabolites from *A. niger*

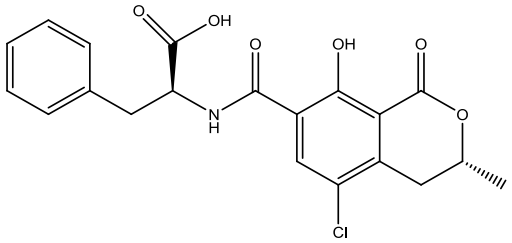

ochratoxin A

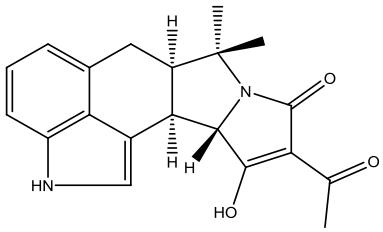

cyclopiazonic acid

3.4. Strain 3: *Epicoccum nigrum*

The third strain selected for investigation of its metabolic content was strain 20076008 which was identified as an *Epicoccum nigrum* strain by ITS sequence comparison. It was selected because of its observed antimicrobial activity against various test strains (Table 14). The antimicrobial activity tests performed on the endophytic fungal extract showed significant antifungal activity for the extract after strain cultivation in medium M5 as a stationary culture and homogenization of mycelium and culture filtrate and then extraction with ethyl acetate.

The following table demonstrates the antimicrobial activity of the fungal extract against *Saccharomyces salmonicolor, Kluyveromyces marxianus, Candida albicans, Penicillium notatum, Penicillium avellaneum, Bacillus subtilis, Aspergillus terreus, Aspergillus niger* and *Aspergillus fumigates* in agar diffusion assay. The most sensitive microorganism was shown to be *Penicillium avellaneum*.

Table 14. Antimicrobial activity[a] of the extract of *Epicoccum nigrum* in medium M5

Strain	*S. salmonicolor*	*K. marxianus*	*C. albicans*	*P. notatum*	*P. alvellaneum*	*B. Subtilis*	*A. terreus*	*A. Niger*	*A. fumigatus*
3 in M5	14	15	14	12	24	12	12	11	11
nystatin	25	23	22	23	25	----	18	20	19

a = measured in terms of the diameter of the inhibition zone in millimeters

The strain was subjected to large scale fermentation (40 L) and afterwards extraction with ethyl acetate yielding an extract with a dry weight of 8 g which was defatted with n-hexane to give a methanolic dry extract of 6 g. Bioactivity-guided fractionation was performed by exposing this methanolic extract to column chromatographic fractionation using chloroform: methanol (9:1) and resulted in the production of five main fractions (F1-F5) which were subjected to antimicrobial activity tests using *Bacillus subtilis* and *Penicillium avellaneum* as test strains in an agar diffusion assay.

The most active fractions were fractions F1 and F3 with the observed antibacterial activity being higher than the antifungal one. Consequently these were subjected to further purification steps involving Sephadex LH-20 column chromatography and preparative HPLC, which were followed by antimicrobial activity tests for the identification of the active secondary metabolite of the fungal extract. The auxin indole carboxylic acid was identified in the HPLC profile of this endophytic extract as well.

3.4.1. Structure elucidation of compound 15 (a diketopiperazine):

A molecular formula of $C_{18}H_{19}O_2N_2$ (*m/z* 295.3015 $[M+H]^+$) was determined for the compound by the HRESIMS. The ^{13}C NMR spectrum revealed the presence of only seven carbon signals, which were shown in the DEPT spectrum to be composed of four methines, one methylenic carbon and two quaternary carbons. This was furthermore confirmed by the HSQC spectrum, which connected the methylinic carbon signal to two different proton signals each appearing as a doublet of doublet in the ^1H NMR spectrum. The ^1H NMR spectrum further revealed the presence of a proton signal not coupled with a carbon signal in the HSQC spectrum indicating the presence of a hydroxyl or an amino group. The HMBC spectrum showed correlations, which led to the identification of the first part of the structure. The presence of a monosubstituted aromatic ring was clearly represented by the carbon signals appearing at δ 136.6, 129.8, 128.2 and 126.5 ppm. The substitution of the aromatic ring at C-5 (δ 136.6 ppm) was confirmed by the HMBC correlations observed between the methylenic protons (H-4) and this quaternary carbon (C-5), the second quaternary carbon C-2 at δ 166.2 ppm as well as the α methine carbon C-3 at δ 55.4 ppm. As the partial structure thus elucidated contained exactly half of the number of carbons and protons deduced by the HRESIMS, it was concluded that the compound was a dimer of two amino acid units giving the final structure of a diketopiperazine (Fig 18) whose characteristic α methine proton was represented by a proton signal at δ 3.99 ppm appearing as a multiplet.

Fig 18. Chemical structure of compound **15**

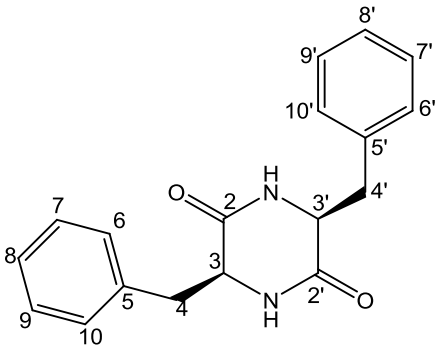

cis-L(-)-3, 6-dibenzyl-2,5-dioxopiperazine

Table 15. NMR spectroscopic data (75 MHz, DMSO-d_6) of compound **15**

Position	δ ^{13}C	δ ^{1}H (*J* in *Hz*)	HMBC
1	NH	*M*	1, 6
2	166.2, qC		
3	55.4, CH	3.66, *m*	1
4a	39.0, CH_2	2.61, *m*	2, 3, 5
4b	39.0, CH_2	2.20, *m*	2, 3, 5
5	136.6, qC		
6	129.8, CH	7.03, *dd J* (2.5; 9.2)	5
7	128.2, CH	7.26, *dd J* (2.6; 9.4)	2
8	126.5, CH	7.21, *dd J* (2.5; 9.4)	3
9	128.2, CH	7.29, *dd J* (2.6; 9.4)	2
10	129.8, CH	7.03, *dd J* (2.5; 9.2)	5
1’	NH	*M*	1, 6
2’	166.2, qC		
3’	55.4, CH	3.66, *m*	1’
4’a	39.0, CH_2	2.6, *m*	2’, 3’, 6’
4’ b	39.0, CH_2	2.20, *m*	2’, 3’, 6’
5’	136.6, qC		
6’	129.8, CH	7.03, *dd J* (2.5; 9.2)	5’
7’	128.2, CH	7.26, *dd J* (2.6; 9.4)	2’
8’	126.5, CH	7.21, *dd J* (2.5; 9.4)	3’
9’	128.2, CH	7.29, *dd J* (2.6; 9.4)	2’
10’	129.8, CH	7.03, *dd J* (2.5; 9.2)	5’

By comparing the obtained structure, the splitting pattern and resonance positions of the geminal methylene and the methine protons with literature data it was found to be the known diketopiperazine which is chemically *cis*-L(-)-3, 6-dibenzyl-2, 5-dioxopiperazine and which has been previously isolated from *Streptomyces noursei* and reported to be of potent anthelmentic activity against the gastrointestinal cestoda *Hymenolepis nana* and a gastrointestinal trematoda *Schistosoma mansoni* [95]. Schistosomiasis is the second worldwide endemy after malaria. The assay performed on this compound to examine its ctotoxic and cytostatic activity showed that it had a weak cytotoxic effect on HeLa cell lines and also weak cytostatic activity on HUVEC and K-562 cell lines with CC_{50} and GI_{50} of more than 50 µg mL^{-1}. Moderate antifungal activity was observed for the compound against *P. avellaneum* (22 mm inhibition zone at a concentration of 250 µg mL^{-1}) and weak antibacterial activity against *B. subtilis* in the agar diffusion assay.

3.4.2. Structure elucidation of compound 16 (epicoccin A):

This compound was obtained as a colorless powder. Its molecular formula was determined as $C_{18}H_{18}N_2O_6S_3$ (10 degrees of unsaturation) by HRESIMS analysis (*m/z* 455.0391 $[M + H]^+$). Analysis of ^1H, ^{13}C, and HMQC NMR data (Table 16) for the compound revealed the presence of four methylenes, eight methines (two oxymethines), two quaternary and four carbonyl carbons. HMBC correlations of H-3, H-6a, and H-7 with the carbonyl group at C-5 (δ 207.8 ppm) led to the identification of one cyclohexanone unit, while correlations of H-3' and H-7' with the other keto group at C-5' (δ 207.4 ppm) revealed the presence of the second cyclohexanone unit. The chemical shifts of C-8 and C-8' (both at δ 64.8 ppm) indicated that these two carbons were attached to hydroxyl groups. HMBC correlations of H-3 with C-1, H-4 with C-2, H-3' with C-1', and H-4' with C-2' indicated that C-1 and C-3 were connected to C-2 and that C-1' and C-3' were connected to C-2'. Considering the downfield chemical shifts of C-2 (δ 74.2 ppm), C-2' (δ 70.5 ppm), C-9 (δ 62.3 ppm), and C-9' (δ 60.2 ppm), the presence of two nitrogen atoms in the compound was concluded. The observation of HMBC correlations of H-9 with C-2 and H-9' with C-2', both C-2 and C-9 and C-2' and C-9' were attached to corresponding nitrogen atoms to complete the diketopiperazine unit. The chemical shifts of C-2, C-7 (δ 45.5 ppm), C-2', and C-7' (δ 41.8 ppm) indicated that these carbons were connected to sulfur atoms. Since only three sulfur atoms are available, it was concluded that a disulfide bridge was present between C-2 and C-7 and a single sulfur bridge was present between C-2' and C-7' based on the observation that the chemical shifts of both C-2 (δ 74.2 ppm) and C-7 (δ 45.5 ppm) are 3.7 ppm downfield from those of C-2' (δ 70.5 ppm) and C-7' (δ 41.8 ppm) in the ^{13}C NMR spectrum. These data led to the identification of the compound as epicoccin A (Fig 19) [96].

Epicoccin A was previously isolated also from an *Epicoccum nigrum* isolate of the fungus *Cordyceps sinensis* and was reported to exhibit activity against *Bacilus subtilis*, affording a zone of inhibition of 12 mm at 100 *μ*g/disk [97]. It is a relatively new member of the epipolythiodioxopiperazine class of compounds that possesses unusual sulfur bridges. Rostratin D, the most closely related known compound, could be a biosynthetic precursor for epicoccin A [97]. Natural products containing the diketoperazine moiety and sulfur bridge(s) have been isolated frequently from fungal sources. These compounds (Fig 20) include the rostratins [97], the epicorazines [98], the leptosins [99], gliotoxin [100], gliocladine [101] and the bionectins [102]. They displayed antiproliferative [103], cytotoxic [99], antitumor [104], immunonodulatory [105], antinematodal [101] and antibacterial activities [102].

Fig 19. Chemical structure of epicoccin A

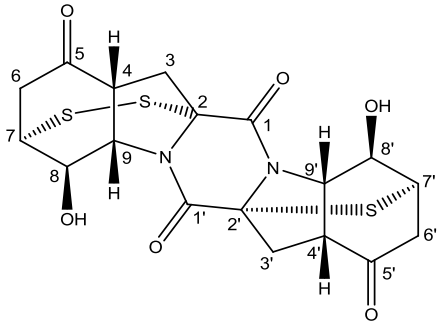

Fig 20. Chemical structures of natural products containing the diketopiperazine moiety and sulfur bridges

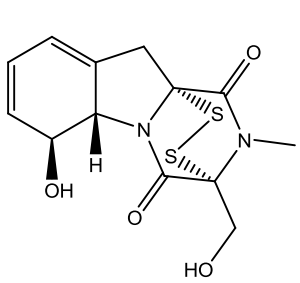

gliotoxin

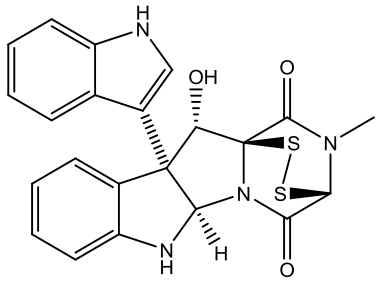

bionectin A

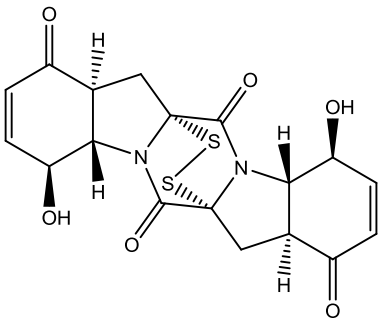

epicorazine A

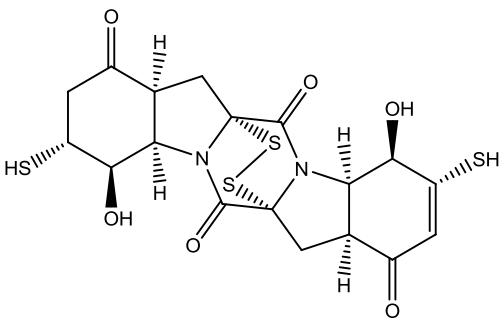

rostratin D

Table 16. NMR spectroscopic data (150 MHz, DMSO-d_6) of epicoccin A

Position	δ ^{1}H (*J* in *Hz*)	δ ^{13}C	HMBC
1			
2			
3a	2.57, *d* (13)	45.6, CH_2	2, 4, 5, 9
3b	2.85, br, *d* (13)	45.6, CH_2	1, 2, 5, 9
4	3.10, br *d* (8.5)	43.4, CH	2, 5, 8
5		207.8, qC	
6a	2.46, *d* (18)	38.0, CH_2	5, 8
6b	3.09, *dd* (18; 12)	38.0, CH_2	4, 5, 7, 8
7	3.74, *dd* (12; 5.1)	45.5, CH	5, 8
8	4.62, br, *dd* (5.1; 3.3)	64.8, CH	4, 6, 9
9	4.48, br *d* (8.5)	62.3, CH	2, 3, 4, 5, 7, 8
8-OH	6.08, *d* (3.3)		7, 8, 9
1’		159.8, qC	
2’		70.5, qC	
3’ a	2.76, *d* (13)	43.3, CH_2	1`, 2`, 5`, 9`
3’ b	2.88, br *d* (13)	43.3, CH_2	1`, 2`, 4`, 5`, 9`
4’	3.05, br *d* (6.8)	45.0, CH	2`, 5`, 6`, 8`
5’		207.4, qC	
6’ a	2.88, *d* (17)	41.3, CH_2	4`, 5`
6’ b	3.11, *dd* (17; 11)	41.3, CH_2	7`, 8`
7’	3.74, br *d* (11)	41.8, CH	2`, 5`, 6`, 8`, 9`
8’	3.98, br *s*	64.8, CH	4`, 6`, 7`
9’	4.62, br *d* (6.8)	60.2, CH	2`, 3`, 8`
8’-OH	6.19, br *s*		7`, 8`, 9`

In the cytotoxic assay, epicoccin A showed weak cytotoxicity against HeLa cell lines as well as weak cytostatic activity against both HUVEC and K-562 cell lines with a CC_{50} value of more than 50 µg mL^{-1} and GI_{50} values of more than 50 and 42.6 µg mL^{-1}, respectively (Fig 21). The compound exerted weak antifungal activity in agar diffusion assay against *P. avellaneum* and showed antibacterial activity against *Bacillus subtilis* by exerting an inhibition zone of 27mm at a concentration of 100 µg mL^{-1}.

Fig 21. Antiproliferative and cytotoxic activity of epicoccin A against HUVEC, K-562 and HeLa cancer cell lines

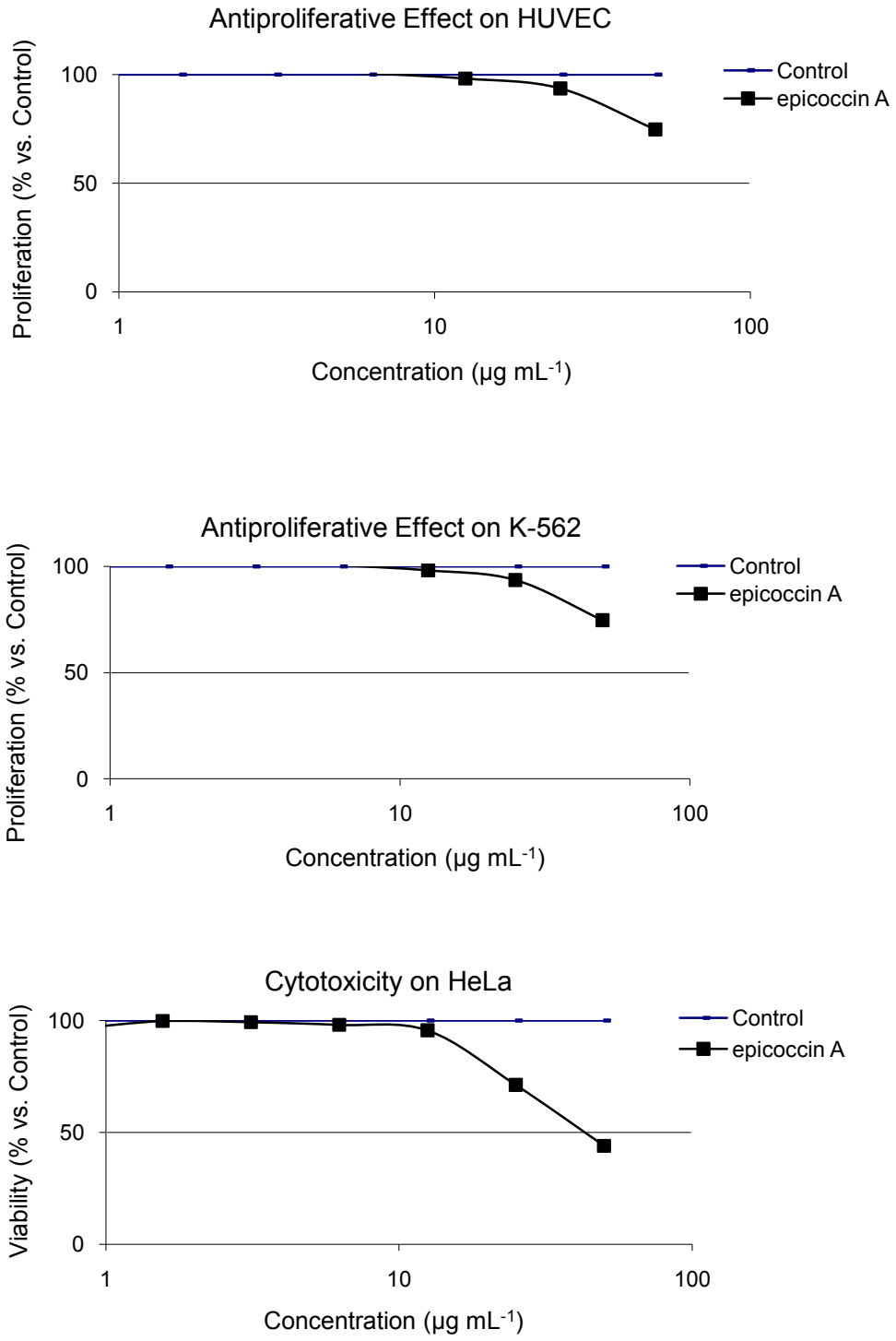

3.4.3. Structure elucidation of compound 17 (adenosyl 9a-D-arabinofuranoside)

Positive ESI-MS showed a molecular ion peak at m/z 268.4 $[M+H]^+$ (base peak) indicating a molecular weight of 267 g/mol for the compound. By dereplication with the database and comparison of the UV spectrum and chromatographic behavior with an authentic sample it was identified as the known adenosyl 9a-D-arabinofuranoside (Fig 22), which has been isolated from an *Actinoplane* sp. and was reported as a herbicide [106] and a potent anti-cancer agent [107]. Furhthermore the compound has been found to inhibit germination of the plant *Arabidopsis thaliana* at 25 µg/mL [106].

Fig 22. Chemical structure of adenosyl 9a-D-arabinofuranoside

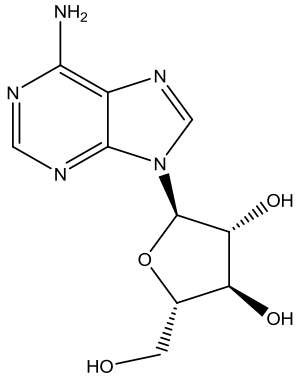

3.5. Strain 4: *Khuskia oryzea*

The strain was identified as *Khuskia oryzea* by ITS sequence comparison. Literature data showed that the only known metabolite of this rarely investigated strain was the antifungal agent griseofulvin [108]. In the following three active constituents of this strain are presented which have never been reported from it before.

The strain was cultivated in four different culture media (M4, M5, M25 and M26) both as a shaken and as a stationary culture and was then subjected to antimicrobial activity screening. Results of the agar diffusion assay performed (Table 17) showed moderate antifungal activity of the fungal extract especially against *Candida albicans* and *Aspergillus terreus* as well as antibacterial activity against *Bacillus subtilis.*

Table 17. Antimicrobial activity[a] of the extract of *Khuskia oryzae* in medium M25

Strain	*Sporobolomyces Salmonicolor*	*Saccharomyces cerevisiae*	*Candida albicans*	*Penicillium notatum*	*Penicillium avellaneum*	*Aspergillus terreus*	*Bacillus subtilis*
K. oryzae	14	0	24	14	14	24	21

a = measured in terms of the diameter of the inhibition zone in millimeters

Therefore, the strain was chosen for large scale fermentation (30 L) in medium M25, where it showed the highest antimicrobial activity. The strain was handeled in the same manner as for the previous strains by the total extraction of culture broth and mycelium with ethyl acetate yielding 7 g of dried crude extract after solvent evaporation. Chromatographic fractionation of the extract was carried out on silica gel using a solvent system of hexane: ethyl acetate starting with a proportion of 9:1 and then gradually increasing the proportion of ethyl acetate till final elution with 100% ethyl acetate. After combining the similar fractions three main fractions were obtained. Activity guided fractionation resulted in the isolation of three pure compounds after several purification steps on Sephadex LH-20 using methanol as a solvent and finally isolation of the pure compounds using RP silica on the preparative HPLC.

3.5.1. Structure elucidation of compound 18 [9-oxo-(10*E*, 12*E*) octadecadienoic acid]:

A molecular formula of $C_{18}H_{31}O_3$ (*m/z* 295.2056 $[M+H]^+$) was suggested for the compound by the HRESIMS thus indicating four degrees of unsaturation. The ^{13}C NMR spectrum revealed the presence of 18 carbons two of which represented a carbonyl and a carboxyl group, respectively. The presence of two olefinic bonds was deduced from the appearance of signals at chemical shift values of δ 128.07, 142.78, 128.97, and 145.36 ppm in the ^{13}C NMR spectrum. The pattern of ^{1}H NMR chemical shifts (Table 18) of the four olefinic protons at δ 6.1 ppm (d, *J* = 15.5 *Hz*), 6.2 ppm (d, *J* = 15.5 *Hz*), 6.3 ppm (d, *J* = 15.5 *Hz*), 7.2 ppm (dd, *J* = 2.8, 8.8, 15.5 *Hz*) suggested the presence of a diene system in the compound and the coupling constants indicated a *trans* configuration of the olefinic protons being thus in clear agreement with a 10*E*, 12*E* diene system. The HMBC experiment showed correlations between H-2 and C-1, C-5 and C-6 as well as between H-10 and C-9 and C-12. Furthermore HMBC correlations (Table 18) were observed between H-11 and C-13 as well as between H-12 and C-11 which served to establish the structure as 9-oxo-(10*E*, 12*E*)-octadecadienoic acid (Fig 23).

Fig 23. Chemical structure of 9-oxo-(10*E*, 12*E*) octadecadienoic acid

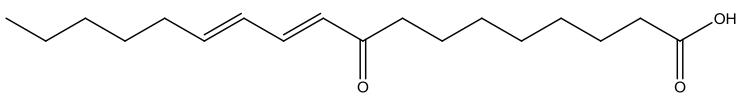

Table 18. NMR data (125 MHz, DMSO-d_6) of 9-oxo-(10*E*, 12*E*) octadecadienoic acid

Position	δ ^{13}C	δ ^{1}H (*J* in *Hz*)	HMBC
1	174.49, qC		
2	33.6, CH_2	2.21, *m*	1, 5, 6
3	27.8, CH_2	1.42, *m*	
4	28.5, CH_2	1.33, *m*	
5	24.4, CH_2	1.51, *m*	1, 4
6	28.4, CH_2	1.30, *m*	
7	23.8, CH_2	1.50, *m*	4
8	39.9, CH_2	2.64, *m*	5, 6, 7, 9
9	200.2, qC		
10	128.1, CH	6.12, *d* (15.5)	9, 12
11	142.8, CH	7.22, *dd* (2.8, 8.8, 15.5)	13
12	129.0, CH	6.24, *d* (15.5)	11
13	145.4, CH	6.30, *d* (15.5)	
14	32.4, CH_2	2.22, *m*	13, 12
15	28.5, CH_2	1.33, *m*	
16	30.8, CH_2	1.34, *m*	
17	21.9, CH_2	1.32, *m*	15
18	13.9, CH_3	0.94, *m*	16, 17

3.5.2. Structure elucidation of compound 19 [8-oxo-(9*E*, 11*E*)- octadecadienoic acid]:

For compound **19** a molecular formula of $C_{17}H_{29}O_3$ (as *m/z* 281.1055 $[M+H]^+$) was deduced from HRESIMS, indicating four degrees of unsaturation. The ^{13}C NMR spectrum revealed the presence of 17 carbon signals with one representing a carbonyl, a carboxyl and four sp^2 carbons. The NMR data (Table 19) of the compound showed great similarity to those of 9-oxo-(10*E*, 12*E*)-octadecadienoic acid, the only difference observed was the absence of one methylenic carbon signal. The presence of a diene system in the structure was supported by the appearance of four olefinic protons in the ^{1}H NMR spectrum. The pattern of ^{1}H NMR chemical shift values of the four olefinic protons and their coupling constants were also characteristic for a 9*E*, 11*E* diene system. The structure of the compound was established by detailed 2D NMR spectroscopic studies including COSY, HMQC and HMBC experiments, which revealed the compound as a new fatty acid called 8-oxo-(9*E*, 11*E*)-octadecadienoic acid (Fig 24). The oxygenated derivatives of fatty acids, known as oxylipins to which this compound belongs are important signaling molecules in animals and terrestrial plants [109]. In animal systems eicosanoids regulate cell differentiation, immune response and homeostasis.

Fig 24. Chemical structure of 8-oxo-(9*E*, 11*E*)-octadecadienoic acid

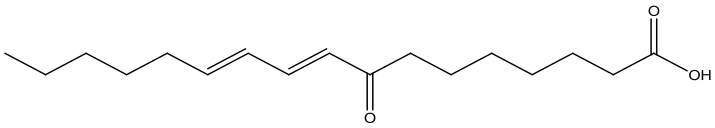

Fig 25. Key HMBC correlations of 8-oxo-(9*E*, 11*E*)-octadecadienoic acid

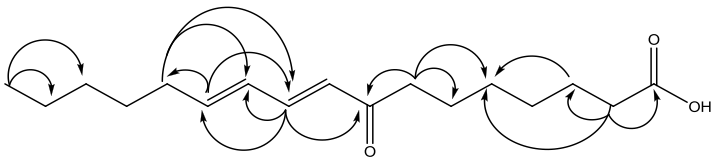

Table 19. NMR data (125 MHz, DMSO-d_6) of 8-oxo-(9*E*, 11*E*)-octadecadienoic acid

Position	$\delta^{13}C$	$\delta^{1}H$ (*J* in *Hz*)	HMBC
1	174.9, qC		
2	33.8, CH_2	2.15, *m*	1, 3, 5
3	24.5, CH_2	1.45, *m*	5
4	28.0, CH_2	1.35, *m*	
5	28.5, CH_2	1.20, *m*	
6	23.9, CH_2	1.40, *m*	
7	40.0, CH_2	2.55, *m*	5, 6, 8
8	200.7, qC		
9	128.2, CH	6.10, *d* (15.5)	
10	143.2, CH	7.15, *dd* (2.7; 8.9; 15.5)	8, 11, 12
11	129.2, CH	6.26, *d* (15.5)	13
12	145.8, CH	6.25, *d* (15.5)	10, 13
13	32.6, CH_2	2.12, *m*	10, 11
14	28.5, CH_2	1.25, *m*	
15	31.0, CH_2	1.22, *m*	
16	22.1, CH_2	1.25, *m*	
17	14.1, CH_3	0.85, *m*	15, 16

In contrast terrestrial plants use derivatives of C18 and C16 fatty acids as developmental or defense hormones. The oxylipin 9-oxo-(10*E*, 12*E)* octadecadienoic acid was previously found in the marine red alga *Chondrus crispus* and was found to be involved in induction of innate immunity of this alga [109]. Furthermore it was found in another study to have good activity against the bacterial plant pathogens *Phytophthora parasitica* and *Cladosprium herbarum* which is why it was suggested to contribute to plant protection not only by induction of defensive responses but also by direct antimicrobial activity in some cases [110]. More recently a study was conducted on the fungitoxic constituents of the basidiomycete *Gomphus floccosus* and detected 9-oxo-(10*E*, 12*E*)-octadecadienoic acids together with two other oxylipins as the active constituents with predominant antifungal activity against *Phomopsis* species [111].

A cytotoxic assay was performed for compound **18** and revealed it of being of weak cytotoxic activity against HeLa cell lines with a CC_{50} value of 43.4 µg mL^{-1} and also weak cytostatic activity against HUVEC and K-562 cancer cell lines with GI_{50} values of 47.0 µg mL^{-1} and 43.2 µg mL^{-1} respectively (Fig 26).

The cytotoxic assay performed on 8-oxo-(9*E*, 11*E*) octadecadienoic acid (**19**) showed moderate cytotoxicity against Hela cell lines and also moderate cytostatic activity against HUVEC and K-562 cell lines with a CC_{50} value of 30.3 µg mL^{-1} for the cytotoxic activity and a GI_{50} value of 27.8 µg mL^{-1} for the cytostatic activity against HUVEC and K-562 cell lines (Fig 26). Compared to the first oxylipin isolated from this strain 8-oxo-(9*E*, 11*E*)-octadecadienoic acid exerts higher cytostatic and cytotoxic activities. In the antimicrobial assay performed against *B. subtilis* and *A. terreus* moderate antibacterial activity was observed for it (inhibition zone 24 mm at a conc of 250 µg mL^{-1}), while no antifungal activity was detected.

Fig 26. Antiproliferative and cytotoxic activities of 9-oxo-(10*E*, 12*E*)-octadecadienoic acid and 8-oxo-(9*E*, 11*E*)-octadecadienoic acid against HUVEC, K-562 and HeLa cell line

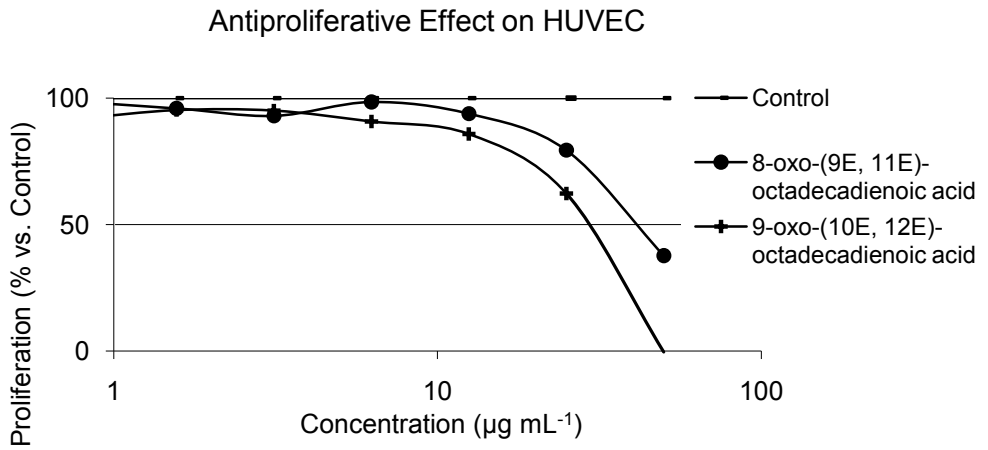

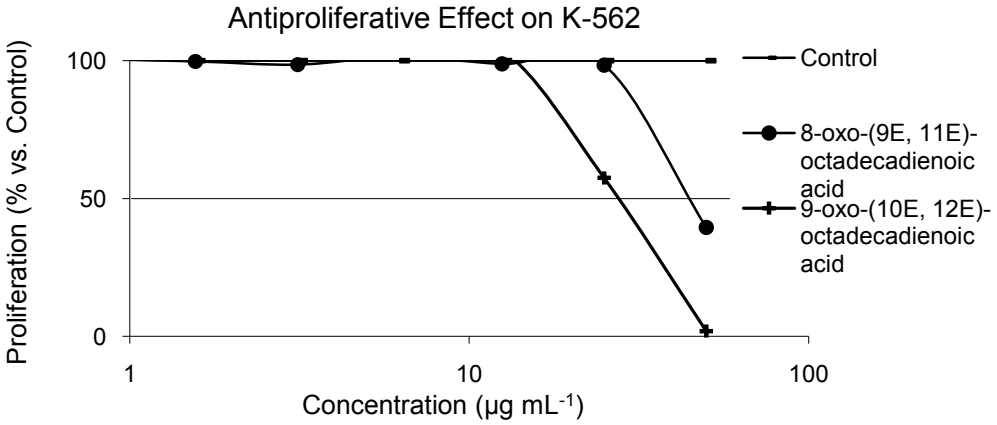

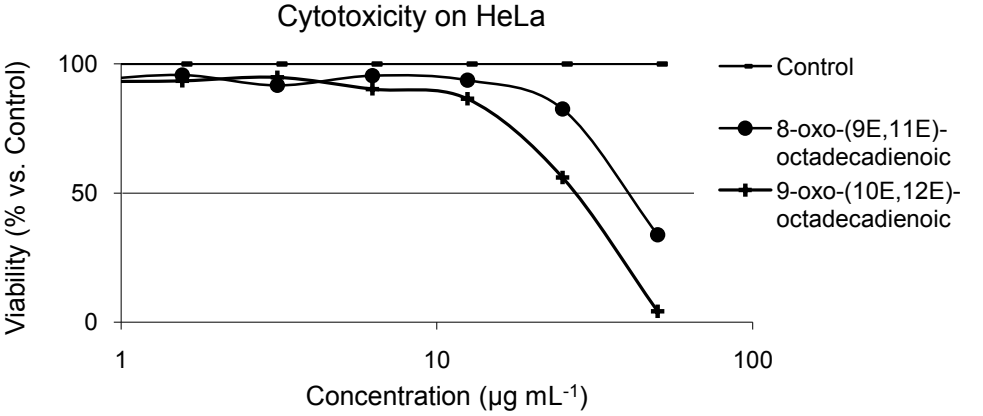

3.5.3. Structure elucidation of compound 20 (sterigmatocystin):

The compound appeared as a yellow solution in methanol and a molecular formula of $C_{18}H_{13}O_6$ (*m/z* 325.2506 $[M+H]^+$) was determined for it by HRESIMS. The ^{1}H-NMR spectrum showed eight proton signals, a hydroxyl proton appearing at δ 13.28 ppm indicating the presence of a chelated phenolic hydroxyl group and a methoxy group at δ 56.88 ppm. The ^{13}C-NMR data (Table 20) revealed the presence of 18 carbon signals and thus together with the ^{1}H-NMR confirmed the suggested molecular formula. The HMBC correlations (Table 20) clearly revealed the first part of the structure as being a benzo-pyrone. The downfield shift of C-7 and C-2 indicates their connection to oxygen atoms and thus reveals this part of the structure as being a tetrahydrodifurano ring system. By comparing the obtained structure with literature data it was found to be the mycotoxin sterigmatocystin (Fig 27), which has been previously isolated from several *Aspergillus* species like *Aspergillus versicolor* and *Aspergillus multicolor* [112]. The xanthone nucleus attached to a bifuran structure it closely resembles the aflatoxins and has similarly been shown to be toxic to mice [113], rats [114] monkeys [115], ducklings [113] and is carcinogenic and mutagenic when injected or fed to rats [116]. Sterigmatocystin and cultures which are capable of its production have been detected in wheat [117] and coffee beans [118]. It belongs to the main 20 mycotoxins that are known to occur in foodstuffs at significant levels and frequency to be of food safety concern [112]. These mycotoxins have been reported to be produced by five fungal genera: *Aspergillus*, *Penicillium*, *Fusarium*, *Alternaria* and *Claviceps* [112]. This is the first report of sterigmatocystin isolation from *K. oryzae.*

A cytotoxic assay was carried out on sterigmatocystin to examine its cytotoxic activity against HeLa cell lines and its cytostatic activity on HUVEC and K-562 cell lines where it proved to be of weak cytotoxicity and also weak cytostatic activity with CC_{50} and GI_{50} values of more than 50 µg mL^{-1}.

Fig 27. Chemical structures of sterigmatocystin and aflatoxin B1

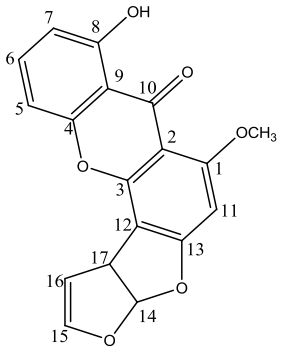

sterigmatocystin

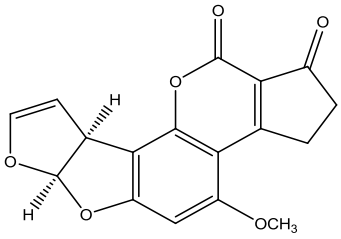

aflatoxin B1

Table 20. NMR spectroscopic data (150 MHz, DMSO-d_6) of sterigmatocystin

position	δ ^{13}C	δ ^{1}H (*J* in Hz)	HMBC
1	110.8, CH	6.72, *d*	8, 17, 9
2	106.6, qC		
3	180.5, qC		
4	136.3, CH	7.62, *t*	8, 4, 9
5	161.4, qC		
6	162.9, qC		
7	102.7, CH	5.53, *t*	3, 15
8	153.4, qC		
9	105.0, qC		
10	145.7, CH	6.74, *d*	9, 17
11	113.4, CH	6.90, *d*	15, 13, 16, 5, 17
12	154.5, qC		
13	106.6, CH	7.00, *d*	4, 9, 7, 14, 17
14	164.5, qC		
15	91.1, CH	6.71, *s*	8, 1, 13, 12
16	108.3, qC		
17	47.3, CH	4.86, *d*	16, 5, 11
18	56.9, OCH_3	3.89, *s*	1

3.6. Strain 5 (20076005):

In the antimicrobial activity screening (Table 21) the strain exhibited significant antifungal effects when cultivated in medium M4 especially against *A. terreus* and was therefore chosen for large scale fermentation (40 L) as a stationary culture. The total extract obtained after solvent extraction weighed 6 g which were subjected to silica gel column chromatography and yielded five main fractions. Antimicrobial activity tests showed that only the first fraction F1 was active. F1 was therefore purified on Sephadex LH-20 and gave three main subfractions F1a, F1b and F1c. Each was then successively purified on Sephadex LH-20 and finally on preparative HPLC to yield three pure compounds.

Table 21. Antimicrobial activity [a] of the extract of strain 5 in medium M4

Strain	*B. subtilis*	*C. albicans*	*A. fumigatus*	*A. terreus*	*A. niger*	*S. Salmonicolor*
Extract	32	30	40	42	30	40
Nystatin	---	25	23	22	28	24

a = measured in terms of the diameter of the inhibition zone in millimeters

3.6.1. Structure elucidation of compound 21 (alternariol):

This compound represented the major secondary metabolite of the strain. A molecular formula of $C_{14}H_{11}O_5$ (*m/z* 259.2106 $[M+H]^+$) was determined by the HRESIMS thus indicating 10 degrees of unsaturation. The number of carbons and hydrogens suggested by the HRESIMS was in agreement with the number of signals detected in the ^{13}C NMR and ^{1}H NMR data (Table 22). The ^{1}H NMR spectrum exhibited signals for four aromatic hydrogens at δ 6.4, 6.6, 6.7 and 7.2 ppm; one methyl group at δ 2.7 ppm and three phenolic hydroxyl groups at δ 10.3, 10.8 and 11.7 ppm. Each two of the four aromatic protons were *meta* coupled with each other thus indicating the presence of two different aromatic rings. The ^{13}C NMR spectrum exhibited signals for a methyl group (δ 25.23 ppm), eight olefinic carbons (δ 97.40, 100.86, 101.59, 104.3, 108.95, 117.52, 138.12, 138.32 ppm), four olefinic carbon atoms bearing oxygen atoms (δ 152.61, 158.41, 164.06, 164.69 ppm) and a carbonyl group (δ 165.39 ppm). From the HMBC correlations it was observed that one phenyl ring contained the two *meta* positioned protons at δ 7.2 and 6.4 ppm together with the two hydroxyls at δ 10.8 and 11.7 ppm. This was concluded from the correlations observed between H-4 (δ 6.4 ppm) and C-6, 2, 3 and those of H-6 (δ 7.2 ppm) with C-2, 4, 7 and 1'. Furthermore HMBC correlations were observed for the second phenyl group suggesting its substitution by one hydroxyl and one methyl group due to the correlations observed between H-3` (δ 6.6 ppm) and C-1', 4', 5', 6' and for H-5` (δ 6.7 ppm) with C-1', 3', 4', 7'. The upfield shift of C-2 (δ 97.40 ppm) suggests its connection to a carbonyl group while the downfield shift observed for C-2' (δ 138.32 ppm) indicates its connection to an ether group. According to literature data the deduced structure was found to be alternariol (Fig 28) [119].

Fig 28. Chemical structure of alternariol

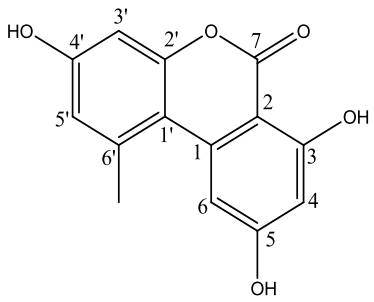

Alternariol is a mycotoxin previously isolated from several *Alternaria* species reported of infecting various fruits, including tomatoes, olives, mandarins, melons, peppers, apples and raspberries [120]. It belongs to the toxins of alternaria, which also include alternariol monomethyl ether and tenuazonic acid (Fig 29) [120]. These mycotoxins have phytotoxic properties and are important in the development of some plant disease processes such as

black spot and seedling chlorosis [120]. They have also been shown to be toxic to chicken embryos. Alternariol was previously isolated from a mangrove endophytic fungus from the South China Sea Coast and was reported to have strong cytotoxic activity against KB cell lines with an IC_{50} value of 4.82 µg mL^{-1}. It has also been reported of having antifungal activity and is a choline esterase inhibitor [121].

Fig 29. Chemical structures of alternaria toxins

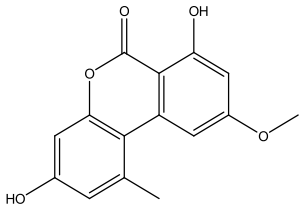

alternariol monomethyl ether

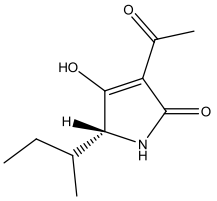

tenuazonic acid

Table 22. NMR spectroscopic data (125 MHz, DMSO-d_6) of alternariol

Position	δ ^{13}C	δ ^{1}H (*J in Hz)*	HMBC
1	138.1, qC		
2	97.4, qC		
3	164.7, qC		
4	100.9, CH	6.4, *d* (1.95)	2, 3, 6
5	164.1, qC		
6	104.3, CH	7.2, *d* (1.95)	2, 4, 7, 1`
7	165.4, qC		
1`	109.0, qC		
2`	138.3, qC		
3`	101.6, CH	6.6, *d* (2.60)	1`, 4`, 5`, 6`
4`	158.4, qC		
5`	117.5, CH	6.7, *d* (2.45)	1`, 3`, 4`, 7`
6`	152.6, qC		
7`	25,2, CH_3	2.7, *s*	1', 5', 6'
OH		10.3, *s*	3`, 4`, 5`
OH		10.8, *s*	4, 6, 7
OH		11.7, *s*	2, 3, 4

3.6.2. Identification of compound 22 (tentoxin):

A molecular weight of 414 g/mol (base peak at 415.23 $[M+H]^+$ in the positive ESI-MS) was suggested for the compound. By dereplication with authentic samples of our database it has been found to have an identical UV chromatogram to that of tentoxin (Fig 30). Also the IR spectrum and chromatographic properties were identical to those of tentoxin. Tentoxin is a phytotoxin, which causes chlorosis in the seedlings of many plants [122]. Chemically, tentoxin is cyclo-[L-leucyl-*N*-methyl-(*Z*)-dehydrophenylalanylglycyl-*N*-methyl-L-alanyl]. The presence of the styrene structure in the dehydrophenylalanyl residue is essential for the chlorotic activity, since dihydrotentoxin has almost no chlorotic effect [122].

Fig 30. Chemical structure of tentoxin

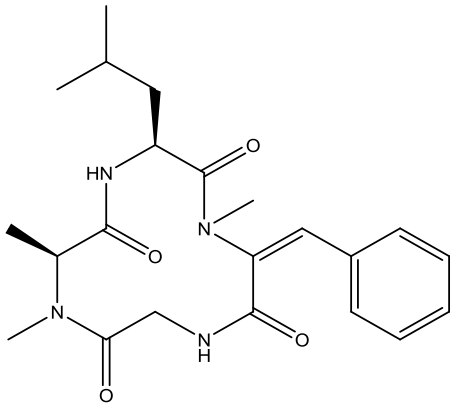

3.6.3. Identification of compound 23 (emodin):

By dereplication with HPLCUV-MS database this compound was found to have a base peak at *m/z* 271.5 $[M+H]^+$ and a UV chromatogram identical to that of emodin. Further comparison with an authentic sample revealed identical IR spectra and chromatographic behavior on thin layer chromatography confirming the identity of this compound as emodin (Fig 31) [123]. There are few reports of emodin isolation from endophytic fungi, which include its detection in an endophytic fungus from the stems of the medicinal herb *Hypericum perforatum* where it was proposed to be the main precursor in the microbial metabolic pathway to hypericin (Fig 31) [124]. It was also identified as a secondary metabolite of the endophytic fungus *Microsphaeropsis* species where it has been suggested to be the precursor of microsphaeropsones A-C (Fig 31) [125]. Further studies also revealed that it inhibited *Vibrio vulnificus* growth and survival in seawater. It was confirmed that *Plygoni Cuspidati* radix showed direct antibacterial activity against *V. vulnificus* due to its high emodin content and prevented the morphologic damages and acute death of HeLa cells caused by this bacterium [126]. Furthermore emodin was isolated from the stem bark of *Ventilago madraspatana* and

showed significantly high antibacterial activity against *B.subtilis* with a MIC of 0.5 µg mL^{-1} and against *P. aeroginosa* with a MIC of 70 µg mL^{-1} [127].

Fig 31. Chemical structures of emodin, microsphaeropsone A and hypericin

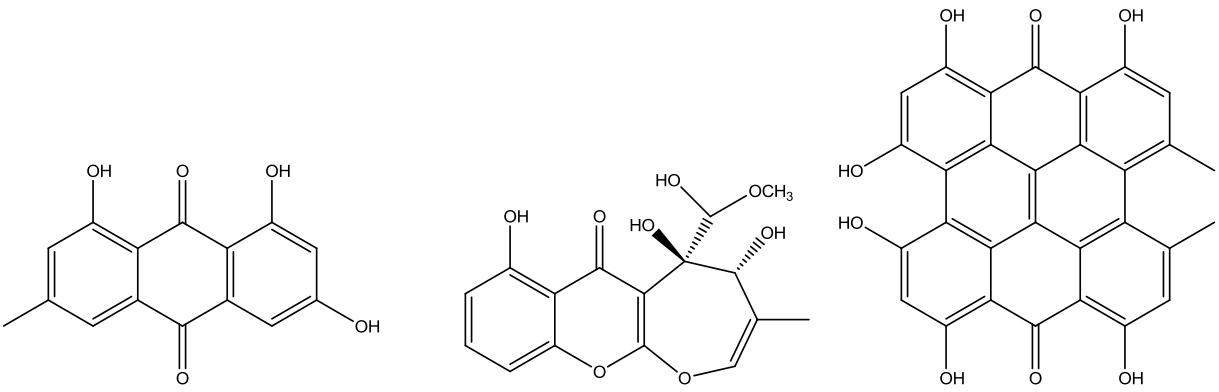

emodin microsphaerpsone A hypericin

3.6.4. Identification of compound 24 (ascaridole):

The compound displayed a base peak at *m/z* 169.3 $[M+H]^+$ in the ESI-MS and was identified using the HPLCUV-MS database as ascaridole (Fig 32). The detection of ascaridole as a secondary metabolite of this endophyte is quite interesting since it is known of exerting several biological activities. Ascaridole was reported to display cytotoxicity, showing IC_{50} values in the range of 6.3 to 18.4 µg mL^{-1} in HL-60 and HCT-8 cell lines. An *in vivo* study, using sarcoma 180 as a tumor model, demonstrated inhibition rates of 33.9% at 10 mg/kg and 33.3% at 20 mg/kg doses [128]. The antitumor activity in sarcoma 180 murine model of ascaridole is probably related to its described cytotoxic activity, and its presence in the essential oil from the leaves of *C. regelianus* could be considered as one of the main reasons for the ethnopharmacological use of this plant in the treatment of cancer [129].

Fig 32. Chemical structure of ascaridole

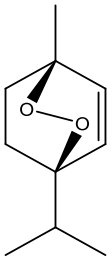

In addition the antifungal activity of the essential oil from the Brazilian epazote (*Chenopodium ambrosioides L*.) was evaluated by the poison food assay with eight postharvest deteriorating fungi (*Aspergillus flavus, Aspergillus glaucus, Aspergillus niger, Aspergillus ochraceous, Colletotrichum gloesporioides, Colletotrichum musae, Fusarium oxysporum*, and *Fusarium semitectum*). Studies revealed that ascaridole is the principal fungitoxic component of the essential oil content of *Chenopodium ambrosioides* [129].

Being of such potent antifungal and cytotoxic activity ascaridole is thus suggested to give an indication for the probable protective effect this endophyte provides for itself against competitors and for the plant against invading pathogenic fungi.

3.6.5. Detection of indole carboxylic acid

Also in this strain the plant auxin indole carboxylic acid could be identified by comparison with an authentic standard which thus seems to be a common metabolite of nearly all studied endophytic fungal strains of *Bidens pilosa*.

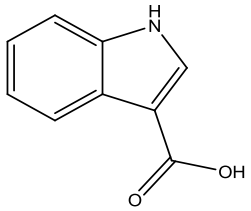

indole carboxylic acid

3.7. Strain 6 (20076002)

The extract of this strain showed antifungal activity when tested against the microbial strains: *S. salmonicolor, K. marxianus, R. rubra, C. albicans, A. niger, A. fumigatus, B. subtilis, P. avellaneum* and *A. terreus* (Table 23). Highest antimicrobial activity was observed for the strain when cultivated in medium M25 as a shaken culture for two weeks. The chemical screening of the strain and the dereplication with our database using HPLCUV-MS proved that the only active constituent produced by this strain was citrinin (Fig 33). The phytohormone indole carboxylic acid was also detected among the metabolic constituents of this strain as well and as shown in the HPLC profiles of the investigated endophytic strains (Fig 34), it is a common metabolite of all studied endophytic strains of *Bidens pilosa*.

Table 23. Antimicrobial activity[a] of strain 6 in medium M25

Strain	*S. salmonicolor*	*K. marxianus*	*R. rubra*	*C. albicans*	*A. niger*	*A. fumigatus*	*B. subtilis*	*P. avellaneum*	*A. terreus*
stationary culture	17	28	0	0	17p	16	25	18	18
shaken culture	13	18	0	24	20p	14	22	17p	25p
nystatin	25	28	0	24	20	20	-	20	20

a = measured in terms of the diameter of the inhibition zone in millimeters

3.7.1. Identification of compound 25 (citrinin):

The compound appeared as the major secondary metabolite of this strain. By comparison with the HPLCUV-MS database it was identified as citrinin (Fig 33). Citrinin is a fungal metabolite known since 1931, when it was isolated from *Penicillium citrinum* and later from the Australian plant *Crotolaria crispata* [130]. It is quite interesting to find citrinin among the active constituents of plant extracts as well since there are only few examples of plant metabolites being produced by fungal endophytes, which suggests the potential presence of genetic cross linking between them. Another example is represented by the cytotoxic agents methylpodophyllotoxin, podophyllotoxin and podophyllotoxin glucoside which are produced by the perennial herb *Podophyllum hexandrum* and its endophyte *Trametes hirsute* [131]. After having been characterized as an antibiotic its activity was later on tested against bacteriophages, sarcomas, protozoa, animal cells and superior plant cells [130].

Several studies indicate that citrinin has a biological action by inhibition of cholesterol and triglyceride synthesis, this inhibition being possibly caused by damage to transport systems and/or interferences in energetic metabolism [130]. Citrinin was also previously noted to cause teratogenic effects in chicken embryos, with malformations primarily in the extremities [132].

Fig 33. Chemical structure of citrinin

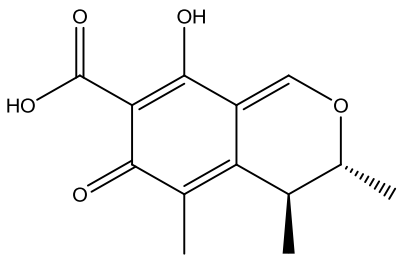

Fig 34. HPLC profiles of the endophytic fungal extracts of *B. pilosa*

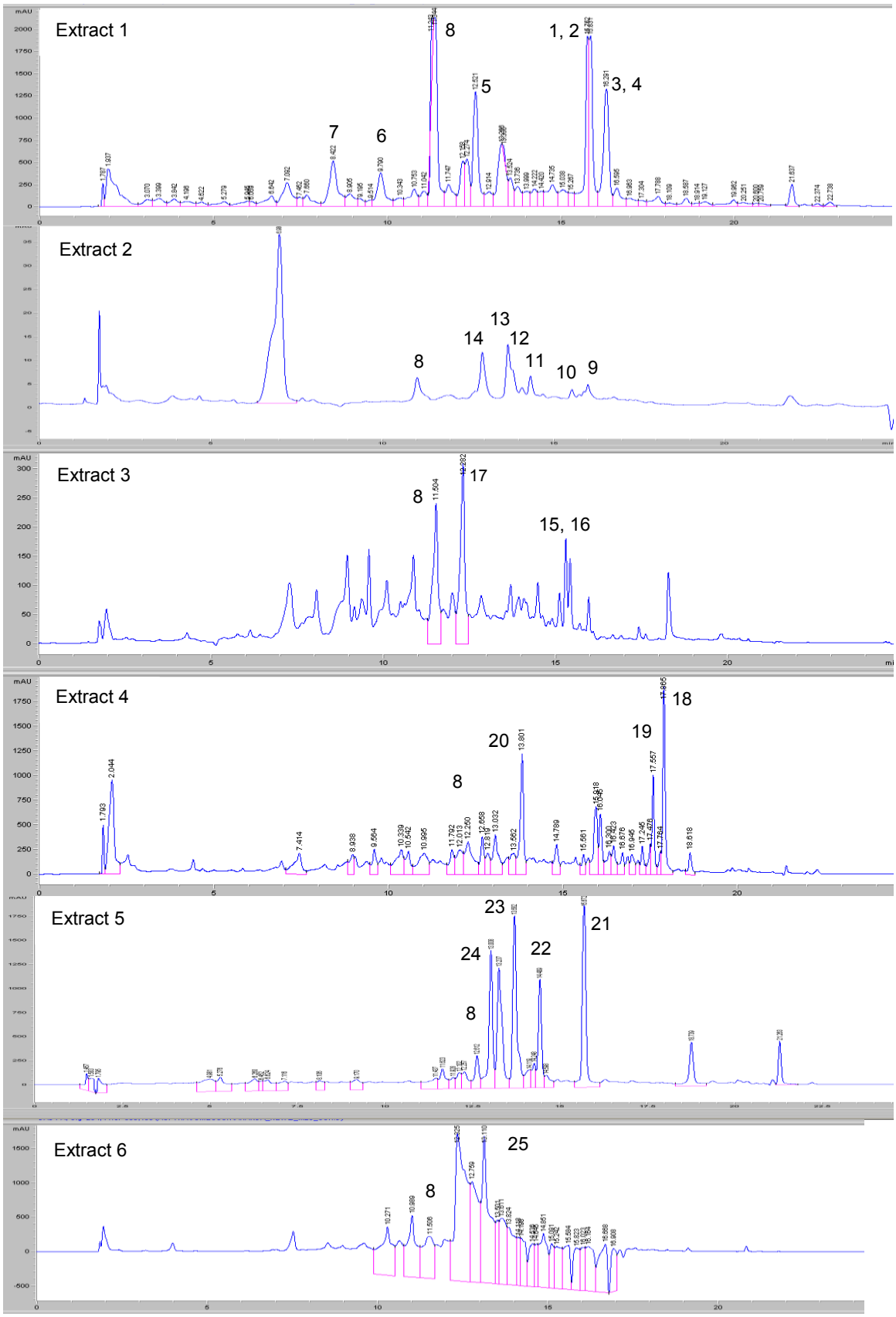

1-25 = isolated bioactive metabolites

3.8. Testing endophyte-endophyte interaction

3.8.1. Effect of antifungal endophytic extracts on the growth of endophytes

To examine the effect of the endophytes of *B. pilosa* on each other's growth, the fungal extracts exhibiting antifungal activity were tested for their antifungal effect on the other endophytic strains of the plant in an agar diffusion assay. Surprisingly the growth of the endophytic strains was not affected by any antifungal endophytic extract of the plant (no inhibition zones were observed). The most surprising observation was, that even though the most sensitive test strain towards the extract of *Botryosphaeria rhodina* was an *Aspergillus* species (*A. terreus*) the endophytic strain *A. neoniger* was not affected by the antifungal activity of this extract at all. It seems that the endophytes have developed protective mechanisms to be resistant against the antifungal activity of their neighbors. From this it was concluded that the antifungal activity observed for the strains was not directed towards the neighboring endophytic fungi but most propably only against "foreign" fungal invaders. This conclusion supports the assumption of plant protection by its endophytes and suggests the absence of competition between these endophytes. The interactions between endophytes of a certain host plant have been rarely examined. A previous study examined the interaction between an endophytic fungus *Guignardia criticarpa* and the most frequently isolated endophytic bacteria of citrus rootstocks. It was observed that metabolites of the endophytic fungus inhibited the growth of *Bacillus* spp. and stimulated the growth of *Pantoea agglomerans* [133].

3.8.2. Effect of mixed fermentations on the metabolic profile of endophytes

The development and growth of fungi depends on successful communication processes within the organism and between organisms of the same or related species as well as with non-related organisms [134]. There are reports of enhanced production of bioactive metabolites and new bioactive metabolite production when microorganisms grow in mixed cultures with other species which was referred to possible synergistc effects produced in such cultures [135].

Thus the interaction between the endophytic strains of *B. pilosa* was examined by the formation of mixed cultures of different endophytic strains. The endophytic fungal strains of *B. pilosa* with the highest antifungal activities were chosen for the cultivation of dual cultures. These dual cultures were formed by combination of the following strains: *Botryosphaeria rhodina* and *Aspergillus neoniger* (A), *B. rhodina* and *Epicoccum nigrum* (B) as well as *B. rhodina* and *Khuskia oryzae* (C). The metabolic profile of each co-culture (Fig 35) was examined and compared to that of the original pure culture (Fig 34). In addition the antifungal

activity of the extracts of the mixed cultures was examined against the test strains *Aspergillus terreus*, *Penicillium notatum* and *Penicillium avellaneum*.

The metabolic profile of each dual culture differed significantly from that of the original cultures. The main difference observed was the absence of the peaks corresponding to the active secondary metabolites of each strain as indicated by HPLC-MS. The phytohormone indole carboxylic acid (**8**) was detected as the major secondary metabolite in the HPLC profiles of mixed cultures (A) and (C) (Fig 35).

Fig 35. HPLC profiles of the dual culture extracts (A-C) of the endophytes of *B. pilosa*

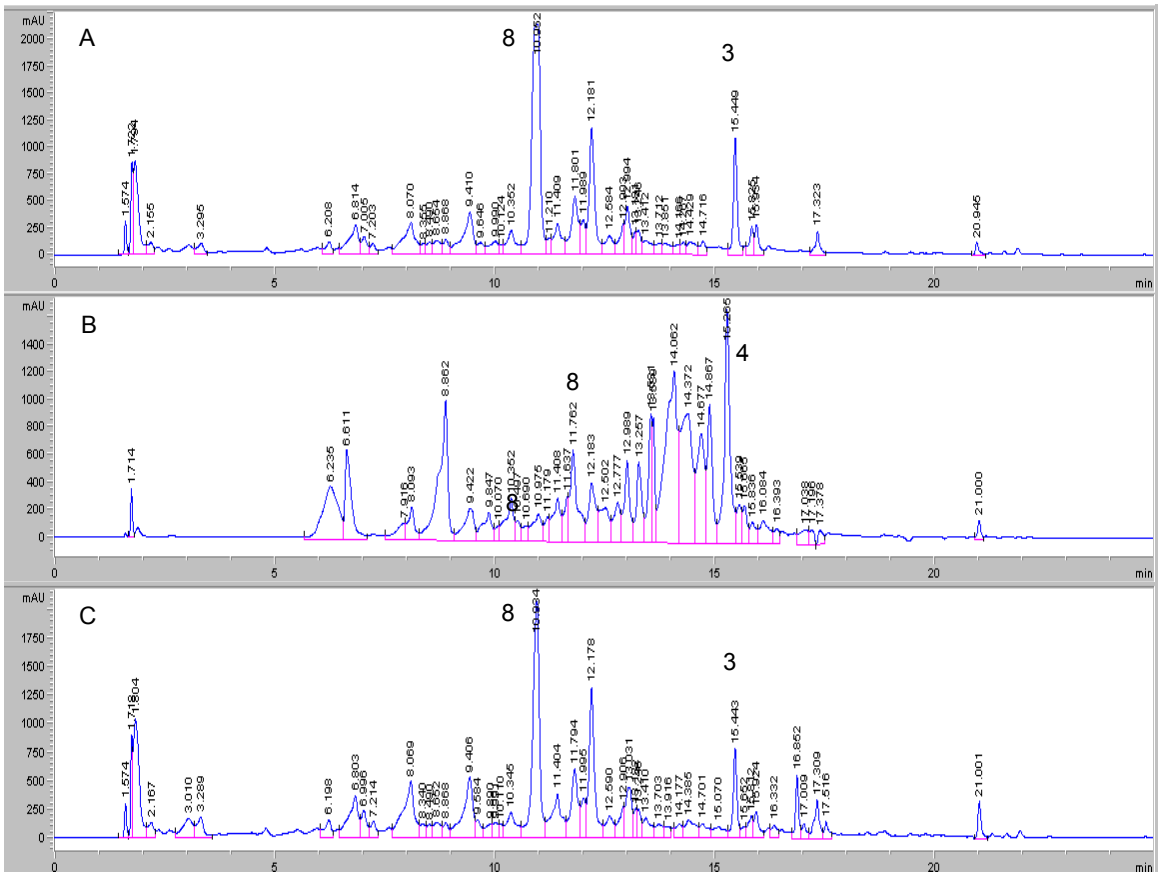

8 = peak representing indole carboxylic acid; 4 = peak representing botryorhodine C; 3 = peak representing botryorhodine D

The antimicrobial activity test showed that the extracts of the dual cultures exerted no antifungal activity in agar diffusion assay against the tested microorganisms (no inhibion zones were produced). Thus it is apparent that the production of the antifungal secondary metabolites of each endophytic strain was inhibited in the coculture, while the production of the phytohormone (**8**) (Fig 35) was maintained in all cultures especially in cocultures A and C. HPLC-MS measurements and dereplication with the database revealed the presence of a

peak (at 15.3 min) corresponding to the secondary metabolite isolated from *B. rhodina*, botryorhodine D (**4**) which has no antifungal activity, in the HPLC profile of coculture B (Fig 35), while a peak (at 15.4 min) representing the production of botryorhodine C (**3**), which has also no antifungal activity, was observed in cocultures A and C.

These results indicate that the endophytes of *B. pilosa* are able of recognizing each other and growing together without exerting any antifungal effects that might inhibit the growth of the other endophytes of the host plant. Furthermore these findings suggest that these endophytes are capable of differentiating foreign invading pathogens from their known neighboring endophytes. Following this recognition there seems to be a depressed production of antifungal secondary metabolites by the endophytes. This could be explained by the fact that fungi are believed to be capable of distinguishing between "self" and "nonself" [134]. This ability either causes a fungus to merge with compatible species or in case of incompatible genetic sequences repulsion can take place as a kind of immune response such as that present in plants [136]. Cells present in a medium communicate with each other either by direct cell-to-cell-interactions or through the signal substances in the fermentation broth [137]. Interactions between the different microorganisms play a critical role in a coculture. Growth of cells of one strain may be enhanced or inhibited by the activities of other microorganisms present in the medium. The same is also true for the formation of secondary metabolites [138]. The endophytes of *B. pilosa* seem to be either capable of interfering with the metabolic pathways of the endophytes they communicate with, thereby inhibiting the production of antifungal secondary metabolites, or most propably they inactivate the antifungal compounds produced. This assumption could also explain their resistance to the antifungal effects of other endophytic strain extracts observed in agar diffusion assay (section 3.8.1.)

3.9. Plant immune Assay

The possibility of enhancing plant defenses by using their associated endophytes opens a new field of study for the use of endophytes in the control of crop pests and diseases [7]. Such an effect can be used in biological control in ecological agriculture. However it must be considered that an endophyte might produce different secondary metabolites in a non-host plant [7]. *Arabidopsis thaliana* has been used as a model plant to study its interactions with endophytes like *Azorhizobium caulinodans* and enterobacteria. The advantage of using *A. thaliana* is that there are defined mutants that may be tested for their colonization by endophytes [7]. Therefore it was interesting to find out if any of the endophytic extracts of *B. pilosa* had a stimulant effect on the immune response of *A. thaliana*. Accordingly a plant immune assay was performed at the Institue for Biochemical Plant Pathology of the

Helmholtz Zentrum in Munich (by the PhD student Clara Steinhauser) to detect the presence of elicitors of plant immune response among the constituents of the different endophytic fungal extracts of *B. pilosa*. In the presence of elicitors plant pathogen recognition would be stimulated in cells of *A. thaliana* resulting in activation of defense mechanisms which causes the production of endogenous signaling compounds. Among the earliest reactions detectable is the production of ROS like NO and H_2O_2 [139]. In the plant immune assay performed the production of H_2O_2 and NO as members of the hypersensitive response in cells of *A. thaliana* was tested. Chitosan was used as a positive control, DAF and DCFDA as indicators for NO and H_2O_2 production respectively. The fluorescence emitted was measured over a time period of 100 min and expressed as Relative Fluorescence Unit (RFU) [139].

None of the endophytic strains tested showed significant induction of nitric oxide or hydrogen peroxide production in *Arabidopsis thaliana*. Compared to the positive control, chitosan, they were all rather inactive and none of them could be considered as containing an elicitor or stimulating immune response in *A. thaliana* (Fig 36a, b).

Fig 36a. Induced H_2O_2 production by strains 1-6

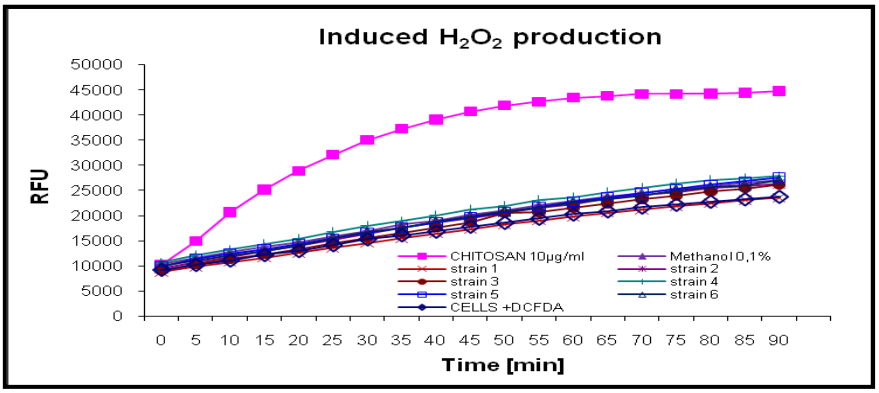

Fig 36b. Induced NO production by strains 1-6

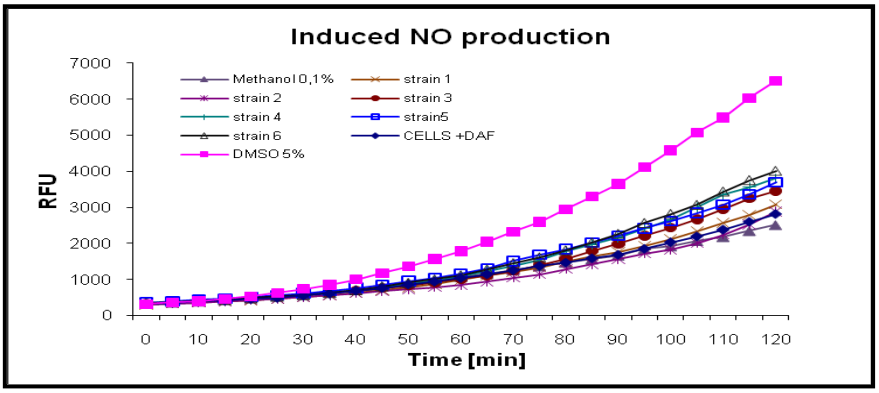

One may speculate about the role of these endophytes in the plant endophyte interaction. They were isolated from a healthy asymptomatic plant which indicates the absence of pathogenic effects at least at the time of isolation from the plant and they did not stimulate immune response in the model plant *A. thaliana* which indicates the absence of elicitors for *A. thaliana*. How they might affect the immune response of their host plant cannot be concluded and still needs deeper long trem studies as the effect on the host plant might differ completely from that on a non host plant. This was shown by a previous study showing that when an endophyte inoculates a nonhost species the pattern of its metabolites differs significantly which suggests that endophytes might respond to specific stimuli from their host [131]. From the results of this plant immune assay it was concluded, that none of the examined endophytes of *B. pilosa* could be considered interesting in the search for crop pests and disease control in ecological agriculture.

3.10. Discussion

In the past decade endophytes have been studied as sources of bioactive natural products. The main reason for this approach is that since endophytes live in association with an eukaryotic host they are not expected to produce compounds that are toxic or harmful to the host [131]. Recently several hypotheses have been made on the role of endophytes in plants and the types of plant endophyte interactions. But still the exact role of endophytes in plants has not been fully declared.

The medicinal plant *Bidens pilosa* was previously investigated for its secondary metabolite constituents and was found to have several biological activities. In addition the plant has been found to be widely spreading in many areas of the world and to be a dominant species wherever it was found [2]. Thus it was necessary to investigate its endophytes and find out if and how they contribute to the dominance and activities of their host plant.

Accordingly eleven endophytic fungal species from the different plant parts (stem, leaf and flower) of *Bidens pilosa* were isolated. The isolation of all these endophytic fungal species from a single plant is not surprising since the most frequently isolated microorganisms from plant tissues are fungi and commonly, several to hundreds of endophyte species can be isolated from a single plant [140]. The taxonomic identification of these endophytic fungi showed a great variability of species which might depend on the environmental conditions under which the host plant was growing [141].

It has been previously reported that different endophyte species are found in different leaf tissues: parenchyma, vascular ducts, dermis etc. This specific distribution might be related to their ability to use different specific substrates [141]. The use of different substrates by endophytes has been demonstrated as a “resource distribution strategy” of the different species living in the same organ [140], to reduce competition between the endosymbionts. This substrate/tissue specialization prevents the host plant from an excessive endophyte population as demonstrated for tropical plants with a high diversity of endophyte species and a “clustered distribution pattern” [141].

Variability of endophytes might depend on the vegetative condition of the host and shows seasonal variation as well, being higher in the spring and is probably dependant on plant physiology [142]. Endophytes live in the intercellular space of the host plant tissues as well as inside the cells causing no visible damage. Therefore the association established between these two organisms was previously considered a classical symbiosis. Plants with associated endophytes have advantages over those without the association including defences against

herbivores resulting in improved biomass and distribution. Moreover the endophyte gains improved access to nutrients and protection from dessication [28].

The metabolic content of the endophytes of *Bidens pilosa* shows high chemical diversity: depsidones (botryorhodines A-D), diphenylethers (botryorhodine E), naphtha-ϒ-pyrones (the aurasperones), anthraquinones (emodin), isocoumarin derivatives (4-hydroxymellein), naphthoquinone spiroketals (preussomerin C), diketopiperazine dimers (asperazine, asperzine A and epicorazine A), epipolythiodioxopiperazines (epicoccin A), oxygenated fatty acids (the octadecadienoic acids), xanthone derivatives (sterigmatocystin), cyclic peptides (tentoxin), diphenyl derivatives (alternariol) and benzopyran derivatives (citrinin).
The metabolites of a single endophyte showed some structural similarities as was observed for the depsidones isolated from *Botryosphaeria rhodina* and the naphthopyrones from *Aspergillus neoniger,* but they also showed a high degree of structural diversity as was observed for the metabolites of *Epiccocum nigrum,* and *Khuskia oryzae.*

Common for all secondary metabolites of the different endophytic fungal species of *Bidens pilosa* was the fact that they were all bioactive metabolites exhibiting either significant antifungal, antibacterial and/or cytotoxic activities. This could be referred to the fact that endophytic fungi are a treasure of bioactive compounds because so many of them inhabit millions of unique biological hosts growing in unusual environments.

Now the question arises about the role of these bioactive metabolites in the plant-endophyte interaction. Several hypotheses have been made to find an answer to this question. It has been suggested that endophytes may contribute to their host plant by producing many bioactive substances to provide protection which aids in the survival of the host plant. Some endophytes are capable of increasing the hosts' effects on other plant species co-growing with them which are usually competitor(s) for the nutrition and the space [2]. This could be the reason why some plants with special endophytes are usually competitive enough to become dominant species [2]. Indeed, the examination of the endophytes of *B. pilosa* showed that this might be true for this plant, as it is known to be a widely spreading, invasive species which might be able to extend its dominance to other regions of the world [39], which could be referred to the bioactive metabolites produced by its endophytes.
This is in agreement with previous reports stating that certain endophytes improve the ecological adaptability of hosts by increasing their tolerance to environmental stresses and resistance to phytopathogens and/or herbivores including some insects feeding on the host plant [2]. This could also be the case with *Bidens pilosa* as several metabolites of its examined endophytes were active against known phytopathogens such as *Fusarium*

oxysporum (e.g. the depsidones, preussomerin C and the oxylipins). It is also quite possible that these endophytes contribute to the reported antifungal activity of the host plant *B. pilosa* against phytopathogens [39]. When each of the antifungal endophytic extracts of *B. pilosa* was tested for antifungal activity against any of the other endophytes isolated from the plant it was found to be inactive which suggests the absence of competition between them and refers to potential mutualistic interactions between them.
None of the natural products isolated from the endophytes of *Bidens pilosa* was identical with the constituents previously isolated from the plant itself.

A very interesting discovery is the detection of the auxin indole carboxylic acid as a major secondary metabolite in all endophytic species of *Bidens pilosa*. The production of this phytohormone by all endophytic species suggests its important role in the host-endophyte interaction. It has been previously noticed that endophyte-infected plants often grow faster than non-infected ones [66]. This effect was referred at least in part to the endophytes' production of phytohormones such as indole-3-acetic acid (IAA), cytokines, and other plant growth-promoting substances [13].
Thus the observed one meter height of *Bidens pilosa* [67] could be referred at least partially to the production of the auxin indole carboxylic acid by all its endophytic fungi. The fact that it was produced by all endophytic strains suggests the presence of potential biosynthesis gene transfer between the different endophytic strains of *B. pilosa.*
Therefore the detected production of bioactive natural products, especially antifungal compounds by the endophytes of *B. pilosa* is not only relevant for a therapeutic potential but it also suggests their possible role in protecting themselves from competitors and the host plant from fungal invaders.
At the time these endophytes were isolated from the plant, it was free from any symptoms of diseases, which could be due to the absence of pathogenic endophytes or due to the presence of latent pathogens. This assumption is based on previous hypotheses suggesting that the asymptomatic endophyte-host interaction involves two actively antagonistic partners. However, a balanced antagonistic endophyte-host interaction does not exclude the possibility that the endophyte may play a beneficial role within its host, for example by inducing defence metabolites potentially active against pathogens, by secreting phytohormones, by supplying the host with nutrients from the rhizosphere and (or) by increasing the metabolic activity of the plant host [143]. Colonisation by endophytes may lead to induced disease resistance, improved growth of the host, protection against pathogenic competitors and insect predators of the host by the synthesis of antagonistic secondary metabolites [1]. Overall it seems that

there is no doubt that both the endophyte and its host determine the outcome of the relationship by the type of products made by both organisms. A fungal endophyte can cause disease symptoms to the host plant under stress conditions. Additionally, it is possible to isolate a latent or weak pathogen from an asymptomatic host plant suggesting that some pathogens may have evolved from endophyte ancestors. It is not clear if some of the plant-isolated fungi, which were thought to be endophytes are actually latent pathogens [6].

This could explain the detection of phytotoxins such as tentoxin, sterigmatocystin, alternariol and hydroxymellein which are known to cause chlorosis in plants as secondary metabolites of the endophytic strains of healthy samples of *Bidens pilosa*. It could be assumed that these toxins are produced by latent pathogens which are waiting for a suitable time of reduced immune response of the plant or senescence to exert their pathogenic effects. On the other hand some endophytic strains produced antifungal compounds with antifungal activity against phytopathogens (botryorhodines A and B, preussomerin C, oxylipins).

At the same time this observed antifungal activity is not affecting any of the other endophytic strains isolated from *B. pilosa*. All these facts let us assume the presence of potential balanced antagonism not only in the host-endophyte interaction but also in the interaction between the different endophytes.

Previously a study was conducted to examine the interaction between an endophytic fungus *Guignardia criticarpa* and the most frequently isolated endophytic bacteria of citrus rootstocks. It was observed that metabolites of the endophytic fungus inhibited the growth of *Bacillus* spp. and stimulated the growth of *Pantoea agglomerans* [133].

The assumed antagonism in the interaction between the endophytes of *B. pilosa* was furthermore supported by the depressed production of antifungal secondary metabolites in dual cultures of endophytic strains exerting high antifungal activities as pure cultures. Upon communication with a known neighboring endophytic strain the endophytes of *B. pilosa* exerted no antifungal effects. This could be referred to the fact that cells present in a medium communicate with each other either by direct cell-to-cell-interactions or through the production of signal substances in the fermentation broth [137]. Interactions between the different microorganisms play a critical role in a coculture and can result in enhanced or inhibited formation of secondary metabolites [138].

Only few fungi are actually capable of causing disease in any one plant, since they must first cross several barriers and overcome plant defences. Pathogens achieve this by their virulence factors, phytotoxic secondary metabolites and exoenzymes. Many fungal endophytes produce phytotoxic metabolites in vitro that are effective against algal and plant test organisms. Thus, being isolated as an endophyte does not exclude the possibility that a

fungus may become pathogenic when the host is stressed or senescent [143]. The plant in turn may possess preformed defence metabolites and, when confronted with a fungal invader, may activate a variety of defence reactions, including not only mechanical defence, e.g. callose and papillae, but also induced defence metabolites. Furthermore an endophyte can act as a pathogen to plant species other than its host [142].

In this case it would stimulate an immune response in the plant and could potentially be used to enhance plant defense responses. Such a reaction could be made use of in ecological agriculture for the biological control of crop pests and diseases. Based on this assumption a plant immune assay has been conducted to find out if any of the isolated endophytic strains of *Bidens pilosa* was producing elicitors that could stimulate immune responses in the model plant *Arabidopsis thaliana* and could then act as potential stimulants of plant immunity for application in agricultural purposes. Results of these screening tests showed the absence of elicitors in the endophytic fungal extracts of *Bidens pilosa.* Since no immune reaction was observed in *Arabidopsis thaliana* in response to any endophytic fungal extract of *Bidens pilosa* it is possible that these endophytes are not exerting a pathogenic effect. These results are quite intriguing as on the other hand the investigation of their metabolic content revealed the presence of some phytotoxins (tentoxin, sterigmatocystin, alternariol, hydroxymellein and adenosyl 9a-D-arabinofuranoside). One might speculate about the role of these endophytes in the interaction with the host plant. Since the endophytic fungal extracts containing these phytotoxins did not stimulate significant immune reponses in *A. thaliana* it follows that their production is in small amounts insufficient of producing defense reactions in the plant. A real understanding of the plant-endophyte interactions needs further deeper, long-term studies on several plant-endophyte systems as more information is required about the virulence degree of an endophytic fungus in the asymptomatic endophyte-host interaction and the host plant response to the endophytic colonization.

4. Materials and methods

4.1. General experimental procedures

NMR spectra were recorded on a Bruker DPX-300 and a Bruker DRX-500 at 300 MHz and 500 MHz for ^{1}H, and 125 MHz for ^{13}C NMR, respectively; chemical shifts are given in δ values (ppm).

IR spectra were recorded on a Bruker FT-IR (IFS 55) spectrometer.

UV spectra were recorded on a Cary 1 Bio UV–vis spectrophotometer (Variant).

HPLC-MS measurements were recorded on an Agilent high performance 1100 series LC/MSD Trap module with an API - electrospray source, PC printer and LC/MSD chemstation software for data aquisition and data analysis.

HRESIMS were recorded on a Finnigan TSQ Quantum Ultra AM Thermo Electron.

Open column chromatography was performed on silica gel 60 (Merck, 0.04–0.063 mm, 230–400 mesh ASTM) and Sephadex LH-20 (Pharmacia).

TLC: silica gel plates (silica gel 60 F254 on aluminium foil or glass, Merck), spots were visualized by spraying with anisaldehyde/sulfuric acid, vanillin/sulphuric acid and Ehrlich`s reagent followed by heating.

Analytical HPLC was conducted on a Shimadzu HPLC system using a Nucleosil 100-5 C18 column (125 x 4.6 mm) with MeCN/0.1% TFA–H2O as eluent (flow rate 1 mL min^{-1}, 15/85 to 100% MeCN in 30 min) and UV detection at 254 nm.

Preparative HPLC was performed on a Shimadzu HPLC system using a Nucleosil 100-5 C18 column (250 x 16 mm, pore diameter 100 Å) using a flow rate of 10 mL min^{-1} starting elution with 25% MeCN and ending with 100% MeCN in 45 min with a UV detector. All solvents used were spectral grade or distilled prior to use.

Lyophilizer drying: All water contained in the fractions was lyophilized with a Virtus Sentry (The Virtus Company Gardiner, New York 12525) apparatus.

4.2. Spray reagents

Vanillin/sulphuric acid: 2.5 g vanillin was added to a solution containing 425 mL methanol, 50 mL acetic acid and 25 mL sulphuric acid. Anisaldehyde/sulphuric acid: 1 mL anisaldehyde was added to 100 mL solution containing 85 mL methanol, 14 mL acetic acid and 1 mL sulphuric acid. Ehrlich's Reagent: 1 g of 4-dimethylaminobenzaldehyde was dissolved in a mixture of 25 mL hydrochloric acid (37%) and 75 mL methanol.

4.3. Microbiological and analytical methods

Pre-screening

The fungal isolates were cultivated in a 1 L scale in 500 mL Erlenmeyer flasks containing 200-300 mL of malt medium, MPG medium, Sbo1, medium, and zeolith medium. The flasks were either shaken for two weeks or left to stand as stationary cultures for three weeks after which culture broth and mycelium were mixed together homogenously and then extracted with ethyl acetate (200 mL). Finally the collected ethyl acetate extract was evaporated to dryness and used for antimicrobial activity tests at a concentration of 100 µg mL^{-1} in methanol.

Storage of strains: deep-freeze storage in a Dewar vessel, Fa. Capillaries for deepfreeze storage: diameter 1.75 mm, length 80 mm, Fa. Hirschmann Laborgeräte, Eberstadt.

Laboratory Shaker: ISF-1-w Adolf Kühner AG. Basel

Autoclave: Albert Dargatz Autoclave, volume 119 L, working temperature 121°C, working pressure 1.2 kg/cm2.

Antimicrobial assay disc: 9 mm diameter, Schleicher & Schuell No. 321 261.

Laminar-Flow-Box: Hareus instrument (Germany)

4.4. Ingredients of different media

All the microbiological work was performed under sterile conditions as usual.

The ingredients of media consisted of:

Malt extract, glucose, caseine peptone, Merck.

Degreased soybean flour, Henselwerk GmbH.

Yeast extract, Oxoid

Oatmeal (Holo Hafergold), Neuform

BiTek Agar-Agar, Difco

Glucose, AppliChem

Maltose, Fluka

Biomalt, Villa Natura

Recepies of the media

All the culture media were autoclaved at 1.2 bar and 121°C for 35 min.

Malt medium (M4)	(g/L)
Malt extract	20
Yeast extract	2
Glucose	10
$(NH_4)_2HPO_4$	0.5
Agar	1
pH	7

MPG-medium (M25)	(g/L)
Glucose	10
Malt extract	20
Soybean flour	2
Yeast extract	1
KH_2PO_4	1
$MgSO_4$.7H2O	0.5
pH	5.5

Zeolith medium (M5)	(g/L)
Glycerin	20
Glucose	2
Peptone	10
NaCl	0.5

Sbo1-Medium(M26)	(g/L)
Glucose	10
Saccharose	10
Yeast extract	0.8
Caseine peptone	2
KH_2PO_4	1
$(NH_4)_2HPO_4$	0.5
$CaCO_3$	0.5
$(NH_4)_2SO_4$	5
pH	6.5

4.5. General laboratory chemicals

Anisaldehyde (4-methoxybenzaldehyde)	Merck
(-)-2-Butanol	Merck
Dimethylsulfoxide	Merck
Formaldehyde	Merck
L-(+)-Ascorbic acid	Merck
Hydrochloric acid	Merck
Potassium hydroxide	Merck
Pyridine	Merck
Concentrated sulphuric acid	Merck
Triflouroacetic acid (TFA)	Merck
Concentrated ammonia solution	Fluka

4.6. Plant collection and endophyte isolation

The plant was collected in October 2006 from the museum of agriculture near Cairo/Egypt and identified by Dr. Abdel Megid (Head of Department of Botany at the Museum of Agriculture, Cairo/Egypt). Plant materials were cut into small pieces, washed with sterilized demineralized water, then thoroughly surface treated with 70% ethanol for 1-2 minutes and ultimately air dried under a laminar flow hood. This is done in order to eliminate surface contaminating microbes. With a sterile scalpel, outer tissues were removed from the plant samples and the inner tissues were carefully dissected under sterile conditions and placed onto malt agar plates containing antibiotic. After 3-4 weeks of incubation at room temperature, hyphal tips of the fungi were removed and transferred to fresh malt agar medium. Plates were prepared in duplicates to eliminate the possibility of contamination. Pure strains were isolated by repeated inoculation.

4.7. Cultivation of pure fungal strains

Fungi were grown on malt agar medium at room temperature for several days. When fungal hyphae almost covered the surface of the MA plate, cultures were stored at 4ºC for a maximum period of 6 months, and then re-inoculated onto fresh MA media.

4.8. Cultivation of dual cultures

Each fungus (*B. rhodina, A. neoniger, E. nigrum and K. oryzae*) was grown on potato dextrose agar (PDA) at 23ºC for 14 days and the mycelium of each plate was cut into 4 pieces each of which was used as an inoculum in a 1 L Erlenmeyer flask, containing 250 mL of MPG medium (M25). Each Erlenmeyer flask was inoculated with two different endophytic fungal strains. Three dual cultures were formed by cultivating *B. rhodina* with *A. neoniger*, *B. rhodina* with *E. nigrum* and *B. rhodina* with *K.oryzae* as standing cultures in medium M25 for 21 days.

4.9. Fungal identification

Fungal strains were identified using a molecular biological protocol by DNA amplification and sequencing of the internal transcribed spacer (ITS) region. This was done by Dr. Grit Walther at the Central Bureau for Schimmelcultures in the Netherlands.

4.10. Cultivation for screening and isolation of secondary metabolites

Each fungus was grown on potato dextrose agar (PDA) at 23ºC for 14 days and the mycelium of each plate was cut into 12 pieces each of which was used as an inoculum in a

1L Erlenmeyer flask, containing 250 mL of the corresponding culture medium. Incubation was carried out for 21 days (23 ºC) under static conditions in case of stationary cultures and for 14 days with shaking in case of shaken cultures. The extract was prepared by homogenizing the culture filtrate and the mycelium of each Erlenmeyer flask and then macerating for 24 h in 200 mL EtOAc, which was then collected by decantation. After evaporation to dryness and defatting with n-hexane the crude extract was obtained. For large scale fermentation the same procedure was carried out using the required amount of culture media and PDA plates for cultivation followed by extraction with ethylacetate as described above.

4.11. Biological screening methods

4.11.1. Antimicrobial screening

Antifungal activity tests were performed by Mrs Schwinger (technical assistant at the department of Biomolecular Chemistry of the Hans Knöll Institute). Activities were studied qualitatively by agar diffusion tests according to the literature [144-145] and quantitatively by determination of minimal inhibitory concentration (MIC) according to the NCCLS guidelines using the broth micro dilution method [145]. Fifty micro liters of the test compound solution in methanol were serially diluted by factor two with the culture medium (RPMI 1640 with L-glutamine, MOPS and without sodium bicarbonate, LONZA Verviers SPRL, Belgium). Then, the wells were inoculated with 50 µl of the test organism to give a final concentration of $6x10^3$ CFU mL^{-1}. After incubation of the microtiter plates at 37°C (*Aspergillus terreus*) for 24 h, the MIC-values were read with a Nepheloscan Ascent 1.4 automatic plate reader (Lab systems, Vantaa, Finnland) as the lowest dilution of compound allowing no visible growth. The MIC for *Fusarium oxysporum* and *Bacillus subtilis* was determined by the agar diffusion method. Fifty microliters of each of the 12 serial twofold dilutions were filled in agar (malt extract agar from Roth, Karlsruhe, Germany; seeded with 0.5 mL of a pretested mycelial solution) holes of 9 mm in diameter. After incubation for 24 h the MIC was read as the lowest concentration giving an inhibition zone.

Test organisms (*Bacillus subtilis* ATCC 6633*, Escherichia coli* SG 458, *Streptococcus aureus* BB 271*, Micrococcus luteus* SG 125 A*, Mycobacterium vaccae* IMET 10670*, Saccharomyces cerevisiae Gi300, Sporobolomyces salmonicolor* SBUG 549*, Candida albicans* ATCC 18804*,Penicillium notatum* JP 36*, Fusarium culmorum* JP 15*, Phoma destructiva* 1015*,Aspergillus fumigatus* ATCC 46645*, Aspergillus terreus)* were suspended in the melted agar medium and poured into Petri dishes. Holes of 9 mm in diameter were cut in the agar and filled with 50 µl of a 100 mg/l solution of the crude extract. Inhibition zones were measured with a ruler after overnight incubation.

4.11.2. Antiproliferative and cytotoxic assays

The tests for antiproliferative and cytotoxic activity were carried out by Dr. Dahse at the Department of Infection Biology of the Hans-Knoll Institute.

Cells and culture conditions

Cells of HUVEC (ATCC CRL-1730), K-562 (DSM ACC 10) and HeLa (DSM ACC 57) were cultured in DMEM (CAMBREX 12-614F), RPMI 1640 (CAMBREX 12-167F) and RPMI 1640 (CAMBREX 12-167F) respectively. All cells were grown in the appropriate cell culture medium supplemented with 10 mL l^{-1} ultraglutamine 1 (Cambrex 17-605E/U1), 500 µl l^{-1} gentamicin sulfate (CAMBREX 17-518Z), and 10 % heat inactivated fetal bovine serum (PAA A15-144) at 37°C in high density polyethylene flasks (NUNC 156340).

Antiproliferative assay

The test substances were dissolved in DMSO before being diluted in DMEM. The adherent cells were harvested at the logarithmic growth phase after soft trypsinization, using 0.25 % trypsin in PBS containing 0.02 % EDTA (Biochrom KG L 2163). For each experiment, approximately 10.000 cells were seeded with 0.1 mL culture medium per well of the 96-well microplates (NUNC 167008).

Cytotoxic assay

For the cytotoxic assay, HeLa cells were pre-incubated for 48 hours without the test substances. The dilutions of the compounds were carried out carefully on the subconfluent monolayers of HeLa cells after the pre-incubation time. Cells were incubated with dilutions of the test substances for 72 hours at 37 °C in a humidified atmosphere and 5 % CO_2.

Method of evaluation

For estimating the influence of chemical compounds on cell proliferation of K-562, the numbers of viable cells present in multiwell plates were determined via CellTiter-Blue® assay. The indicator dye resazurin was used to measure the metabolic capacity of cells as an indicator of cell viability. Viable cells of untreated control retain the ability to reduce resazurin into resorufin, which is highly fluorescent. Nonviable cells rapidly lose metabolic capacity, do not reduce the indicator dye, and thus do not generate a fluorescent signal. Under our experimental conditions, the signal from the CellTiter-Blue® reagent is proportional to the number of viable cells. The adherent HUVEC and HeLa cells were fixed by glutaraldehyde and stained with a 0.05 % solution of methylene blue for 15 min. After gentle washing the

stain was eluted with 0.2 mL of 0.33 N HCl in the wells. The optical densities were measured at 660 nm in SUNRISE microplate reader (TECAN). The GI_{50} and CC_{50} values were defined as being where the dose response curve intersected the 50% line, compared to untreated control. The comparisons of the different values were performed with software Magellan (TECAN).

4.12.3. Spectrofluorometric assay

The spectrofluorometric assay was performed by Clara Steinhauser at the Institute for Biochemical Plant Pathology of the Helmholtz Zentrum in Munich.

Cell culture

Suspension cells were generally grown in the dark on a rotary shaker at 120 rpm and 27°C. Every week two gram cells were sub-cultured with a sifter in 40 mL fresh growth medium modified after Murashige & Skoog (Murashige and Skoog, 1962) in a 200 mL cell culture flask. For *Arabidopsis thaliana* cells HaM or PS Medium were taken. All experiments were performed using cells in the logarithmic growth phase, 5-6 days after sub-culturing.

Detection of NO

Microscopy

The detection of NO (carried out by Mrs Clara Steinhauser, PhD student at the Institute for Plant Pathology of the Helmhotz zentrum in Munich) was done with NO-reactive fluorescent indicators in conjunction with fluorescence microcopy. The nitric oxide indicators used were DAF-FM and DAF-FM diacetate.

NO and ROS quantification

An induction of NO and ROS in *Arabidopsis* suspension cells was confirmed by photometrical measurement of fluorescence intensities of DAF-FM and H2DCF-DA respectively using a Genios plate reader (Tecan, Crailsheim) with usual FITC excitation and emission filters. Chitosan treated cells were stained by addition of 10 µl DAF-FM or H2DCF-DA (both dyes at 10 µM) to 300 µl of cells in a black 96 well microplate (Greiner Bio-One, Essen). The fluorescence intensity was measured every min over a time period of 100 min and expressed in relative fluorescence units (RFU). The plate was rocked before measuring for 5 sec.

4.13. Isolation and identification of metabolites

4.13.1. *Botryosphaeria rhodina*

The strain was isolated from the sterilized stem parts of the host plant *Bidens pilosa*. In the antimicrobial prescreening the crude extract exhibited strong antifungal activity particularly against *Aspergillus niger.* The fungus was cultured in all four different media (M4, M5, M25 and M26) both as a shaken and stationary culture after which the antifungal activity of each extract was examined. Both the chemical and biological analyses showed that the antimicrobial activity of the fungal extract and the production of secondary metabolites were highest using a stationary culture (21 days) at 23 °C of M25. The major products of the extract were botryorhodine A, B and C. Activity-guided isolation started by subjecting the extract to fractionation on a silica gel column using (hexane: EtOAc / 1:1) as eluent which resulted in 9 main fractions. The fractions exhibiting antimicrobial activity were successively purified on silica gel using ($CHCl_3$: MeOH / 9:1); Sephadex LH-20 (MeOH) and finally RP-18 Silica on preparative HPLC starting gradient elution with 25 % acetonitrile in H_2O and ending with 100 % acetonitrile after 45 minutes, to give botryorhodine A (8 mg), botryorhodine B (5 mg), botryorhodine C (2 mg), botryorhodine D (3 mg), preussomerin C (5 mg), botryorhodine E (2.5 mg). The plant growth promoting auxin indole acetic acid and the phytotoxin 4-hydroxymellein were isolated using Sephadex LH-20 (MeOH) and identified by comparison of their chromatographic, UV and MS data with authentic samples.

4.13.2. *Aspergillus neoniger*

The strain was obtained from the leaves of the host plant *B. pilosa*. Large scale fermentation (performed by Mrs Schwinger, technical assistant at the Department of Biomolecular Chemistry of the Hans Knöll Institute) of this endophytic strain was carried out as a stationary culture in medium M5. The crude extract was dissolved in methanol and examined by TLC and analytical HPLC. The antimicrobial activity of the fungal extract was confirmed by agar diffusion assay against the most sensitive strain *A. terreus*. Chromatographic fractionation was started using Silica gel column with a mixed solvent system of $CHCl_3$: methanol / 9:1 (250 mL) followed by gradual increase in polarity until final elution with 100 % methanol. Further fractionation was carried out on Sephadex LH-20 using methanol as a solvent. Final purification of the obtained secondary metabolites was achieved by the preparative HPLC starting with a gradient solvent system of 25 % acetonitrile in H2O until 100 % acetonitrile. Identification of the isolated compounds was carried out using 1 and 2D NMR experiments including ^{1}H-^{13}C NMR, COSY, HSQC, DEPT and HMBC. This resulted in the identification of six compounds: asperpyrone D (4 mg), aurasperone A (6 mg),

dianhydroaurasperone C (8 mg), aurasperone D (5 mg), asperazine (3 mg) and asperazine analogue (2 mg), as well as indole carboxylic acid (2 mg) which was obtained as a side-product during the purification steps.

4.13.3. *Epicoccum nigrum*

The strain was isolated from the flowering parts of the host plant *Bidens pilosa*. Fourteen days malt agar-plate cultures (23 ºC) were prepared and the well grown agar plate cultures were used to inoculate a liquid malt medium. The residue (7.5 g) of the evaporated ethyl acetate extract from 30 l of culture was first pre-screened and then applied to a silica gel column in chloroform. Elution was performed with 300 mL portions of $CHCl_3$, $CHCl_3$/MeOH (9:1), $CHCl_3$/MeOH (7:3), $CHCl_3$/MeOH (1:1) and MeOH. The fractions obtained were separated using Sephadex LH 20 and HLPC on reverse phase column (RP18 Spherisorb, 25 mm x 250 mm) using a binary gradient (water/acetonitrile 95:5 to 5:95; 30 min). The individual peaks were collected and purified by the same preparative procedure to get the purified compounds.

4.13.4. *Khuskia oryzae*

The strain was isolated from the stem of the host plant *Bidens pilosa and* was cultivated in a large scale (20 L) as a stationary culture in medium M25. The dried crude extract (3.2 g) was subjected to silica gel chromatography (silica gel 60, Merck, 0,063~0.1 mm, column 4 x 60 cm), using stepwise $CHCl_3$, and $CHCl_3$–MeOH (9:1, 8:2, 1:1, v / v) as eluents. Final purification was achieved by preparative HPLC (Sperisorb ODS-2 RP18, 5 µm (Promochem), 250 x 25 mm, water/methanol 7:3), 10 mL/minute, UV-detection 210 nm). These purifaction steps resulted in the isolation and identification of four secondary metabolites: sterigmatocystin (3 mg), 9-oxo-(10E, 12E)-octadecadienoic acid (2.7 mg), 8-oxo-(9E, 11E)-octadecadienoic acid (3.2 mg) and indole carboxylic acid.

4.13.5. Strain 20076005

This strain was isolated from the sterilized leaves of *Bidens pilosa* and was cultivated in medium M4 as a shaken culture. The residue obtained after extraction with ethyl acetate and evaporation to dryness (6 g) from 40 l of culture was first pre-screened and then applied to a silica gel column in chloroform. Elution was performed with 500 mL portions of $CHCl_3$, $CHCl_3$/MeOH (9:1), and $CHCl_3$/MeOH (7:3). The fractions obtained were then separated using Sephadex LH-20 and HLPC on reverse phase column (RP8 Spherisorb, 25 mm x 250 mm) using a binary gradient (water/acetonitrile 95:5 to 5:95; 30 min). The individual peaks were collected and purified by the same preparative procedure. After purification on

preparative HPLC the following compounds were identified: alternariol (4.2 mg), ascaridole (3.5 mg), tentoxin (2.7 mg), emodin (2.5 mg) as well as indole carboxylic acid (2 mg).

4.13.6. Strain 20076002

The strain was isolated from the sterilized stem parts of *Bidens pilosa* and was cultivated in M25 as a shaken culture. The fractionation performed on the ethyl acetate extract obtained from small scale fermentation of this fungal strain resulted in the isolation of the major secondary metabolite which has been identified as citrinin (4.2 mg) by comparison with an authentic sample.

5. Summary

In the past decade endophytes have gained increasing attention due to their production of bioactive natural products.

The objective of this thesis was the investigation of the bioactive secondary metabolites of the endophytic fungal strains of the important medicinal plant *Bidens pilosa* (*Asteraceae*). This was done in an attempt of understanding the plant endophyte interactions in this plant and to search for new bioactive natural products.

Eleven different fungal strains were isolated from different plant parts (leaves, stems and flowers). The antimicrobial activity screening showed that six out of the eleven strains were antimicrobially active and therefore they were chosen for further chemical investigations. Activity-guided fractionation resulted in the isolation and structure elucidation of 25 pure compounds representing different structural subclasses: depsidones (botryorhodines A-D), diphenylethers (botryorhodine E), naphthopyrones (the aurasperones), anthraquinones (emodin), isocoumarin derivatives (4-hydroxymellein), naphthoquinone spiroketals (preussomerin C), diketopiperazine dimers (asperazine, asperzine A and *cis*-L-(-)-3, 6-dibenzyl-2, 5-dioxopiperazine), epipolythiodioxopiperazines (epicoccin A), oxygenated fatty acids (the octadecadienoic acids), xanthone derivatives (sterigmatocystin), cyclic peptides (tentoxin), diphenyl derivatives (alternariol) and benzopyran derivatives (citrinin).

Predominantly the antifungal and cytotoxic activity of the isolated compounds was examined. Furthermore a plant immune assay was performed in an attempt to find potential elicitors of immune response which could be used in enhancing plant immunity and controlling crop diseases.

The first strain was identified as a *Botryosphaeria rhodina* strain. Through bioactivity-guided fractionation the isolation and full characterization of four depsidones, botryorhodines A–D (1-4), which have not been isolated from a natural source before was achieved. Botryorhodines A and B were found to be significantly active against a variety of pathogenic fungi. This antifungal activity is not only relevant for a potential therapeutic application, but also suggests that endophytes might be involved in protecting the host plant from invasion of phytopathogens. Botryorhodines A and B also showed significant antiproliferative effects with botryorhodine A exhibiting higher cytostatic activity. From the same strain the potent antifungal compound preussomerin C was also isolated which is active against several phytopathogenic fungi. In addition a new diphenyl ether (botryorhodine E) with moderate cytostatic activity was also identified. Furthermore hydroxymellein which is known to be of significant antimicrobial activity was identified as a secondary metabolite of this strain as well. The major peak observed in the HPLC profile of this endophytic fungal extract represented

the plant auxin indole carboxylic acid which is known for stimulating plant growth and elongation.

The second strain investigated was identified as *Aspergillus neoniger* which showed significant cytotoxic activity in the screening assays. Four known naphthopyrones: aurasperone A, asperpyrone D, dianhydroaurasperone C, and aurasperone D have been isolated from this endophyte strain. In addition asperazine and a new asperazine analogue (asperazine A) have been identified as major metabolites of this strain as well. Significant cytotoxicity has been detected for aurasperone D and asperpyrone D against K-562, HUVEC and HeLa cell lines. Weak cytotoxicity was observed for asperazine, asperazine A and aurasperone A. No cytotoxicity was detected for dianhydroaurasperone C. Asperazine exerted higher cytotoxic activity than its analogue. Similar to the first endophytic strain indole carboxylic acid has been observed as a major product in the HPLC profile of this fungal extract.

An *Epicoccum nigrum* strain was selected for investigation of its metabolic content due to its observed high antifungal activity against several fungal species in the antimicrobial screening assay especially against *A. terreus*. From this strain two diketopiperazines, epicoccin A and *cis*-L-(-)-3, 6-dibenzyl-2, 5-dioxopiperazine, have been isolated, as well as the antiviral compound adenosyl 9α-D-arabinofuranoside.

From a *Khuskia oryzae* strain two oxylipins were identified: a new 8-oxo-(9*E*, 11*E)*-octadecadienoic acid with moderate cytotoxic activity and 9-oxo-(10*E*, 12*E*)-octadecadienoic acid, as well as the phytotoxic mycotoxin sterigmatocystin. In the cytotoxic assay performed 8-oxo-(9*E*, 11*E*)-octadecadienoic acid was slightly less active than its analogue 9-oxo-(10*E*, 12*E*)-octadecadienoic acid. This is the first report of the production of bioactive metabolites from *K. oryzae* other than griseofulvin.

Furthermore the antifungal phytotoxin alternariol has been isolated and identified as the major secondary metabolite of the fifth strain. In addition the phytotoxin tentoxin, the antibacterial secondary metabolite emodin and the antitumoral and antifungal compound ascaridole were also identified in this strain. The production of a phytotoxin like tentoxin by an endophyte isolated from healthy plant parts of *B.pilosa* lets us assume its potential latent pathogenicity.

The last strain investigated contained the antifungal compound citrinin as the only active constituent.

A plant immune assay was carried out on all endophytic fungal extracts to examine the effect of their constitutents on the immune system of the model plant *Arabidopsis thaliana*. The assay was performed in collaboration with the Institute of Biochemical Plant Pathology of the

Helmholtz Zentrum in Munich and aimed to detect the production of nitric oxide or H_2O_2 by the plant cells, which serve as indicators of plant defense reactions.

All strains gave weak or no production of H_2O_2 and NO, thus indicating the absence of elicitors of immune response in these endophytic fungal extracts.

It was interesting to find out that nearly all endophytic fungi of *Bidens pilosa* exhibited antimicrobial activity. When the most active strains were examined for their active constituents, they were all found to produce potent antifungal compounds. This supports the hypothesis that endophytes produce bioactive natural products to protect the plant from phytopathogens and themselves from competitors.

Surprisingly, these strains were not exerting antifungal effects against each other in agar diffusion assays which suggests the potential presence of mutualism in the host-endophyte and endophyte-endophyte interactions. Furthermore mixed fermentations of endophytic strains exerting antifungal activity in their pure cultures were formed. Surprisingly no antifungal activity was exhibited by the extracts of these cocultures. These results indicate that these endophytic strains are capable of recognizing each other. Upon communicating with each other they seem to interfere with the metabolic pathways of neighboring endophytes, thereby depressing their production of antifungal secondary metabolites or inactivating them.

Interestingly the plant auxin indole carboxylic acid has been detected in all endophytic fungal strains of *Bidens pilosa*. Certainly this phytohormone serves to stimulate plant growth and elongation and also indicates the possible presence of genetic cross linking between the different endophytic fungi of *Bidens pilosa*.

After having identified these secondary metabolites from the different endophytic fungal strains of *B. pilosa* it seems that these bioactive metabolites contribute to the known dominance of this plant species. Its one meter height is most probably stimulated by the production of the auxin indole carboxylic acid by all its endophytic strains. The antifungal activity of some secondary metabolites against phytopathogens suggests a plant protective effect exerted by their endophytes against microbial predators.

6. Zusammenfassung

In den letzten zehn Jahren gewannen Endophyten zunehmende Aukmerksamkeit im Gebiet der Naturstoffforschung wegen ihrer Produktion von bioaktiven Naturstoffen.

Das Ziel dieser Arbeit war die Untersuchung der endophytischen Sekundärmetabolite der Heilpflanze *Bidens pilosa* (*Asteraceae*) und die Evaluierung ihrer zytotoxischen und antimikrobiellen Wirkung. Dies wurde durchgeführt, um Informationen über die Pflanze-Endophyt Interaktion zu erhalten und um neue bioaktive Naturstoffe zu entdecken. Elf verschiedene endophytische Pilze wurden aus den verschiedenen Pflanzenteilen (Stengel, Blatt und Blume) isoliert. Alle Stämme wurden einem chemischen und biologischen Screening unter Variation der Kultivierungsbedingungen unterzogen. Bei diesem Screening erwiesen sich sechs Stämme und ihre Metabolite als antimikrobiell wirksam. Daher wurden diese Stämme im größeren Maßstab kultiviert, so dass ihre Sekundärstoffe isoliert und identifiziert werden konnten. Anhand der von Bioaktivität geleiteten Chromatographie wurden 25 Substanzen identifiziert, die sich als strukturell vielfältige, teils neue Naturstoffe erwiesen: Depsidone (Botryorhodine A-D), Diphenylether (Botryorhodine E), Naphthopyrone (Aurasperone), Anthrachinone (Emodin), Isocoumarin Derivate (4-hydroxymellein), Naphthochinon Spiroketal (Preussomerin C), Diketopiperazin Dimere (Asperazin, Asperzin A und *cis*-L-(-)-3, 6-Dibenzyl-2, 5-Dioxopiperazin), Epipolythiodioxopiperazin (Epicoccin A), oxygenierte Fettsäuren (Octadecadiensäuren), Xanthon Derivate (Sterigmatocystin), zyclische Peptide (Tentoxin), Diphenyl Derivate (Alternariol) and Benzopyran Derivate (Citrinin).

Der erste Stamm wurde als *Botryosphaeria rhodina* identifiziert. Vier neue Depsidone (Botryorhodine A-D) wurden aus diesem Stamm isoliert und mittels ein- und zweidimensioneller NMR Spektroskopie strukturell aufgeklärt. Botryorhodine A und B zeigten besondere antifungale Wirkung gegen mehrere pathogene Pilze, weshalb sie nicht nur für potentielle therapeutische Anwendungen von Interesse wären, sondern ebenfalls in der Pflanze-Endophyt Interaktion von Bedeutung sind. Beide Substanzen wiesen potente antiproliferative Wirkung auf, wobei Botryorhodine A die höhere zytostatische Aktivität zeigte. Ebenso wurde aus diesem Stamm der antifungale Naturstoff Preussomerin C erhalten, der für seine Wirkung gegen phytopathogene Pilze bekannt ist. Des Weiteren wurde ein neuer Diphenylether (Botryorhodine E) isoliert, der moderate zytostatische Wikung aufwies. Der antimikrobielle Sekundärmetabolit Hydroxymellein und das Pflanzenhormon Indolcarboxylsäure, das für seine wachstumsstimulierende Wirkung auf Pflanzen bekannt ist, wurden ebenfalls aus diesem Stamm isoliert.

Der zweite Stamm wurde als *Aspergillus neoniger* identifiziert. In der zytotoxischen Testung wies der Pilzextrakt besondere zytotoxische Wirkung auf. Vier bekannte Naphthopyrone wurden aus diesem endophtischen Pilz erhalten: Aurasperon A, Aurasperon D, Asperpyron D und Dianhydroaurasperon C. Ebenso wurden Asperazin und ein Asperazin-Analogon (Asperazine A) als Hauptprodukte dieses Stammes erhalten. Besondere zytotoxische Wirkung zeigten Aurasperon D und Asperpyron D gegen K-562-, HUVEC- und HeLa-Zelllinien. Dagegen konnte für Asperazin, sein Analogon und Aurasperon A nur schwache zytotoxische Wirkung nachgewiesen werden. Analog zum ersten Stamm produzierte auch dieser Endophyt das Phytohormon Indolcarboxylsäure.

Ein *Epicoccum nigrum* Stamm zeigte im antimikrobiellen Screening antifungale Wirkung gegen mehrere Pilzstämme. Zwei bekannte Diketopiperazine (*cis*-L-(-)-3, 6-Dibenzyl-2, 5-Dioxopiperazine und Epicoccin A) wurden aus diesem Stamm isoliert, sowie die antivirale Substanz adenoside 9α-D-Arabinofuranosid.

Des Weiteren wurde ein *Khuskia oryzae* Stamm bearbeitet, der in der Literatur nur für die Produktion von Griseofulvin bekannt ist. Zwei Oxylipine wurden aus diesem Stamm identifiziert, wobei 8-Oxo-(9*E*, 11*E*)-octadecadienoic acid sich als ein neues Oxylipin erwies. In der zytotoxischen Testung zeigte diese Substanz schwächere Aktivität als das zweite Oxylipin 9-Oxo-(10*E*, 12*E*)-octadecadienoic acid gegen die untersuchten Zelllinien. Ebenso wurde das phtotoxische Mykotoxin Stergmatocystin aus diesem Stamm erhalten.

Als Hauptprodukt des fünften Stammes wurde der phytotoxische und antifungale Naturstoff Alternariol produziert. Ebenso wurde festgestellt, dass dieser Stamm das Phytotoxin Tentoxin, den antibakteriellen Naturstoff Emodin, sowie die antitumorale und antifungale Substanz Ascaridol produziert. Die Produktion von Phytotoxinen in diesem Stamm, der aus infektionslosen Pflanzenteilen isoliert wurde, könnte auf potentielle latente Pathogenität dieses Pilzstammes deuten.

Als einziges aktives Hauptprodukt wurde die antifungale Substanz Citrinin im sechsten Stamm nachgewiesen.

Zur weiteren Evaluierung der biologischen Aktivität dieser endophytischen Pilzstämme wurden ihre Extrakte nach ihrer Wirkung auf das Immunsystem der Modelpflanze *Arabidopsis thaliana* geprüft. Die Testung wurde in Zusammenarbeit mit dem Institut für Biomolekulare Pflanzenpathologie (Helmholtz Zentrum) in München durchgeführt und hatte zum Ziel die Identifikation von Elicitoren der pflanzlichen Abwehr in den Pilzextrakten. Ergebnisse ergaben jedoch schwache oder keine Produktion reaktiver Sauerstoffspezies, was auf die Abwesenheit von Elicitoren des pflanzlichen Immunsystems in den endophytischen Pilzextrakten deutet.

Zur Untersuchung der Interaktion zwischen den Endophyten wurde die Wirkung der antifungalen Pilzextrakte auf das Wachstum der anderen endophytischen Pilzstämme der Pflanze getestet. Die durchgeführten Testungen ergaben, dass keiner dieser Stämme von dieser Aktivität beeinflußt wurde, was auf die wahrscheinliche Abwesenheit von Konkurrenz unter den endophytischen Pilzstämmen hindeutet und eine mutualistische Interaktion vermuten lässt.

Außerdem wurden gemischte Kulturen aus den endophytischen Pilzstämmen gebildet, die als reine Kulturen besondere antifungale Wirkung zeigten. Überraschenderweise zeigten die Extrakte dieser Kokulturen keine antifungale Wirkung mehr. Es wurde festgestellt, dass die Produktion der antifungalen Sekundärmetabolite unterdrückt oder gehemmt wurde. Diese Ergebnisse deuten darauf hin, dass die Endophyten der Wirtspflanze *B. Pilosa* ihre benachbarten endophytischen Pilzstämme erkennen können. In Kontakt mit ihnen sind sie anscheinend in der Lage, die Produktion antifungaler Sekundärmetabolite zu hemmen oder produzierte antifungale Metabolite zu deaktivieren.

Ebenso ist von Bedeutung die Tatsache, dass fast alle endophytischen Pilze dieser Arzneipflanze besondere antimikrobielle Wirkung nachwiesen. Die Unterschung der aktivsten Stämme führte zur Identifizierung mehrerer antifungaler Sekundärmetabolite, was darauf hindeutet, dass diese bei der Verteidigung der Wirtspflanze gegen pathogene Pilze, sowie der Verteidigung der Endophyten gegen konkurrierende endophytische Pilzstämme eine Rolle spielen.

Es wurde festgetstellt, dass alle untersuchten Endophyten der Wirtspflanze *Bidens pilosa* das pflanzliche Hormon Indolcarboxylsäure produzieren, was die Anwesenheit eines Austausches biosynthetischer Gene zwischen Pflanze und Endophyt vermuten lässt.

Die Produktion der beschriebenen bioaktiven Sekundärmetabolite unterstützt die Vermutung, dass die Endophyten von *Bidens pilosa* zur bekannten schnellen Verbreitung und Dominanz dieser Pflanze beitragen. Ihre ein Meter Höhe wird sicherlich durch die Produktion des Wachstumshormons Indolcarboxylsäure von ihren Endophyten stimuliert.

7. References

1. Zhang, H. W., Y. C. Song, and R. X. Tan, Biology and chemistry of endophytes. Nat. Prod. Rep., 2006. **23**(5): p. 753-771.
2. Strobel, G., B. Daisy, U. Castillo, and J. Harper, Natural products from endophytic microorganisms. J. Nat. Prod., 2004. **67**(2): p. 257-268.
3. White, J. F., G. Morganjones, and A. C. Morrow, Taxonomy, life-cycle, reproduction and detection of *Acremonium* endophytes. Agricult. Ecosyst. Env., 1993. **44**(1-4): p. 13-37.
4. Aly, A. H., R. Edrada-Ebel, I. D. Indriani, V. Wray, W. E. Muller, F. Totzke, U. Zirrgiebel, C. Schachtele, M. H. Kubbutat, W. H. Lin, P. Proksch, and R. Ebel, Cytotoxic metabolites from the fungal endophyte *Alternaria* sp. and their subsequent detection in its host plant *Polygonum senegalense.* J. Nat. Prod., 2008. **71**(6): p. 972-980.
5. Schulz, B. and C. Boyle, The endophytic continuum. Mycol. Res., 2005. **109**: p. 661-686.
6. Kogel, K. H., P. Franken, and R. Huckelhoven, Endophyte or parasite-what decides? Curr. Opin. Plant Biol., 2006. **9**(4): p. 358-363.
7. Saikkonen, K., P. Wali, M. Helander, and S. H. Faeth, Evolution of endophyte-plant symbioses. Trends Plant. Sci., 2004. **9**(6): p. 275-280.
8. Stierle, A., G. Strobel, and D. Stierle, Taxol and taxane production by *Taxomyces andreanae*, an endophytic fungus of Pacific yew. Science, 1993. **260**(5105): p. 214-216.
9. Strobel, G. A., Microbial gifts from rain forests. Can. J. Plant Pathol. Rev. Can. Phytopathol., 2002. **24**(1): p. 14-20.
10. Faeth, S. H., and W. F. Fagan, Fungal endophytes: Common host plant symbionts but uncommon mutualists. Integr. Comp. Biol., 2002. **42**(2): p. 360-368.
11. Siegel, M. R. and L. P. Bush, Defensive chemicals in grass-fungal endophyte associations. Recent Adv. Phytochem., 1996. **30**: p. 81-118.
12. Casabuono, A. C. and A. B. Pomilio, Alkaloids from endophyte-infected *Festuca argentina.* J. Ethnopharm., 1997. **57**(1): p. 1-9.
13. Tan, R. X. and W. X. Zou, Endophytes: a rich source of functional metabolites. Nat. Prod. Rep., 2001. **18**(4): p. 448-459.
14. Strobel, G. A., Rainforest endophytes and bioactive products. Crit. Rev. Biotechnol., 2002. **22**(4): p. 315-333.
15. Strobel, G. and B. Daisy, Bioprospecting for microbial endophytes and their natural products. Microbiol. Mol. Biol. Rev., 2003. **67**(4): p. 491-502.
16. Clay, K., Fungal endophytes of plants: Biological and chemical diversity. Nat. Toxins, 1993. **1**(3): p. 147-149.
17. Larsen, T. O., J. Smedsgaard, K. F. Nielsen, M. E. Hansen, and J. C. Frisvad, Phenotypic taxonomy and metabolite profiling in microbial drug discovery. Nat. Prod. Rep., 2005. **22**(6): p. 672-695.
18. Bisby, G. R., Geographical distribution of fungi. Botanical Rev., 1943. **9**: p. 466-482.
19. Strobel, G. A., R. V. Miller, C. Miller, M. Condron, D. B. Teplow, and W. M. Hess, Cryptocandin, a potent antimycotic from the endophytic fungus *Cryptospsporiopsis* cf. *quercina.* Microbiol., 1999. **145**(8): p. 1919-1926.
20. Li, J.Y., J. K. Harper, D. M. Grant, B. O. Tombe, B. Bashyal, W. M. Hess, and G. A. Strobel, Ambuic acid, a highly functionalized cyclohexenone with antifungal activity from *Pestalotiopsis* spp. *and Monochaetia* sp. Phytochem., 2001. **56**(5): p. 463-468.
21. Li, J. Y. and G. A. Strobel, Jesterone and hydroxyjesterone antioomycete cyclohexenenone epoxides from the endophytic fungus *Pestalotiopsis jesteri.* Phytochemistry, 2001. **57**(2): p. 261-265.

22. Brady, S.F., S.M. Bondi, and J. Clardy, The guanacastepenes: a highly diverse family of secondary metabolites produced by an endophytic fungus. J. Am. Chem. Soc., 2001. **123**(40): p. 9900-9901.
23. Ma, Y. M., Y. Li, J. Y. Liu, Y. C. Song, and R. X. Tan, Anti-Helicobacter pylori metabolites from *Rhizoctonia sp.* Cy064, an endophytic fungus in *Cynodon dactylon.* Fitoterapia, 2004. **75**(5): p. 451-456.
24. Hellwig, V., T. Grothe, A. Mayer-Bartschmid, R. Endermann, F. U. Geschke, T. Henkel, and M. Stadler, Altersetin, a new antibiotic from cultures of endophytic *Alternaria* sp. taxonomy, fermentation, isolation, structure elucidation and biological activities. J. Antibiot., 2002. **55**(10): p. 881-892.
25. Guo, B. Y., J. R. Dai, S. Ng, Y. C. Huang, C. Y. Leong, W. Ong, and B. K. Carte, Cytonic acids A and B: Novel tridepside inhibitors of HCMV protease from the endophytic fungus *Cytonaema* species. J. Nat. Prod., 2000. **63**(5): p. 602-604.
26. Singh, S. B., D. L. Zink, Z. Q. Guan, J. Collado, F. Pelaez, P. J. Felock, and D. J. Hazuda, Isolation, structure, and HIV-1 integrase inhibitory activity of xanthoviridicatin E and F, two novel fungal metabolites produced by *Penicillium chrysogenum.* Helv. Chim. Acta, 2003. **86**(10): p. 3380-3385.
27. Wani, M.C., H. L., Taylor, M. E. Wall, P. Coggon, A. McPhail, Plant antitumor agents. Isolation and structure of taxol, a novel antileukemic and antitumor agent from *Taxus brevifolia.* J. Am. Chem. Soc., 1971. **93**(9): p. 2325.
28. Verma, V. C., R. N. Kharwar, and G. A. Strobel, Chemical and functional diversity of natural products from plant associated endophytic fungi. Nat. Prod. Commun., 2009. **4**(11): p. 1511-1532.
29. Schiff, P. B. and S. B. Horowitz, Taxol stabilizes microtubules in mouse fibroblast cells. Proc. Natl. Acad. Sci., 1980. **77**: p. 1561-1565.
30. Young, D. H., E. J. Michelotti, C. S. Sivendell, and N. E. Kraus, Antifungal properties of taxol and various analogues. Experientia, 1992. **48**(9): p. 882-885.
31. Greig, N. H., T. T. Soncrant, H. U. Shetty, S. Momma, Q. R. Smith, S. I. Rapoport, Brain uptake and anticancer activities of vincristine and vinblastine are restricted by their low cerebrovascular permeability and binding to plasma constituents in rat. Cancer Chemoth. Pharm., 1990. **26**(4): p. 263-268.
32. Kharwar, R.N., V. C. Verma, G. Strobel, D. Ezra, The endophytic fungal complex of *Catharanthus roseus (L.)* Curr. Sci., 2008. **95**(2): p. 228-233.
33. Ishii, T., K. Hayashi, T. Hida, Y. Yamamoto, and Y. Nozaki, TAN-1813, a novel Ras-farnesyltransferase inhibitor produced by *Phoma* sp. taxonomy, fermentation, isolation and biological activities in vitro and in vivo. J. Antibiot. (Tokyo), 2000. **53**(8): p. 765-778.
34. Ratnayake, A. S., W. Y. Yoshida, S. L. Mooberry, and T. Hemscheidt, The structure of microcarpalide, a microfilament disrupting agent from an endophytic fungus. Org. Lett., 2001. **3**(22): p. 3479-3481.
35. Wagenaar, M., J. Corwin, G. A. Strobel, and J. Clardy, Three new chytochalasins produced by an endophytic fungus in the genus *Rhinocladiella.* J. Nat. Prod., 2000. **63**(12): p. 1692-1695.
36. Ding, G., Y. C. Song, J. R. Chen, C. Xu, H. M. Ge, X. T. Wang, R. X. Tan, Chaetoglobosin U, a cytochalasan alkaloid from endophyfle *Chaetomium globosum* IFB-E019. J. Nat. Prod., 2006. **69**(2): p. 302-304.
37. Horiuchi, M. and Y. Seyama, Antiinflammatory and antiallergic activity of *Bidens pilosa* L. var. *radiata* Scherff. J. Health Sci., 2006. **52**(6): p. 711-717.
38. Oliveira, F. Q., V. Andrade-Neto, A. U. Krettli, and M. G. Brandao, New evidences of antimalarial activity of *Bidens pilosa* roots extract correlated with polyacetylene and flavonoids. J. Ethnopharmacol., 2004. **93**(1): p. 39-42.

39. Deba, F., T. D. Xuan, M. Yasuda, and S. Tawata, Herbicidal and fungicidal activities and identification of potential phytotoxins from *Bidens philosa* L. var. *radiata* Scherff. Weed Biol. Management, 2007. **7**: p. 77-83.
40. Wang, J., H. Yang, Z.-W. Lin, and H.-D. Sun, Flavonoids from *Bidens pilosa* var. *radiata.* Phytochemistry, 1997. **46**(7): p. 1275-1278.
41. Geissberger, P. and U. Sequin, Constituents of *Bidens pilosa* L.: do the components found so far explain the use of this plant in traditional medicine? Acta Trop., 1991. **48**(4): p. 251-261.
42. Bezivin, C., S. Tomasi, I. Rouaud, J. G. Delcros, and J. Boustie, Cytotoxic activity of compounds from the lichen: *Cladonia convoluta.* Planta Med., 2004. **70**(9): p. 874-877.
43. Lohezic-Le Devehat, F., S. Tomasi, J. A. Elix, A. Bernard, I. Rouaud, P. Uriac, and J. Boustie, Stictic acid derivatives from the lichen *Usnea articulata* and their antioxidant activities. J. Nat. Prod., 2007. **70**(7): p. 1218-1220.
44. Pittayakhajonwut, P., A. Dramae, S. Madla, N. Lartpornmatulee, N. Boonyuen, and M. Tanticharoen, Depsidones from the endophytic fungus BCC 8616. J. Nat. Prod., 2006. **69**(9): p. 1361-1363.
45. Abdou, R., K. Scherlach, H. M. Dahse, I. Sattler, and C. Hertweck, Botryorhodines A-D, antifungal and cytotoxic depsidones from *Botryosphaeria rhodina*, an endophyte of the medicinal plant *Bidens pilosa.* Phytochemistry, 2010. **71**(1): p. 110-116.
46. Elix, J. A., L. Lajide, and D. J. Galloway, Metabolites from the lichen genus *Psoroma.* Aust. J. Chem., 1982. **35**: p. 2325-2333.
47. Elix, J. A., U. A. Jenie, L. Arvidsson, P. M. Jörgennsen, and P. W. James, New depsidones from the lichen genus *Erioderma.* Aust. J. Chem., 1986. **39**: p. 719-722.
48. Fernandez, E., A. Reyes, M. E. Hidalgo, and W. Quilhot, Photoprotector capacity of lichen metabolites assessed through the inhibition of the 8-methoxypsoralen photobinding to protein. J. Photochem. Photobiol. B, 1998. **42**(3): p. 195-201.
49. Neamati, N., H. Hong, A. Mazumder, S. Wang, S. Sunder, M. C. Nicklaus, G. W. Milne, B. Proksa, and Y. Pommier, Depsides and depsidones as inhibitors of HIV-1 integrase: discovery of novel inhibitors through 3D database searching. J. Med. Chem., 1997. **40**(6): p. 942-951.
50. Shimada, A., I. Takahashi, T. Kawano, and Y. Kimura, Chloroisosulochrin, chloroisosulochrin dehydrate and pestheic acid, plant growth regulators, produced by *Pestalotiopsis theae.* Z. Naturforsch. B, 2001. **56**: p. 797-803.
51. Adeboya, M. O., R. L. Edwards, T. Lassoee, D. J. Maitland, L. Shields, and A. J. S. Walley, Metabolites of the higher fungi. Part 29. Maldoxin, maldoxone, dihydromaldoxin, isodihydromaldoxin and dechlorodihydromaldoxin. A spirocyclohexadienone, a depsidone and three diphenyl ethers: key in the depsidone biosynthetic pathway from a member of the fungus genus *Xylaria.* J. Chem. Soc. Perk. T 1, 1996. **12**: p. 1419-1425.
52. Jayasuriya, H., R. G. Ball, D. L. Zink, J. L. Smith, M. A. Goetz, R. G. Jenkins, M. Nallin-Omstead, K. C. Silverman, and G. F. Bills, Barcelonic acid A, a new farnesyl-protein transferase inhibitor from a *Phoma* species. J. Nat. Prod., 1995. **58**: p. 986-991.
53. Ohashi, H., H. Akiyama, K. Nishikori, and J. Mochizuki, Asterric acid, a new endothelin binding inhibitor. J. Antibiot., 1992. **45**: p. 1684-1685.
54. Jung L. H, L. J. Hyeong, H. B. Yeon, K. H. Sub, and L. J. Joon, Fungal metabolites, asterric acid derivatives inhibit vascular endothelial growth factor (VEGF)-induced tube formation of HUVECs. J. Antibiot., 2002. **55**: p. 552-556.
55. Weber, H. A., and J. B. Gloer, The Preussomerins: novel antifungal metabolites from the *Coprophilous* fungus *Preussia isomera* Cain. J. Org. Chem., 1991. **56**: p. 4355-4360.

56. Dong JY, S. H. Li, J. H. Tang, Y. S. Sun, R. Wang, L. Zhou, Y. P. Wang, L. M. Shen, K. Z. Wang, and C. R. Zhang, YMF 1029A-E, Preussomerin analogues from the fresh water derived fungus YMF 1.01029. J. Nat. Prod., 2008. **71**: p. 952-956.
57. Macias-Rubalcava, M. L., B. E. Hernandez-Bautista, M. Jimenez-Estrada, M. C. Gonzalez, A. E. Glenn, R. T. Hanlin, S. Hernandez-Ortega, A. Saucedo-Garcia, J. M. Muria-Gonzalez, and A. L. Anaya, Naphthoquinone spiroketal with allelochemical activity from the newly discovered endophytic fungus *Edenia gomezpompae.* Phytochemistry, 2008. **69**(5): p. 1185-1196.
58. Garson, M. J., J. Staunton, and P. G. Jones, New polyketide metabolites from *Aspergillus melleus*: Structural and stereochemical studies. J. Chem. Soc., Perk. T. 1, 1984: p. 1021-1026.
59. Cole, J. C., and R. H. Cox, Handbook of toxic metabolites. Academic press, New York, 1981: p. 129-151.
60. Venkatasubbalah, P. W. S., Phytotoxins of *Botryosphaeria obtusa.* J. Nat. Prod., 1990. **53**(6): p. 1628-1630.
61. Cabras, A., M.A. Mannoni, S. Serra, A. Andolfi, M. Fiore, and A. Evidente, Occurrence, isolation and biological activity of phytotoxic metabolites produced in vitro by *Sphaeropsis sapinea*, pathogenic fungus of *Pinus radiata.* Eur. J. Plant Pathol., 2006. **115**: p. 187-193.
62. Aldridge D. C., S. Galt, D. Giles, and W. B. Turner, Metabolites of *Lasiodiplodia theobromae.* J. Chem. Soc., 1971: p. 1623-1627Venkatasubbalah P, W.S., *Phytotoxins of Botryosphaeria obtusa.* J. Nat. Prod., 1990. **53**(6): p. 1628-1630.
63. Hoeller U., G. M. Koening, A. D. Wright, Three new metabolites from marine derived fungi of the genera *Coniothyrium* and *Microsphaeropsis.* J. Nat. Prod., 1999. **62**: p. 114-118.
64. He, G., H. Matsuura, and T. Yoshihara, Isolation of an alpha-methylene-gamma-butyrolactone derivative, a toxin from the plant pathogen *Lasiodiplodia theobromae.* Phytochemistry, 2004. **65**(20): p. 2803-2807.
65. Cheplick, G. P., K. Clay, and S. Marks, Interactions between infection by endophytic fungi and nutrient limitation in the grasses *Lolium perenne* and *Festuca arundinacea.* New Phytologist, 1989. **111**(1): p. 89-97.
66. Gasoni, L., and B. D. Gurfinkel, The endophyte *Cladorrhinum foecundissimum* in cotton roots: phosphorus uptake and host growth. *Mycol. Res.*, 1997. **101**(7): p. 867-870.
67. Muchuweti, M., C. Mupure, A. Ndhlala, T. Murenje, and M. A. N. Benhura, Screening of antioxidant and radical scavenging activity of *Vigna ungiculata*, *Bidens pilosa* and *Cleome gynandra.* 2007, 2007. **2**(3): p. 161-168.
68. Sassa, T., A. Ishizaki, M. Nukina, M. Ikeda, and T. Sugiyama, Isolation and identification of new antifungal macrophorins E, F and G as malonyl meroterpenes from *Botryosphaeria berengeriana.* Biosci. Biotechnol. Biochem., 1998. **62**(11): p. 2260-2262.
69. Elix, J. A., J. H. Wardlaw, and W. Obermeyer, 2-Hydroxyvirensic Acid, a new depsidone from the lichen *Sulcaria sulcata.* Aust. J. Chem., 2000. **53**: p. 233-235.
70. Elix, J. A., J. H. Wardlaw, W. Obermeyer, and A. W. Archer, 2-Methoxypsoromic acid, a new lichen depsidone from *Pertusaria* and *Sulcaria* species. Aust. J. Chem., 1999. **52**: p. 717-719.
71. Elix, J. A., J. H. Wardlaw, and I. Yashimura, Sublobaric Acid and oxolobaric acid, two new depsidones from the lichen *Anzia hypoleucoides* Aust. J. chem., 1997. **50**: p. 763-765.
72. Rezanka, T. and I. A. Guschina, Brominated depsidones from *Acarospora gobiensis*, a lichen of central Asia. J. Nat. Prod., 1999. **62**: p. 1675-1677.

73. Poch, G. K. and J. B. Gloer, Auranticins A and B: two new depsidones from a mangrove isolate of the fungus *Preussia aurantiaca.* J. Nat. Prod., 1991. **54**(1): p. 213-217.
74. Ito, C., M. Itoigawa, Y. Mishina, H. Tomiyasu, M. Litaudon, J. P. Cosson, T. Mukainaka, H. Tokuda, H. Nishino, and H. Furukawa, Cancer chemopreventive agents. New depsidones from *Garcinia* plants. J. Nat. Prod., 2001. **64**(2): p. 147-150.
75. Xu, Y. J., P. Y. Chiang, Y. H. Lai, J. J. Vittal, X. H. Wu, B. K. Tan, Z. Imiyabir, and S. H. Goh, Cytotoxic prenylated depsidones from *Garcinia parvifolia.* J. Nat. Prod., 2000. **63**(10): p. 1361-1363.
76. Lang, G., A. L. Cole, J. W. Blunt, W. T. Robinson, and M. H. Munro, Excelsione, a depsidone from an endophytic fungus isolated from the New Zealand endemic tree *Knightia excelsa.* J. Nat. Prod., 2007. **70**(2): p. 310-311.
77. Müller, K., Pharmaceutically relevant metabolites from lichens. Appl. Microbiol. Biotechnol., 2001. **56**(1-2): p. 9-16.
78. Rosenblueth, M. and E. Martinez-Romero, Bacterial endophytes and their interactions with hosts. Mol. Plant Microbe Interact., 2006. **19**(8): p. 827-837.
79. He, G. C., H. Matsuura, and T. Yoshihara, Isolation of an alpha-methylene-7-butyrolactone derivative, a toxin from the plant pathogen *Lasiodiplodia theobromae.* Phytochemistry, 2004. **65**(20): p. 2803-2807.
80. Ghosal, S., K. Biswas, and D. K. Chakrabarti, Toxic naphthopyrones from *Aspergillus niger.* J. Agric. Food Chem., 1979. **27**(6): p. 1347-1351.
81. Akiyama, K., S. Teraguchi, Y. Hamasaki, M. Mori, K. Tatsumi, K. Ohnishi, and H. Hayashi, New dimeric naphthopyrones from *Aspergillus niger.* J. Nat. Prod., 2003. **66**(1): p. 136-139.
82. Zhan, J., G. M. Gunaherath, E. M. Wijeratne, and A. A. Gunatilaka, Asperpyrone D and other metabolites of the plant-associated fungal strain *Aspergillus tubingensis.* Phytochemistry, 2007. **68**(3): p. 368-372.
83. Varoglu, M., T. H. Corbett, F. A. Valeriote, and P. Crews, Asperazine, a selective cytotoxic alkaloid from a sponge-derived culture of *Aspergillus niger.* J. Org. Chem., 1997. **62**(21): p. 7078-7079.
84. Hauser, D., H. P. Weber, and H. P. Sigg, Isolation and configuration of Chaetocin. Helv. Chim. Acta, 1970. **53**(5): p. 1061-1073.
85. Fridrichsons, J., M. F. MacKay, and A. M. Mathieson, The absolute molecular structure of (+) kreysiginine. Tetrahedron, 1970. **26**(8): p. 1869-1877.
86. Ikeda, S., M. Sugita, A. Yoshimura, T. Sumizawa, H. Douzono, Y. Nagata, and S. Akiyama, *Aspergillus* species strain M39 produces two naphthopyrones that reverse drug resistance in human KB cells. Int. J. Cancer, 1990. **45**(3): p. 508-513.
87. Ovenden, S. P., G. Sberna, R. M. Tait, H. G. Wildman, R. Patel, B. Li, K. Steffy, N. Nguyen, and B. M. Meurer-Grimes, A diketopiperazine dimer from a marine-derived isolate of *Aspergillus niger.* J. Nat. Prod., 2004. **67**(12): p. 2093-2095.
88. Nielsen, K. F., S. Gravesen, P. A. Nielsen, B. Andersen, U. Thrane, and J. C. Frisvad, Production of mycotoxins on artificially and naturally infested building materials. Mycopathologia, 1999. **145**(1): p. 43-56.
89. Suda, S. C., and R.W. Curtis, Antibiotic properties of malformin. Appl. microbiol. 1966. **14**(3): p. 475.
90. Haenni A., R. M. Vetter, W. Roux, L. Barbier and M. Lederer, Chemical structure of aspergillomarasmines A and B. Helv. Chim. Acta. 1965. **1** (48):p. 729-50.
91. Mikami T., T. Nagasa, T. Matsumoto, M. Suzuki, S. Suzuki, and N. Kumano, Mitogenic effect of the mannans from *Saccharomyces cerevisiae* on mouse spleen lymphocytes. Microbiol Immunol. , 1982. **26**(10): p. 913-922.
92. Orth, R., Mycotoxins of *Aspergillus oryzae* strains for use in the food industry as starters and enzyme producing molds. Ann. Nutr. Aliment. , 1977. **31**(4-6): p. 617-624.

93. Pier AC, E. L. Belden, J. A. Ellis, E. W. Nelson, and L. R. Maki, Effects of cyclopiazonic acid and aflatoxin singly and in combination on selected clinical, pathological and immunological responses of guinea pigs. Mycopathologia. 1989. **105**(3):135-42.,
94. Abarca, M. L., F. Accensi, J. Cano, and F. J. Cabanes, Taxonomy and significance of black aspergilli. Antonie Van Leeuwenhoek, 2004. **86**(1): p. 33-49.
95. Walchshofer, N., M. E. Sarciron, F. Garnier, P. Delatour, A. F. Petavy and J. Paris, Anthelmentic activity of 3, 6-dibenzyl-2,5-dioxopiperazine, cyclo (L-Phe-L-Phe). Amino acids, 1997. **12**: p. 41-47.
96. Zhang, Y. G., S. C. Liu, Y. S. Che, and X. Z. Liu, Epicoccins A-D, epipolythiodioxopiperazines from a Cordyceps-colonizing isolate of *Epicoccum nigrum.* J. Nat. Prod., 2007. **70**: p. 1522-1525.
97. Tan, R. X., P. R. Jensen, P. G. Williams, and W. Fenical, Isolation and structure assignments of rostratins A-D, cytotoxic disulfides produced by the marine-derived fungus *Exserohilum rostratum.* J. Nat. Prod., 2004. **67**(8): p. 1374-1382.
98. Baute, M. A., G. Deffieux, R. Baute, and A. Neveu, New antibiotics from fungus *Epicoccum nigrum*. Fermentation, isolation and antibacterial properties. J. Antibiot., 1978. **31**(11): p. 1099-1101.
99. Yamada, Y., F. Sun, I. Tsuritani, and R. Honda, Genetic differences in ethanol metabolizing enzymes and blood pressure in Japanese alcohol consumers. J. Hum. Hypertens., 2002. **16**(7): p. 479-486.
100. Bauer, J., M. Gareis, A. Bott and B. Gedek, Isolation of a mycotoxin (gliotoxin) from a bovine udder infected with *Aspergillus fumigatus.* J. Med. Vet. Mycol., 1989. **27**: p. 45-50.
101. Dong, J. Y., H. P. He, Y. M. Shen, and K. Q. Zhang, Nematicidal epipolysulfanyldioxopiperazines from *Gliocladium roseum.* J. Nat. Prod., 2005. **68**(10): p. 1510-1513.
102. Zheng, C. J., C. J. Kim, K. S. Bae, Y. H. Kim, and W. G. Kim, Bionectins A-C, epidithiodioxopiperazines with anti-MRSA activity, from *Bionectra byssicola* F120. J. Nat. Prod., 2006. **69**(12): p. 1816-1819.
103. Kleinwachter, P., H. M. Dahse, U. Luhmann, B. Schlegel, and K. Dornberger, Epicorazine C, an antimicrobial metabolite from *Stereum hirsutum* HKI 0195. J. Antibiot., 2001. **54**(6): p. 521-525.
104. Takahashi, C., Y. Takai, Y. Kimura, A. Numata, N. Shigematsu, and H. Tanaka, Cytotoxic metabolites from a fungal adherent of a marine alga. Phytochemistry, 1995. **38**(1): p. 155-158.
105. Fujimoto, H., M. Sumino, E. Okuyama, and M. Ishibashi, Immunomodulatory constituents from an Ascomycete, *Chaetomium seminudum.* J. Nat. Prod., 2004. **67**(1): p. 98-102.
106. Isaac, B. G., S. W. Ayer, L. J. Letendre, and R. J. Stonard, Herbicidal nucleosides from microbial sources. J. Antibiot. (Tokyo), 1991. **44**(7): p. 729-732.
107. Baker, B. R., W. W. Lee, W. A. Skinner, A. P. Martinez, and E. Tong, Potential anticancer agents. Non-classical antimetabolites. Some factors in the design of exoalkylating enzyme inhibitors, particulary of lactic dehydrogenase. J. Med. Pharm. Chem., 1960. **2**: p. 633-657.
108. Broadbent, D. H., H. G. Hemming, and M. Lehan, Production of Griseofulvin by *Khuskia oryzae.* Trans. Br. mycol. Soc., 1974. **62**(3): p. 625-626.
109. Bouarab, K., F. Adas, E. Gaquerel, B. Kloareg, J. P. Salaun, and P. Potin, The innate immunity of a marine red alga involves oxylipins from both the eicosanoid and octadecanoid pathways. Plant Physiol., 2004. **135**(3): p. 1838-1848.
110. Prost, I., S. Dhondt, G. Rothe, J. Vicente, M. J. Rodriguez, N. Kift, F. Carbonne, G. Griffiths, M. T. Esquerre-Tugaye, S. Rosahl, C. Castresana, M. Hamberg, and J. Fournier, Evaluation of the antimicrobial activities of plant oxylipins supports their

involvement in defense against pathogens. Plant Physiol., 2005. **139**(4): p. 1902-1913.
111. Cantrell, C. L., B. P. Case, E. E. Mena, T. M. Kniffin, S. O. Duke, and D. E. Wedge, Isolation and identification of antifungal fatty acids from the basidiomycete *Gomphus floccosus.* J. Agric. Food Chem., 2008. **56**(13): p. 5062-5068.
112. Steyn, P. S., Mycotoxins, general view, chemistry and structure. Toxicol. Lett., 1995. **82-83**: p. 843-851.
113. Lillehoj, E. B. and A. Ciegler, Biological activity of sterigmatocystin. Mycopathol. Mycol. Appl., 1968. **35**(3): p. 373-376.
114. Purchase, I. F. and J. J. van der Watt, Acute toxicity of sterigmatocystin to rats. Food Cosmet. Toxicol., 1969. **7**(2): p. 135-139.
115. van der Watt, J. J. and I. F. Purchase, Subacute toxicity of sterigmatocystin to rats. S. Afr. Med. J., 1970. **44**(6): p. 159-160.
116. Dickens, F., H. E. Jones, and H. B. Waynforth, Oral, subcutaneous and intratracheal administration of carcinogenic lactones and related substances: the intratracheal administration of cigarette tar in the rat. Br. J. Cancer, 1966. **20**(1): p. 134-144.
117. Scott, P. M., W. Van Walbeek, B. Kennedy, and D. Anyeti, Mycotoxins (ochratoxin A, citrinin, and sterigmatocystin) and toxigenic fungi in grains and other agricultural products.J. Agric. Food Chem., 1972. **20**(6): p. 1103-1109.
118. Purchase, I. F. and M. E. Pretorius, Sterigmatocystin in coffee beans. J. Assoc. Anal. Chem., 1973. **56**(1): p. 225-226.
119. Raistrick, H., C. E. Stickings, and R. Thomas, Studies in the biochemistry of microorganisms. Alternariol and alternariol monomethyl ether, metabolic products of *Alternaria tenuis.* Biochem. J., 1953. **55**(3): p. 421-433.
120. Griffin, G. F. and F. S. Chu, Toxicity of the *Alternaria* metabolites alternariol, alternariol methyl ether, altenuene, and tenuazonic acid in the chicken embryo assay. Appl. Environ. Microbiol., 1983. **46**(6): p. 1420-1422.
121. Doupnik, B., and E. K. Sobers, Mycotoxicosis: toxicity to chicks of *Alternaria longipes* isolated from tobacco. Appl. Microbiol., 1968. **16**(10): p. 1596-1597.
122. Liebermann, B., R. Ellinger, E. Pinet, Isotentoxin, a conversion product of the phytotoxin tentoxin. Phytochemistry, 1996. **42**(6): p. 1537-1540.
123. Izhaki, I., Emodin – a secondary metabolite with multiple ecological functions in higher plants. New Phytol., 2002. **155**: p. 205-217.
124. Kusari, S., M. Lamshöft, S. Zühlke, and M. Spiteller, An endophytic fungus from *Hypericum perforatum* that produces hypericin. J. Nat. Prod., 2008. **71**(2): p. 159-162.
125. Krohn, K., S. F. Kouam, G. M. Kuigoua, H. Hussain, S. Cludius-Brandt, U. Florke, T. Kurtan, G. Pescitelli, L. Di Bari, S. Draeger, and B. Schulz, Xanthones and oxepino[2, 3-b]chromones from three endophytic fungi. Chemistry, 2009. **15**(44): p. 12121-12132.
126. Kim, J. R., D. R. Oh, M. H. Cha, B. S. Pyo, J. H. Rhee, H. E. Choy, W. K. Oh, and Y. R. Kim, Protective effect of P*olygoni cuspidati* radix and emodin on *Vibrio vulnificus* cytotoxicity and infection. J. Microbiol., 2008. **46**(6): p. 737-743.
127. Basu, S., A. Ghosh, and B. Hazra, Evaluation of the antibacterial activity of *Ventilago madraspatana* Gaertn., *Rubia cordifolia* Linn. and *Lantana camara* Linn.: isolation of emodin and physcion as active antibacterial agents. Phytother. Res., 2005. **19**(10): p. 888-894.
128. Efferth, T., A. Olbrich, A. Sauerbrey, D. D. Ross, E. Gebhart, and M. Neugebauer, Activity of ascaridol from the anthelmintic herb *Chenopodium anthelminticum* L. against sensitive and multidrug-resistant tumor cells. Anticancer Res., 2002. **22**(6C): p. 4221-4224.
129. Dembitsky, V., I. Shkrob, and L. O. Hanus, Ascaridole and related peroxides from the genus *Chenopodium.* Biomed. Pap. Med. Fac. Univ. Palacky Olomouc Czech Repub, 2008. **152**(2): p. 209-215.

130. De Carvalho, J. C., B. O. Oishi; A. Pandey, and C. R. Soccol, Biopigments from *Monascus*: Strains Selection, Citrinin Production and Colour Stability. Braz. Arch. Biol. Techn., 2005. **48**(6): p. 885-894.
131. Gimenez, C., R. Cabrera, M. Reina, and A. Gonzalez-Coloma, Fungal endophytes and their role in plant protection. Curr. Org. Chem., 2007. **11**: p. 707-720.
132. Ciegler, A. V., R. F. Vesonder, and L. K. Jackson, Production and biological activity of patulin and citrinin from *Penicillium expansum.* Appl. Environ. Microbiol., 1977. **33**(4): p. 1004-1006.
133. Welington, L.A., W. Macheroni, C. I. Aguilar-Vildoso, P. A. V. Barroso, H. O. Saridakis and J. L. Azevedo, Variability and interactions between endophytic bacteria and fungi isolated from leaf tissues of citrus rootstocks. Can. J. Microbiol., 2001. **47**: p. 229-236.
134. Glass, N.L., D. J. Jacobson and P. K. T. Shiu, The genetics of hyphal fusion and vegetative incompatibility in filamentous ascomycete fungi. Annu. Rev. Genet., 2000. **34**: p. R165-R186.
135. Scherlach, K. and C. Hertweck, Triggering cryptic natural product biosynthesis in microorganisms. Org. Biomol. Chem., 2009. **7**: p. 1753-1760.
136. Glass, N.L. and S. J. Saupe, Vegetative incompatibility in filamentous ascomycetes. Osiewacz, H.D. (Ed.) Molecular Biology of Fungal Development. , 2002: p. 109-131.
137. Meyer, V. and U. Stahl, The influence of co-cultivation on expression of the antifungal protein in *Aspergillus giganteus.* J. Basic Microb., 2003. **43**(1): p. 68-74.
138. Keller, L. and M.G. Surette, Communication in bacteria: an ecological and evolutionary perspective. Nat. Rev. Microbiol., 2006. **4**(4): p. 249-258.
139. Delledonne, M., A. Polverari, and I. Murgia, The functions of nitric oxide-mediated signaling and changes in gene expression during the hypersensitive response. Antioxid. Redox Sign., 2003. **5**(1): p. 33-41.
140. Moon, C. D., B. A. Tapper, and B. Scott, Identification of *Epichloe* endophytes in planta by a microsatellite-based PCR fingerprinting assay with automated analysis. Appl. Environ. Microbiol., 1999. **65**(3): p. 1268-1279.
141. Rodrigues, K. F., The foliar fungal endophytes of the Amazonian palm *Euterpe oleracea.* Mycol., 1994. **86**: p. 376-385.
142. Mayer, A. M., Plant-fungal interactions: a plant physiologist's viewpoint. Phytochemistry, 1989. **28**(2): p. 311-317.
143. Schulz, B. and C. Boyle, The endophytic continuum. Mycol. Res., 2005. **109**(6): p. 661-686.
144. Afonin, S., R. W. Glaser, M. Berditchevskaia, P. Wadhwani, K. H. Guhrs, U. Mollmann, A. Perner, and A. S. Ulrich, 4-fluorophenylglycine as a label for 19F NMR structure analysis of membrane-associated peptides. Chem. Biochem., 2003. **4**(11): p. 1151-1163.
145. Wayne, P. A., Reference method for broth dilution susceptibility testing of filamentous fungi; Approved Standard. M38-A, USA, NCCls, 2002: p. 22.

8. Appendix

8.1. Physicochemical data of the isolated compounds

Botryorhodine A
Yellowish-white amorphous powder; UV (MeOH) λ_{max} (logε) 203 (3.63), 220 (4.32), 326 (sh) (0.43) nm; IR (film) ν_{max} 3651, 2886, 2332, 1683, 1456, 1197, 1147, 1061, 850, 727, 669 cm^{-1}; HRESIMS *m/z* 299.0547 $[M-H]^-$ calcd *m/z* 299.0550 for $C_{16}H_{11}O_6$; NMR data see table 3, 4.

Botryorhodine B (nordechloropannarin)
White amorphous powder; UV (MeOH) λ_{max} (logε) 207 (3.87), 227 (3.22), 328 (sh) (0.43); IR (film) ν_{max} 3442, 2888, 2346, 1683, 1446, 1207, 1143, 847, 726, 669 cm^{-1}; HRESIMS *m/z* 313.0722 $[M-H]^-$ calcd *m/z* 313.0707 for $C_{17}H_{13}O_6$; NMR data see table 3, 4.

Botryorhodine C
White amorphous powder; UV (MeOH) λ_{max} (logε) 209 (3.72), 271 (1.16) nm; IR (film) ν_{max} 3335, 2340, 1670, 1450, 1199, 1146, 849, 726, 666 cm^{-1}; HRESIMS *m/z* 315.0858 $[M-H]^-$ calcd *m/z* 315.0863 for $C_{17}H_{15}O_6$; NMR data see table 3, 4.

Botryorhodine D
Yellowish white amorphous powder; UV (MeOH) λ_{max} (logε) 217 (4.043); 269 (2.73) nm; IR (film) ν_{max} 3306, 2889, 2340, 1678, 1460, 1200, 1147, 850, 727, 667 cm^{-1}; HRESIMS *m/z* 301.0705 $[M-H]^-$ calcd *m/z* 301.0707 for $C_{16}H_{13}O_6$; NMR data see table 3, 4.

Botryorhodine E
Yellowish powder, UV (MeOH) λ_{max} (logε) 213 (4.50), 246 (3.7), 292 (3.6) nm. IR (film) ν_{max} 3384, 3278, 3219, 1709, 1656, 1614, 1595 and 1470 cm^{-1}. HRESIMS *m/z* 275.1050 $[M+H]^+$ calcd 275.1054 for $C_{15}H_{15}O_5$. NMR data see table 8.

Preussomerin C

Yellowish amorphous powder, $[\alpha]_D^{20}$ -156 (*c* 0.03; MeOH); UV (MeOH) λ_{max} (logε) 303 (3.813), 254 (7.480) nm; IR (film) ν_{max} 3700, 3650, 3360, 1020, 2860, 1685, 1590, 1520, 1470, 1415, 1330, 1280, 1210 cm^{-1}; HREIMS *m/z* 395.0850 $[M-H]^-$,calcd 395.0845 for $C_{21}H_{17}0_8$. NMR data see table 7.

3R, 4R (-)-4-hydroxymellein

Colourless oil, $[\alpha]_D^{20}$ -36.0 (*c* 0.78, methanol); IR (film) ν_{max} 3384, 1669, 1617, 1584, 1493 cm^{-1}. UV (MeOH) λ_{max} (logε) 244 (3.76), 312 (3.68) nm. HRESIMS *m/z* 195.1549 $[M+H]^+$ calcd 194.1552 for $C_{10}H_{10}O_4$.

Indole carboxylic acid
UV (MeOH) λ_{max} (logε) 260 (3.30), 280 (2.27). HRESIMS *m/z* 181.1023 $[M+H]^+$ for $C_9H_8O_2N_1$.

Asperpyrone D
Yellow powder, UV (MeOH) λ_{max} (log ε): 384 (3.86), 281 (4.68), 248 (4.62), 225 (4.52) nm; IR (film) νmax: 3425, 2928, 2858, 2365, 2338, 1655, 1616, 1570, 1427, 1380, 1261, 1204, 1165 and 1065 cm^{-1}. HRESIMS *m/z* 557.1431 $[M+H]^+$ calcd 557.1448 for $C_{31}H_{24}O_{10}$. NMR data see table 10, 11.

Aurasperone A
Yellow powder, UV (MeOH) λ_{max} (log ϵ) 225 (4.52), 258 (4.42), 280 (4.53), 325 (3.90), 400 (3.68) nm; IR (film) v_{max}: 3350 (broad), 1680, 1630, 1550, 1470, 1400, 1055 cm^{-1}; HRESIMS *m/z* 571.1053 $[M+H]^+$ calcd 571.1056 for $C_{32}H_{26}O_{10}$. NMR data see table 10, 11.

Aurasperone D
Yellow solid, UV (MeOH) (log ϵ) 235-240 (4.70), 280 (4.71), 320-325 (4.18), 380 (3.85) nm; IR (film) v_{max}, 3400 (broad), 1652, 1600, 1580, 1495, 1404, 1018 cm^{-1}; HRESIMS *m/z* 557.1050 $[M+H]^+$, calcd 557.1054 for $C_{31}H_{24}O_{10}$. NMR data see table 10, 11.

Dianhydroaurasperone C
Yellow amorphous powder, UV (MeOH) λ_{max} (log ϵ): 225 (4.36), 255 (4.43), 280 (4.93), 325 (3.57), 405 (3.76) nm; IR (film) v_{max}, 3450 (broad), 1675, 1630, 1550, 1486, 1423, 1023 cm^{-1}; HRESIMS: *m/z* 557.1540 $[M+H]^+$ calcd 557.1545 $[M+H]^+$ for $C_{31}H_{24}0_{10}$. NMR data see table 10, 11.

Asperazine
White powdery flakes, $[\alpha]_D^{20}$ +53 (*c*, 0.2, CH3OH); UV (MeOH) λ_{max}: 300, 285, 225 nm; IR (film) λ_{max} 3448, 3365, 2931, 1681, 1673, 1667, 1651, 1444, 1314, 1093, 743, 700 cm^{-1}. HRESIMS, *m/z* 665.3501 $[M + H]^+$ calcd 665.3504 for $C_{40}H_{37}N_6O_4$. NMR data see table 12.

Asperazine A
White powder, $[\alpha]_D^{20}$ +132 (*c* 0.004, MeOH); UV (MeOH) λ_{max}: 240, 300 nm; IR (film) λ_{max} 3584, 2960, 2922, 2851, 1666 cm^{-1}; HRESIMS *m*/*z* 665.3290 $[M+H]^+$ calcd, 665.3293 for $C_{40}H_{37}N_6O_4$. NMR data see table 12.

Epicoccin A
Colourless powder, $[\alpha]_D^{20}$ +365 (*c* 0.06, MeOH); UV (MeOH) λ_{max} 204 nm; IR (film) *v*max 3453, 2938, 1706, 1672, 1655, 1410, 994 cm-1; HRESIMS *m*/*z* 455.0391 $[M + H]^+$, calcd, 455.0400 $[M+H]^+$ for $C_{18}H_{19}N_2O_6S_3$. NMR data see table 17.

***cis*-L-(-)-3, 6-dibenzyl-2, 5-dioxopiperazine**
Pale yellow powder, $[\alpha]_D^{20}$ -104.24 (*c* 1.2, MeOH). IR (film) *v*max 1690, 1670, 1620 cm^{-1}. HRESIMS *m/z* 295.3015 $[M+H]^+$; calcd 295.3019 $[M+H]^+$ for $C_{18}H_{19}N_2O_2$. NMR data see table 17.

Adenosyl-9α-D-arabinofuranoside
White solid crystals, IR (film): 3315, 3154, 2914, 2845, 1662, 1602, 1570, 1466, 13330, 1299, 1106 cm^{-1}. HRESI-MS: *m/z* 268.3991 $[M+H]^+$ calcd 268.3995 for $C_{10}H_{13}N_5O_4$,

Sterigmatocystin
Pale yellow powder, $[\alpha]_D^{20}$ -363 (*c* 1.0, $CHCl_3$), UV (MeOH) λ_{max} (log ϵ) 233 (27200), 248 (34000), 275sh (7700), 330 (19200) nm; IR (film): 3125, 1655, 1635, 1610, 1595 cm^{-1}; HRESIMS *m/z* 325.2506 $[M+H]^+$ calcd 325.2510 $[M+H]^+$ for $C_{18}H_{13}0_6$. NMR data see table 21.

Alternariol
Reddish white needles, UV (MeOH) λ_{max} 206.1, 255.8, 299.8 and 339.7 nm; HRESIMS *m/z* 259.2106 $[M+H]^+$, calcd 259.2109 for $C_{14}H_{11}O_5$. NMR data see table 23.

Emodin

Pale yellow, UV (MeOH) λ_{max} (log ϵ) 222 (4.47); 253 (4.38); 266 (4.29); 289 (4.36); 438 (4.16) nm. IR (film): 3377, 2925, 1629, 1481, 1456, 1336, 1211, 1103, 1033 cm^{-1}. HRESIMS *m*/*z* 271.4652 $[M+H]^+$, calcd 271.4656 for $C_{15}H_{11}O_5$.

Tentoxin

Colourless needles, $[a]_D^{20}$ - 117 (*c* 0.3, MeOH). UV (MeOH) λ_{max} 220, 280, 300 nm. IR (film) vmax: 3350, 2950, 1450, 1670, 1630, 1520, 760, 700 cm^{-1}. HRESIMS *m/z*: 415.2254 $[M+H]^+$, calcd 415.2259, for $C_{22}H_{30}N_4O_4$.

8.2. NMR spectra of the isolated compounds

Fig 1a. ^{1}H NMR spectrum of botryorhodine A

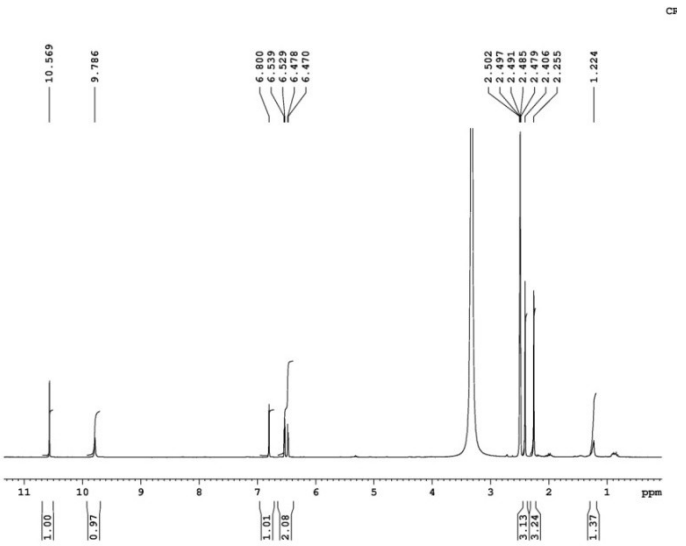

Fig 1b. ^{13}C NMR spectrum of botryorhodine A

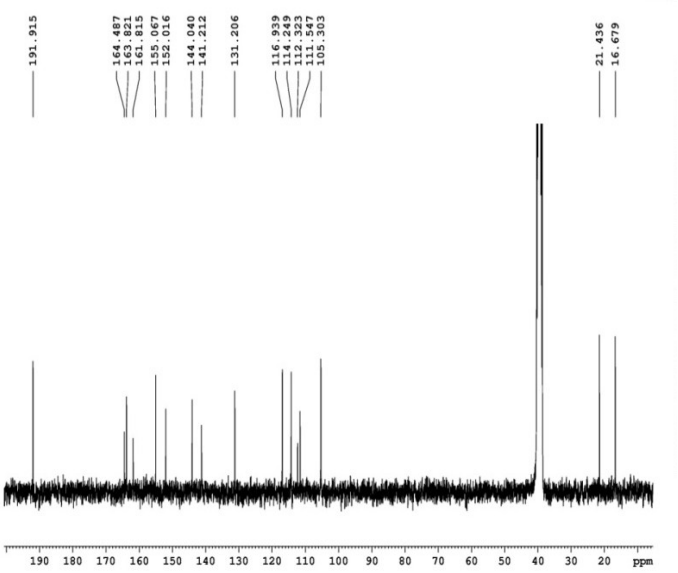

Fig 1c. HMBC spectrum of botryorhodine A

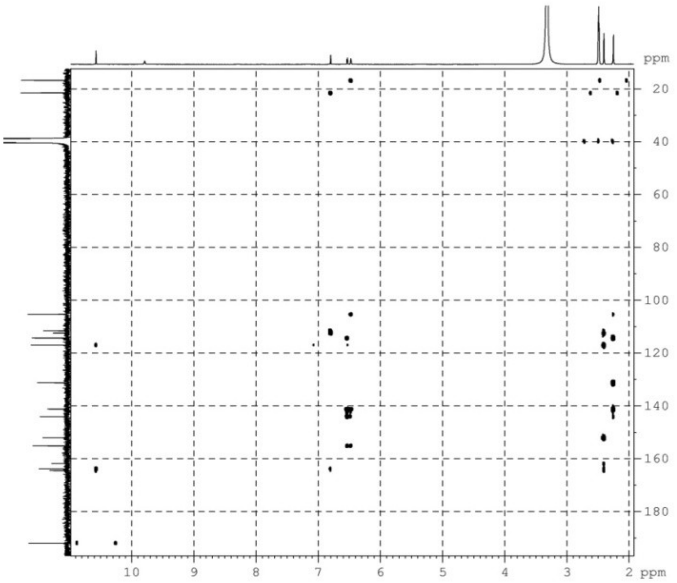

Fig 2a. ^{1}H NMR spectrum of botryorhodine B

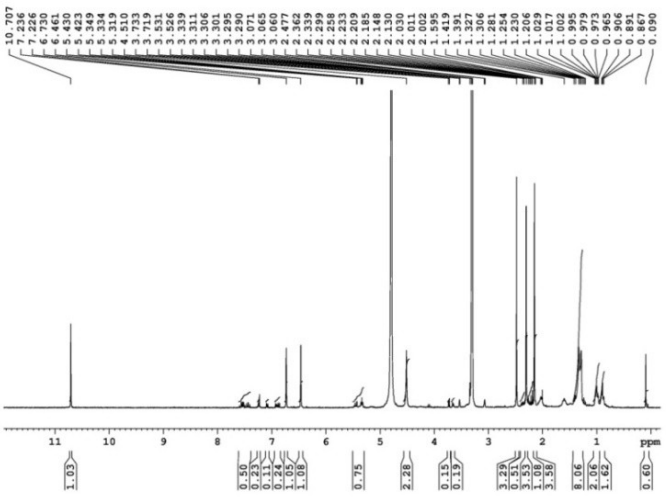

Fig 2b. ^{13}C NMR spectrum of botryorhodine B

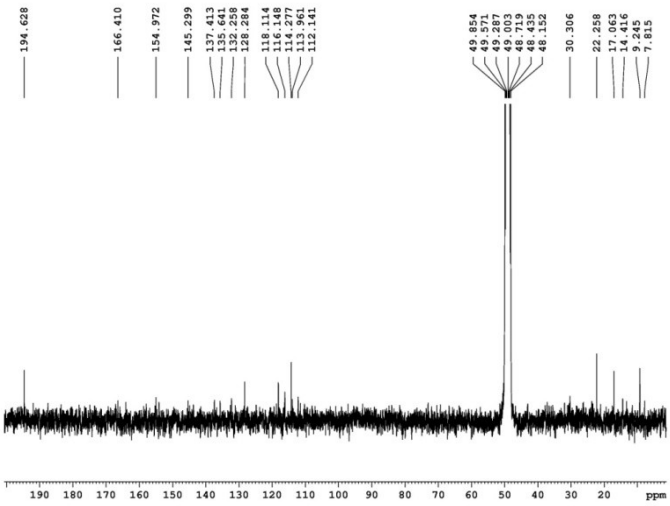

Fig 2c. HMBC spectrum of botryorhodine B

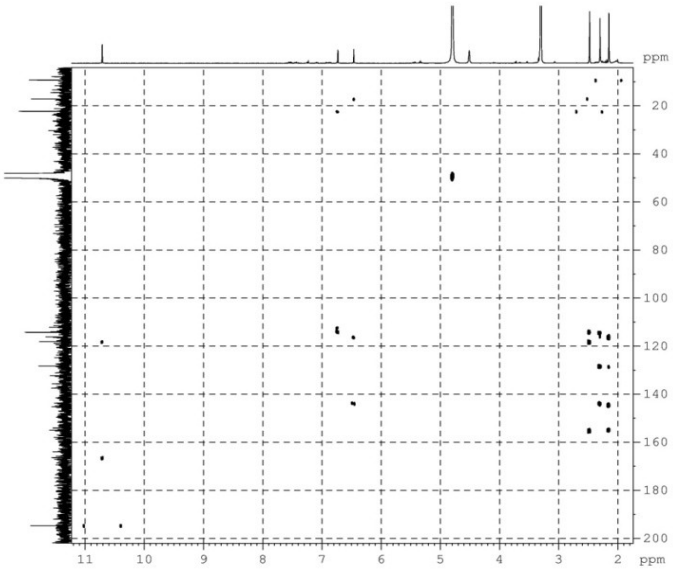

Fig 3a. ^{1}H NMR spectrum of botryorhodine C

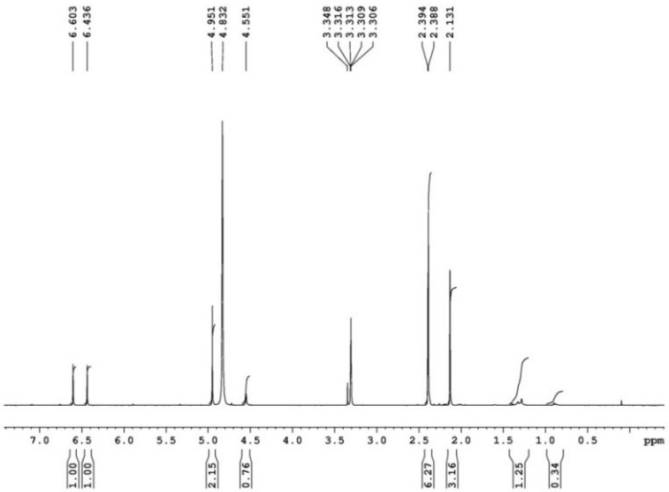

Fig 3b. ^{13}C NMR spectrum of botryorhodine C

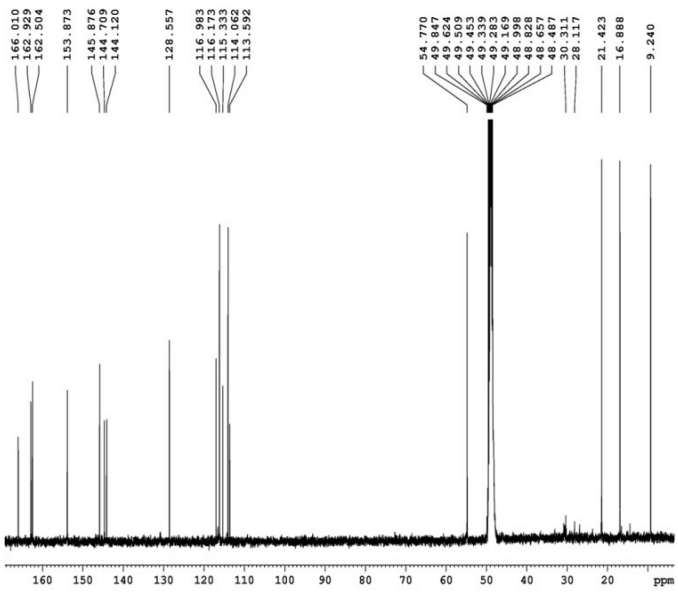

Fig 3c. HMBC spectrum of botryorhodine C

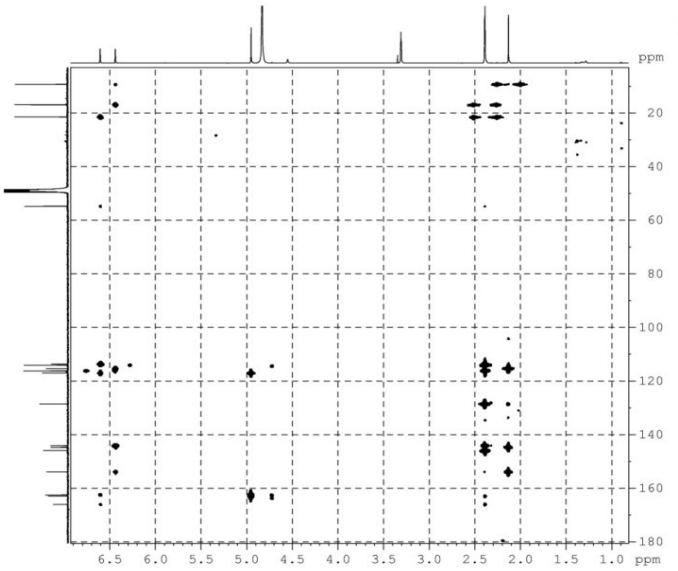

Fig 4a. ^{1}H NMR spectrum of botryorhodine D

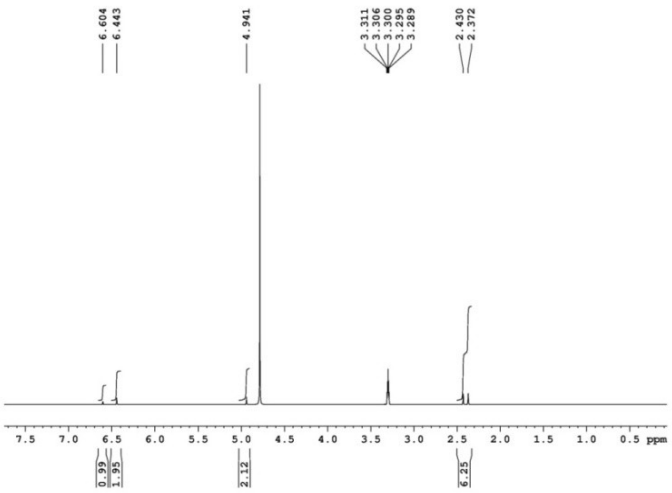

Fig 4b. ^{13}C NMR spectrum of botryorhodine D

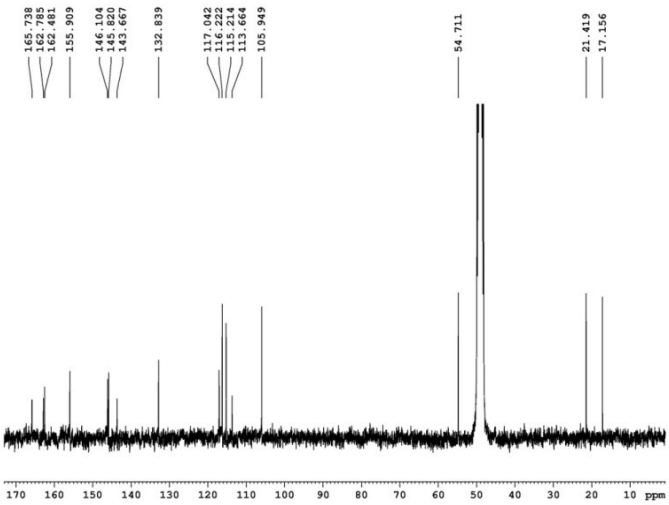

Fig 4c. HMBC spectrum of botryorhodine D

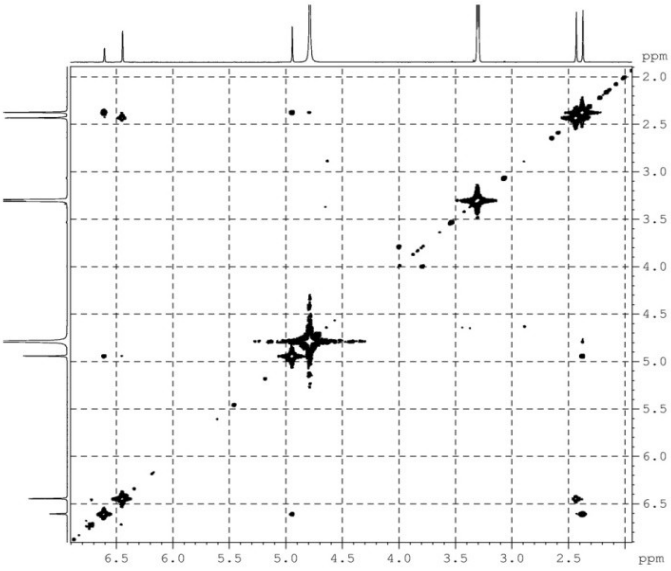

Fig 5a. ^{1}H NMR spectrum of botryorhodine E

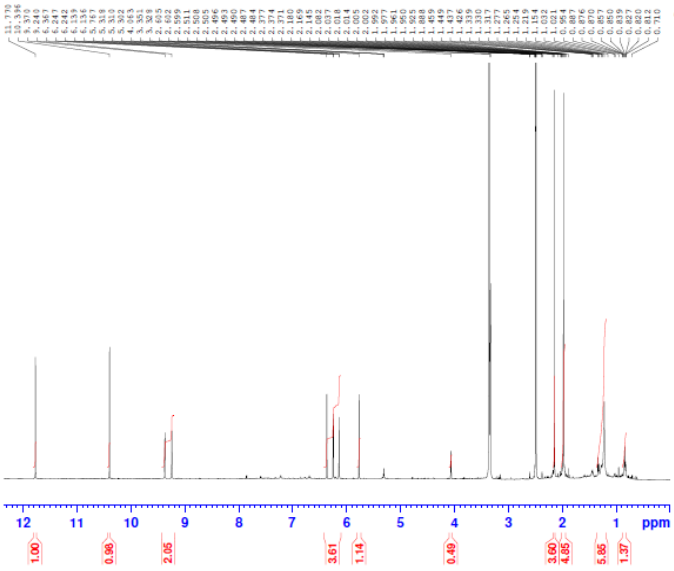

Fig 5b. ^{13}C NMR spectrum of the new diphenyl ether

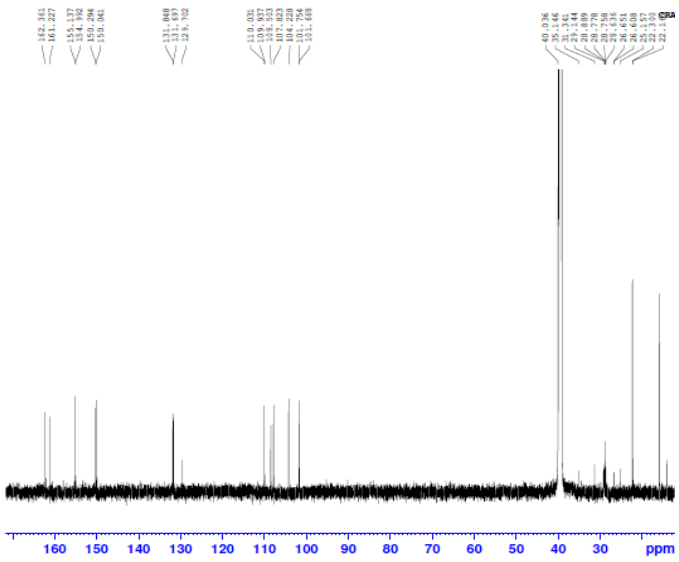

Fig 5c. HMBC spectrum of the new diphenyl ether

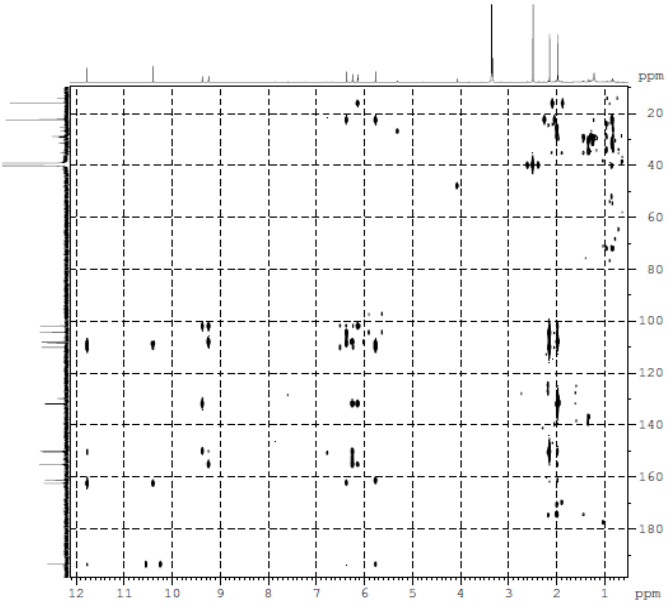

Fig 6a. ^{1}H NMR spectrum of asperazine

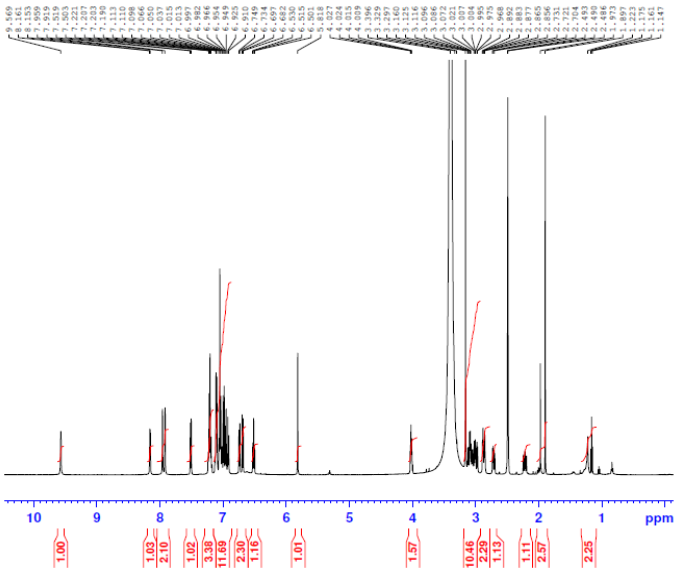

Fig 6b. ^{13}C NMR spectrum of asperazine

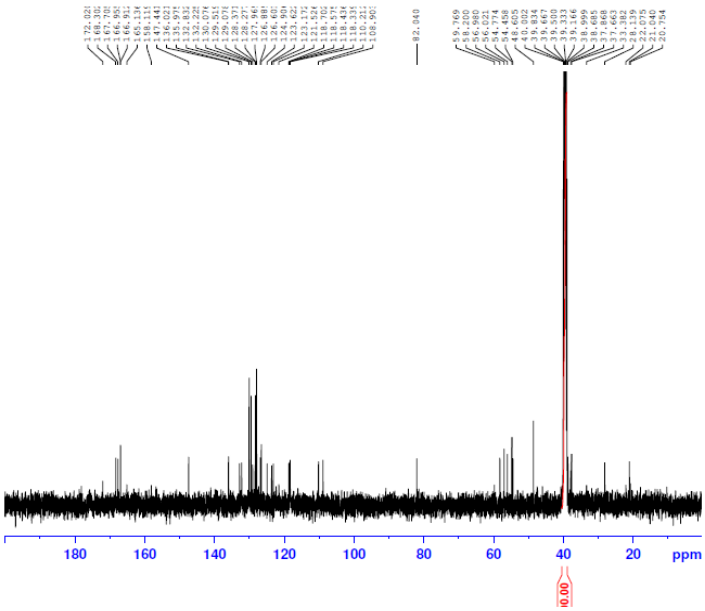

Fig 7a. ^{1}H NMR spectrum of asperazine A

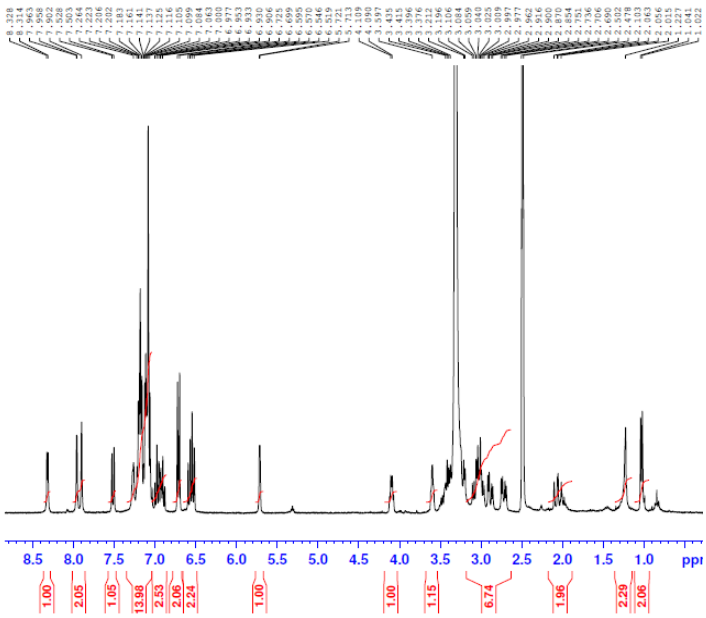

Fig 7b. ^{13}C NMR spectrum of asperazine A

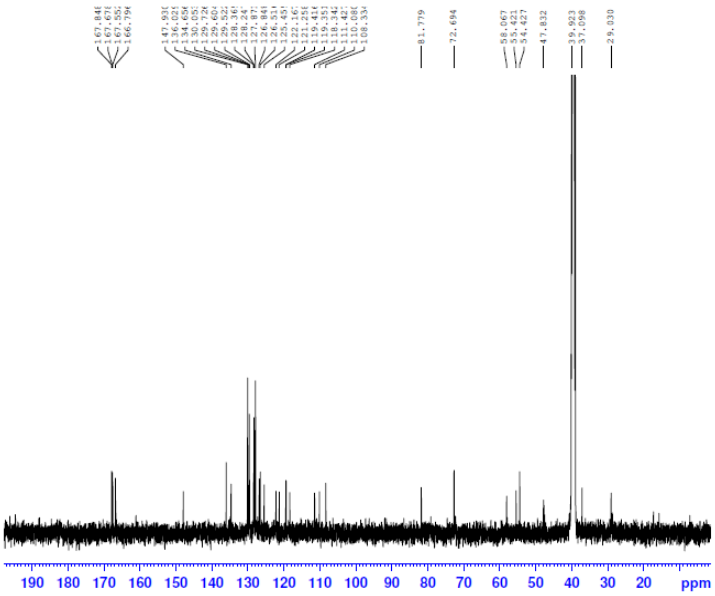

Fig 7c. HMBC spectrum of asperazine A

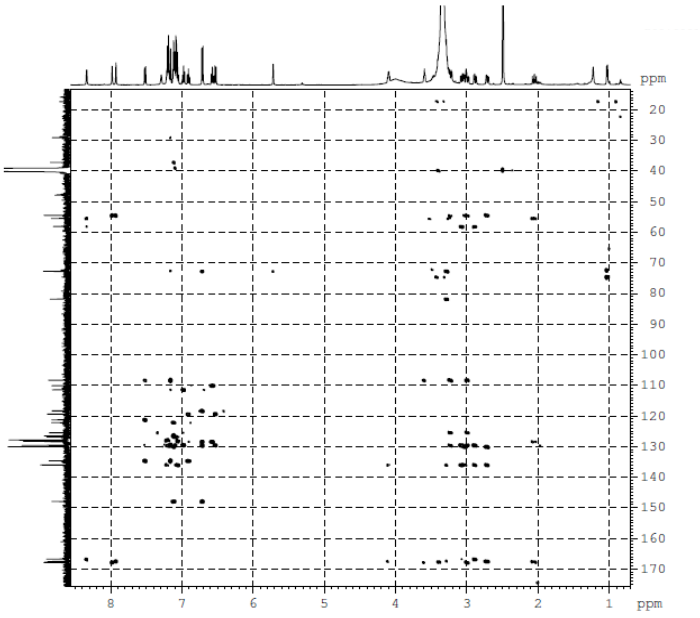

Fig 8a. ^{1}H NMR spectrum of 9-oxo-10, 12 octadecadienoic acid

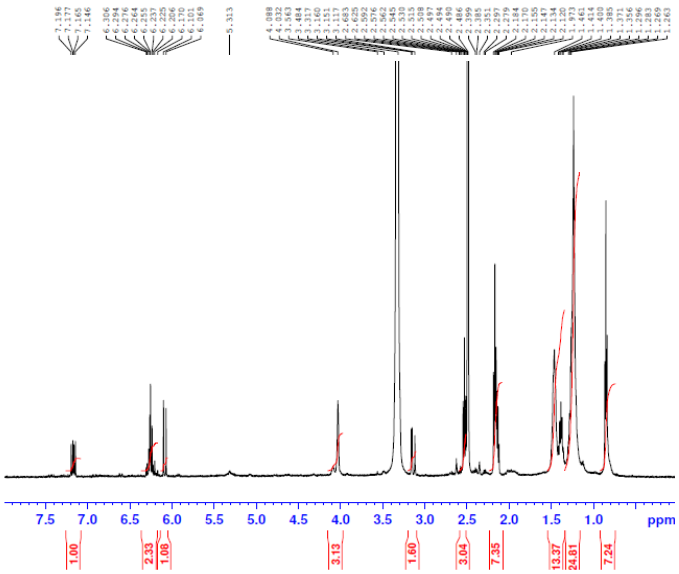

Fig 9a. ^{1}H NMR spectrum of 8-oxo-9, 11 octadecadienoic acid

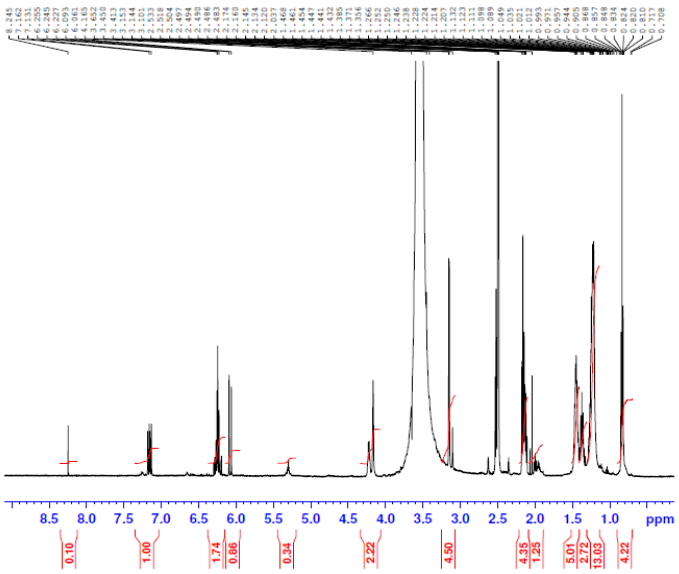

Fig 9b. ^{13}C NMR spectrum of 8-oxo-9, 11 octadecadienoic acid

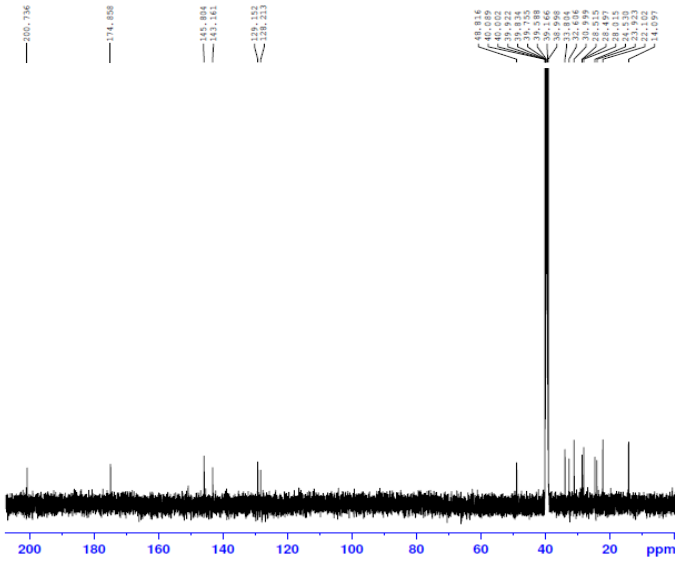

Fig 9c. HMBC spectrum of 8-oxo-9, 11 octadecadienoic acid

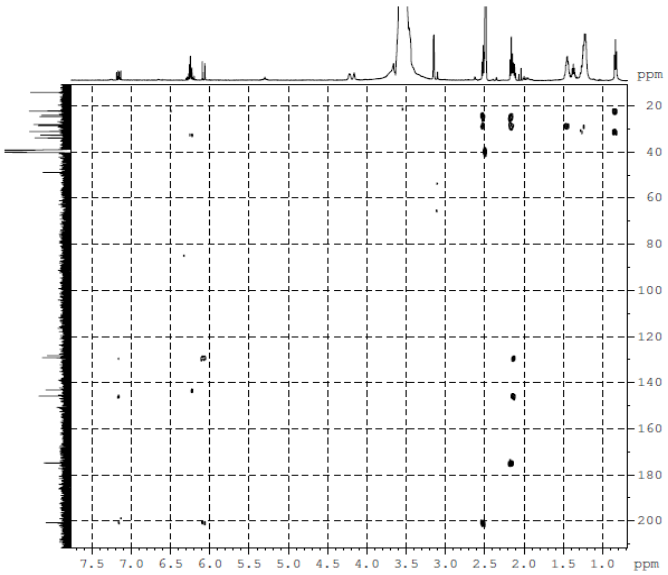

Publication

Abdou, R., K. Scherlach, H. M. Dahse, I. Sattler, and C. Hertweck, Botryorhodines A-D, antifungal and cytotoxic depsidones from *Botryosphaeria rhodina*, an endophyte of the medicinal plant *Bidens pilosa.* Phytochemistry, 2010. **71**(1): p. 110-116.

Acknowledgements

This study was accomplished at the Leibniz Institute for Natural Product Research and Infection Biology, Hans Knöll Institute, Jena from 11. 2006 till 3. 2010 under the supervision of Prof. Dr. Christian Hertweck.

I would like to express my sincere gratitude to Prof. Dr. Christian Hertweck for his valuable scientific guidance, constant support and great help during the course of this study.
Many thanks to Prof. Dr. Christian Hertweck also for giving me the opportunity to pursue my doctoral study in his research group and giving me the chance to use the excellent work facilities at the Department of Biomolecular Chemistry of the Hans-Knöll Institute.

I refer my deepest thanks to Dr. Kirstin Scherlach for her valuable suggestions, fruitful discussions and especially for sharing her expertise in NMR data interpretation.

I would like to express my gratitude to Dr. Hans-Martin Dahse for performing the cytotoxic assays at the Department of Infection Biology of the Hans-Knöll Institute and for helping me in interpreting the results.

I would like to thank also Dr. Isabell Sattler for guiding my first step in this study and for arranging the collaboration with the Institute of Biochemical Plant Pathology of the Helmhotz Zentrum in Munich and the Centralbureau for Schimmelcultures in the Netherlands

Many thanks to Dr. Keishi Ishida and Dr. Markus Nett for their kind help and valuable discussions.

I refer my appreciation to Dr. Grit Walther for carrying out the taxonomic identification of the isolated endophytic fungal strains at the Centralbureau for Schimmelcultures in the Netherlands.

Special thanks for the friendly cooperation with Dr. Uta von Rad and Clara Steinhauser and the performance of the plant immunological study at the Institute of Biochemical Plant Pathology (Helmholtz Zentrum) in Munich and for helping me in interpreting the data.

My deepest thanks for the continuous support and help of Mrs. Heinecke for HPLC-MS measurements and for dereplication with the database, Mrs. Perner for measuring the

HRESIMS spectra, Mrs. Rhein for carrying out the NMR measurements, Mrs. Schwinger for performing the fermentations of the fungal strains and the agar diffusion assays and Mrs. Valentin for handling the cultures made for the screening assays.

Special thanks to all my colleagues for their support especially Basile Ndjeioung and Patricia Gomes for their kind help, continuous encouragement and nice working atmosphere.

I refer my thanks to Frau Klose for her helpfulness and Dr. Dorit Schmidt and Mr. Jan Kößling for their great help in administrative matters.

I am very grateful to the Egyptian government for supporting me financially during the course of this study and for giving me the chance of pursuing this study in Germany.

Last but not least I would like to express my profound gratitude to all members of my family especially my husband for his continuous support and help throughout this study. My warm thanks to my parents and sisters for their unforgettable support and continuous encouragement.

Selbstständigkeitserklärung

Hiermit erkäre ich, dass mir die geltende Promotionsordnung bekannt ist und dass ich die Dissertation selbstständig angefertigt habe. Alle benutzten Hilfsmittel, persönlichen Mitteilungen und Quellen in meiner Arbeit habe ich angegeben. Diese Dissertation wurde weder als Prüfungsarbeit für staatliche oder andere wissenschftliche Prüfungen noch als Dissertation bei einer anderen Hochschule eingereicht.

Randa Abdou

Jena, den 20.8. 2010